

PLATINUM INDUCED NUCLEOLAR STRESS: A STUDY OF MOLECULAR
LEVEL FACTORS

by

CHRISTINE ELLEN FORCE MCDEVITT

A DISSERTATION

Presented to the Department of Chemistry and Biochemistry
and the Division of Graduate Studies at the University of Oregon
in partial fulfillment of the requirements
for the degree of
Doctor of Philosophy

September 2021

DISSERTATION APPROVAL PAGE

Student: Christine Ellen Force McDevitt

Title: Platinum Induced Nucleolar Stress: A Study of Molecular Level Factors

This dissertation has been accepted and approved in partial fulfillment of the requirements for the Doctor of Philosophy degree in the Department of Chemistry and Biochemistry by:

Ramesh Jasti	Chairperson
Victoria DeRose	Advisor
Michael Haley	Core Member
Michael Pluth	Core Member
Eric Selker	Institutional Representative

and

Andrew Karduna	Interim Vice Provost for Graduate Studies
----------------	---

Original approval signatures are on file with the University of Oregon Division of Graduate Studies.

Degree awarded September 2021

© 2021 Christine Ellen Force McDevitt
This work is licensed under a Creative Commons
Attribution NonCommercial-NoDerivs (United States) License.



DISSERTATION ABSTRACT

Christine Ellen Force McDevitt

Doctor of Philosophy

Department of Chemistry and Biochemistry

September 2021

Title: Platinum Induced Nucleolar Stress: A Study of Molecular Level Factors

Platinum anti-cancer drugs are widely used in the United States being used in 10-20% of cancer therapy treatments today. These drugs have been in use for many years with cisplatin being in use for over 40 years. The mechanism of platinum compounds was believed to be through the DNA damage response pathway; however, recently it has been identified and confirmed that oxaliplatin causes cell death through ribosome biogenesis stress or nucleolar stress. Here we explore the structural and molecular level factors that influence why oxaliplatin causes nucleolar stress. Chapter II explores the structural characteristics of oxaliplatin that influence why this compound causes nucleolar stress. We identify new platinum compounds that also exploit this cell death pathway and find that there is a correlation between size and hydrophobicity but that the orientation of the ligand strongly influences whether compounds cause nucleolar stress. The orientation of the ligand can cause compounds with similar size and hydrophobicity to no longer cause nucleolar stress. Chapter III explores the properties of phenanthriplatin, another platinum compound reported to cause nucleolar stress, and other monofunctional platinum compounds. We found that no structural connection exists between oxaliplatin and phenanthriplatin that explain why both compounds cause stress and could indicate that

they are working by two different binding events in cells to cause the same outcome. Chapter IV further explores the non-labile ligand of oxaliplatin (1,2-diaminocyclohexane) and finds that while the addition of a methyl to the scaffold is tolerated, the addition of an acetamide causes the compounds to no longer cause nucleolar stress. This further indicates that the interaction responsible for oxaliplatin causing nucleolar stress is highly selective and could work as a lock and key type mechanism. These structure studies are helpful to determine what the constraints for the interaction are but do not identify potential biomolecular targets of these compounds. In chapter V we report synthetic work towards two click-capable platinum compounds that can be used to directly probe the platinum atoms. A second generation click compound utilizing a cyclopropene-tetrazine bioorthogonal pair can be used for live cell imaging while an CuAAC oxaliplatin mimic could help to uncover the target of oxaliplatin that causes nucleolar stress. Chapter VI examines two types of binding that could occur, a bidentate adduct to a biomolecule such as a double strand of DNA and a mono adduct such as binding to NPM1, through computational modeling. These models illuminate the possibility of asymmetric molecules to exhibit flexibility at interfaces particularly when binding to biomolecules through a monoadduct. These studies help to illuminate the molecular factors that could influence platinum induced nucleolar stress and be used to further understand these platinum compounds and their activities as medicine.

This dissertation contains published and unpublished co-authored material.

CURRICULUM VITAE

NAME OF AUTHOR: Christine Ellen Force McDevitt

GRADUATE AND UNDERGRADUATE SCHOOLS ATTENDED:

University of Oregon, Eugene, OR

University of Arizona, Tucson, AZ

DEGREES AWARDED:

Doctor of Philosophy, Chemistry, 2021, University of Oregon

Bachelor of Science, Biochemistry, 2016, University of Arizona

AREAS OF SPECIAL INTEREST:

Chemical Biology

Platinum Chemotherapeutics

Nucleolar Stress

PROFESSIONAL EXPERIENCE:

Graduate Employee, University of Oregon, 2016-2021

Undergraduate Researcher, University of Arizona, 2014-2016

GRANTS, AWARDS, AND HONORS:

Knight Campus Undergraduate Scholars Mentor, 2019

HHMI, Janelia Junior Scientist Workshop on Solving Biological Problems with Chemistry, 2019

PUBLICATIONS:

Emily C. Sutton, **Christine E. McDevitt**, Matthew V. Yglesias, Rachael M. Cunningham, and Victoria J. DeRose. "Tracking the Cellular Targets of Platinum Anticancer Drugs: Current Tools and Emergent Methods." *Inorganica Chimica Acta*, June 26, 2019, 118984.

Christine E. McDevitt, Matthew V. Yglesias, Austin M. Mroz, Emily C. Sutton, Min Chieh Yang, Christopher H. Hendon, and Victoria J. DeRose. "Monofunctional Platinum(II) Compounds and Nucleolar Stress: Is Phenanthriplatin Unique?" *JBIC Journal of Biological Inorganic Chemistry*, September 7, 2019.

Sutton, Emily C.*, **Christine E. McDevitt***, Jack Y. Prochnau, Matthew V. Yglesias, Austin M. Mroz, Min Chieh Yang, Rachael M. Cunningham, Christopher H. Hendon, and Victoria J. DeRose. 2019. "Nucleolar Stress Induction by Oxaliplatin and

Derivatives.” *Journal of the American Chemical Society* 141 (46): 18411–15. *co-first authors

Hannah C. Pigg, Emily C. Sutton, Matthew V. Yglesias, **Christine E. McDevitt**, Victoria J. DeRose. “Time-Dependent Studies of Oxaliplatin and Other Nucleolar Stress Inducing Compounds.” *in preparation*

Christine E. McDevitt, Andres S. Guerrero, Haley Smith, Victoria J. DeRose,. “Structure-Function Investigation of the 4,5 Position on 1,2-diaminocyclohexane of Oxaliplatin.” *In preparation*

ACKNOWLEDGEMENTS

Firstly, my advisor, Dr. Victoria DeRose who has supported me both within my research as well as navigating other aspects of graduate school. She has been instrumental to me to finish graduate school and pushed me and supported me in pursuing my love of teaching. I would also like to thank my committee chair Dr. Ramesh Jasti and my other committee members— Dr. Michael Haley, Dr. Michael Pluth and Dr. Eric Selker. In particular, Dr. Michael Haley and his lab. I also want to remember Dr. Jeffrey McKnight who, as an outside member, was always involved and interested in my research.

I also want to thank all the members of the DeRose lab. The collaborative and positive energy that has been in our lab has sustained me through my time. I would like to thank Dr. Emily Sutton who has become a good friend for her openness to all of my confusion and excitement about our projects together. I have enjoyed all the time we have talked in lab about all aspects of life and the insights that you have taught me with your view of the world. I am so grateful that we got to spend my entire graduate career in the same lab. I would also like to thank our current members, Matt Yglesias and Hannah Pigg. One of our newest members, Dillon Willis and Andres Guerrero. I am thankful to have worked with all of you. I also want to thank former members Rachael Cunningham and Former lab members whose work came before mine and set the tone for my projects—Dr. Alan Moghaddam and Dr. Jonathan White, Dr. Emily Reister, and Geri Laudenbach. I am thankful for the undergraduate researchers who have worked with me. Firstly, Jack Prochnau who's curiosity sparked a whole new side of our projects. Additionally, Nathan Nguyen with his orange jacket and Haley Rice.

I am also thankful for the people who have helped me to learn and connect with the teaching experience. I have worked with many different professors over the years and seen their joy as they teach the subjects they are most passionate about. In particular, Dr. Tom Stevens, who's commitment to both helping me to develop classroom skills and to his students is something that I will continue to aspire to. And thanks to Dr. Kenneth Prehoda who I worked together with for many years. I have also learned much from Dr. Diane Hawley and Dr. Michael Koscho.

I also want to thank my cohort and classmates. I will remember the nights after cumulative exams and baseball games where I got to spend time with everyone. I want to thank Jeremy Bard who has shared his experiences with me job searching. I also want to thank Annie Gilbert, Haley Smith, and Kaylin Fosnacht as well as Dr. Terri Lovell, Dr. Curtis Colwell, Dr. Brittany White, Dr. Matthew Cerda and Dr. Andrea Steiger, Dr. Hazel Fargher, and Dr. Ruth Maust.

I want to thank both of my best friends, Vi Tran and Alexis Elmore. I want to thank all of my family for their support through the process. I am thankful for my mom and dad for their care and consideration. I am thankful for my sister who I have watched overcome so many setbacks and find what she really loves. Her singlemindedness to get what she wanted is something that I look up to. And I want to thank my new family, the Forces, who have been my family here in Oregon. And finally, I am so thankful for my wife. This past year has been one of the hardest with the pandemic as well as trying to job search. We have handled the uncertainty amazingly and it's definitely because we had each other. I am so thankful to you and so happy to be your wife.

For all of the Forces and McDevitts

TABLE OF CONTENTS

Chapter	Page
CHAPTER I: INTRODUCTION.....	1
Background	1
Ribosome biogenesis stress caused by oxaliplatin	4
Detection of platinum using pre-tethered fluorophores	5
Click chemistry for post-treatment tethering of platinum compounds	7
Bridge to Chapter II.....	11
CHAPTER II: NUCLEOLAR STRESS INDUCTION BY OXALIPLATIN AND DERIVATIVES	12
Nucleolar Stress Induction by Oxaliplatin and Derivatives	12
Bridge to Chapter III	21
CHAPTER III: MONOFUNCTIONAL PLATINUM (II) COMPOUNDS AND NUCLEOLAR STRESS: IS PHENANTHRIPLATIN UNIQUE?.....	23
Introduction	23
Results and discussion.....	26
Oxaliplatin and phenanthriplatin cause NPM1 relocalization	26
Picoplatin does not cause NPM1 relocalization	29
NPM1 relocalization is not a general property of monofunctional platinum compounds.....	29
Steric bulk is not sufficient to predict NPM1 relocalization	31
Hydrophobicity is not sufficient for predicting NPM1 relocalization.....	33
Conclusions	34
Bridge to Chapter IV	36
CHAPTER IV: STRUCTURE-FUNCTION INVESTIGATION OF THE 4,5 POSITION ON 1,2-DIAMINOCYCLOHEXANE OF OXALIPLATIN	38
Introduction	38
Results	41
Limited tolerance for substitutions at the DACH 4- position.....	41

Chapter	Page
Axial vs equatorial substitutions to the DACH ring do not change the mechanism of action	43
DMSO may inactivate platinum compound's abilities to cause nucleolar stress	44
Installation of a double bond at the 4,5 position is tolerated	46
Changes to hydrophobicity do not explain why compounds no longer cause nucleolar stress	48
Discussion	48
Bridge to Chapter V	51
CHAPTER V: SYNTHESIS OF CLICK CAPABLE PLATINUM DERIVATIVES	53
Introduction	53
Second generation click capable platinum compounds for live cell imaging	55
Synthesis and characterization of a click capable oxaliplatin mimic	61
Bridge to Chapter VI	64
CHAPTER VI: MODELING AND VISUALIZING STRESS INDUCING PLATINUM COMPOUNDS	66
Introduction	66
Modeling platinum compounds binding to DNA	67
Platinum compounds interacting with NPM1	72
CHAPTER VII: CONCLUDING REMARKS	77
Summary	77
Future directions	81
APPENDIX A: SUPPLEMENTARY INFORMATION FOR CHAPTER II	84
Supplementary figures	84
Supplementary tables	89
Materials and methods	91
APPENDIX B: SUPPORTING INFORMATION FOR CHAPTER III	101
Materials and Methods:	101

Chapter	Page
APPENDIX C: SUPPORTING INFORMATION FOR CHAPTER IV	106
Materials and methods	106
NMR spectra	110
APPENDIX D: SUPPLEMENTARY INFORMATION FOR CHAPTER V	114
Materials and methods	114
Supplemental NMRs	117
REFERENCES CITED.....	120

LIST OF FIGURES

Figure	Page
1.1. Chemical structures of FDA approved platinum chemotherapeutics	2
1.2. Cellular uptake and aquation of cisplatin.....	4
2.1. Compounds tested for inducing nucleolar stress via NPM1 relocalization	13
2.2. Nucleolar stress induced by Pt(II) compounds	14
2.3. Quantification of NPM1 relocalization induced by Pt(II) compounds	16
2.4. Size and hydrophobicity correlate to stress induction	19
2.5. Computed volume and distance measurements	20
3.1. Platinum compounds used in this study.....	24
3.2. NPM1 relocalization	27
3.3. Two-ring structural isomers related to phenanthriplatin.....	31
3.4. Optimized structures of Platinum (II) compounds.....	32
4.1. Compounds used in this study	40
4.2. NPM1 relocalization of axial and equatorial oxaliplatin derivatives.....	43
4.3. NPM1 relocalization of DACH-PT and methyl oxaliplatin derivatives	45
4.4. NPM1 relocalization caused by DACHene and DACH-Am.....	47
4.5. Computational model of DACHene.....	47
5.1. Platinum compounds incorporation and subsequent click reactions	53
5.2. CuAAC platinum derivatives.....	53
5.3. dPAGE analysis of Pt(II)-cyclopropene derivative bound to DNA.....	59
6.1. Cisplatin and Oxaliplatin binding to DNA	67

Figure	Page
6.2. Platinum compounds bound to DNA APP and Benzaplatin.....	68
6.3. Two bound confirmations of APP	69
6.4. DNA bount to PlatMeEn and pentaplatin	70
6.5. Methyl oxaliplatin derivatives binding to DNA	71
6.6. Cysteine 275 bound to cisplatin and oxaliplatin.....	73
6.7. Two possible confirmations of APP and Benzaplatin	74
A.1. NPM1 assay and quantification scheme	83
A.2. Additional images for compounds tested.....	84
A.3. Quantification of nucleolar stress induction for ligands and solvents	85
A.4. Histograms of NPM1 intensity for individual nuclei.....	86
A.5. DFT-optimized structures of compounds	87
C.1. NMR for EqMe-Pt.....	109
C.2. NMR for AxMe-Pt	109
C.3. Stacked NMR showing AxMe-Pt and EqMe-Pt	110
C.4. NMR for EqEt-Pt	111
C.5. NMR for AxEt-Pt.....	112
D.1. Carbon NMR from cyclopropene scheme 1	116
D.2. NMRs of DACH-Am.....	117
D.3. Crude NMRs of azide containing oxaliplatin mimic	118

LIST OF SCHEMES

scheme	Page
4.1. Synthetic scheme used to synthesize axial and equatorial methyl derivatives	41
4.2. Synthetic scheme used for ethyl axial and equatorial derivatives	42
5.1. Scheme 1 to create cyclopropene Pt(II) derivative	56
5.2. Scheme 2 to create cyclopropene Pt(II) derivative	58
5.3. Oxaliplatin mimic scheme	62

LIST OF TABLES

Table	Page
1.1. Click capable platinum compounds and their biological uses	9
3.1. Steric bulk measurements for platinum compounds	32
3.2. Gibbs free energy of transfer	34
A.1. IC50 values in A549 cells of Pt(II) compounds at 24 hours	88
A.2. IC50 values in A539 cells at 48 hours	88
A.3. Volume and hydrophobicity data	89

CHAPTER I: INTRODUCTION

Background

Platinum chemotherapeutic drugs are used in 10-20% of cancer regimes in the United States.¹ There are currently three FDA-approved platinum anticancer drugs in the US. The first drug, cisplatin, was serendipitously discovered when Barnett Rosenberg and Loretta Van Camp were studying the effects of electric fields on bacteria.² When performing the study they used a platinum electrode and observed that *E. coli* cells had elongated. After the initial observation (sometimes credited to Van Camp)³⁻⁵ it was determined that cisplatin was being formed in solution due to the platinum electrode and the ammonium buffer and that this compound was responsible for inhibiting the bacteria's cell division.⁶ This finding was followed up by testing tumor growth in mice and, eventually led to cisplatin becoming the first platinum chemotherapeutic medicine.

After the discovery of cisplatin, many platinum compounds were synthesized and tested for their anti-tumor properties. Of the thousands of platinum compounds synthesized, only carboplatin and oxaliplatin have been approved for use in the United States.⁶ Carboplatin was approved in 1989 followed by oxaliplatin in 1996 (**Figure 1.1**).⁷ Although more platinum compounds have undergone clinical trials in the United States after oxaliplatin's approval, none have been FDA-approved. However, a few more platinum drugs have been approved in other countries such as

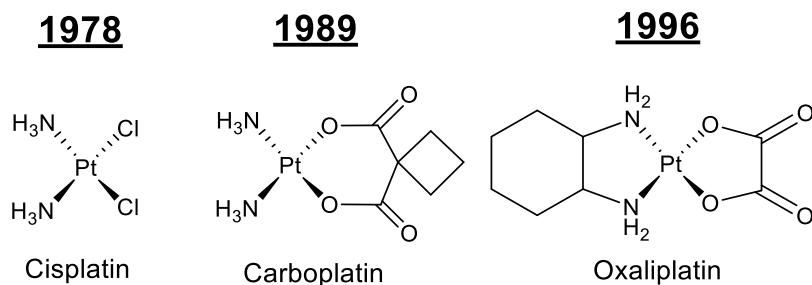


Figure 1.1: Pt(II) anticancer drugs currently approved for use in the United States. Included are years of FDA approval.

nedaplatin in Japan, lobaplatin in China, and heptaplatin in Korea.⁸ In the United States, other platinum compounds have entered clinical trials but have not been approved such as phenanthriplatin.⁹ Phenanthriplatin structure differs from other approved compounds because it is a monofunctional platinum compound.

Despite the last platinum drug being FDA-approved more than 20 years ago, platinum chemotherapeutics are still widely used. Platinum drugs are used in 10-20% of cancer therapies today in conjunction with many other medicines.¹ Despite their efficacy in stopping tumor growth, these drugs come with many severe side effects. Cisplatin's side effects include peripheral neuropathy (nerve damage), hearing loss (ototoxicity), and kidney damage (nephrotoxicity), nausea and vomiting.⁷ The addition of other medications can alleviate some symptoms of these platinum drugs, particularly nausea and vomiting. However, some side effects can become permanent with no way to predict whether patients will exhibit them as is the case for peripheral neuropathy.¹⁰ The side effects of platinum drugs severely limits their long term use.

Clinical research into cisplatin and oxaliplatin show that these two drugs have different side effect profiles and efficacies for different cancer types. Cisplatin is

particularly effective against testicular cancer. Since cisplatin was introduced in the treatment of testicular cancer along with other drugs, the US death rate from testicular cancer has dropped by two thirds.¹ Oxaliplatin is known to be more effective against colon cancer and lung cancer.⁷ The reasons behind why these two drugs are effective in different cancer types and have different side effects is currently not well understood.

The mechanism of action for these drugs is believed to be similar to cisplatin (**Figure 1.2**).¹¹ Cisplatin is injected intravenously where the chloride concentration of the blood is high. The high chloride concentration inhibits the displacement of the chloride ligands of cisplatin. Cisplatin is then transported into the cells using copper transporter 1 or through diffusion. The interior of the cell has a significantly lowered chloride concentration causing cisplatin to aquate. The aquated species is considered the activated species. The water ligands can then be displaced in order to bind to biomolecules that could include nitrogen, sulfur and oxygen ligands. Cisplatin can bind to many different species within cells; however, its activity is believed to be through coordination to genomic DNA leading to DNA damage and cell death. Only 1-10% of cisplatin that enters the cells binds to DNA while the majority of cisplatin binds to other biomolecules as well as small molecules in the cell.¹²⁻¹⁴

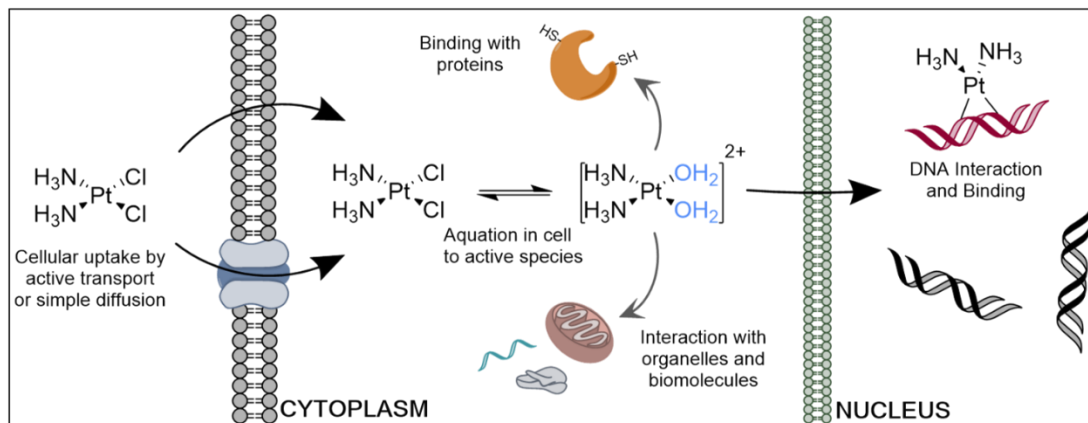


Figure 1.2: Cellular uptake and aquation of cisplatin. Diagram by Matthew Yglesias

The most well-studied mechanism of action of Pt(II)-based chemotherapeutics is the formation of Pt(II) lesions on DNA, which can lead to inhibition of replication and ultimately cell death via DNA damage response (DDR) pathways.¹⁵ Pt(II) lesions primarily form 1,2-intrastrand crosslinks on adjacent guanines, although they can also form 1,2-intrastrand crosslinks on AG dinucleotides, 1,3-intrastrand crosslinks on nonadjacent guanines, interstrand crosslinks, and monofunctional adducts.¹⁵ This pattern has been observed both *in vitro* and *in vivo*, and has been described in detail in previous reviews.^{11,15,16} All known Pt(II) compounds with exchangeable ligands are capable of forming these adducts with DNA and the downstream influence of these adducts has been heavily investigated.

Ribosome biogenesis stress caused by oxaliplatin

Until recently, it was believed that the cytotoxicity of all Pt(II) compounds could be attributed solely to their DNA crosslinking abilities and subsequent induction of the DNA Damage Response (DDR), a known trigger of apoptotic pathways.¹⁷ As the body of research on Pt(II) reagents has grown, a more complex picture has emerged of the

mechanisms of action behind these ubiquitous drugs.¹⁷ A striking relatively recent discovery is that oxaliplatin, but not cisplatin or carboplatin, causes cytotoxicity via disruptions in ribosome biogenesis rather than DDR.¹⁸ In addition to oxaliplatin, the mono-adduct forming phenanthriplatin also induces nucleolar stress.¹⁹ Ribosome biogenesis occurs in the nucleolus, a conserved and highly structured organelle in eukaryotes. Disruptions of the nucleolus or ribosome biogenesis trigger the nucleolar stress response, which leads to cell death or senescence via activation of the tumor suppressor p53. Because its molecular mechanisms are not yet fully understood, and due to its potential role as a chemotherapeutic target, this fascinating stress process is an area of intense interest in the fields of molecular biology and medicine.²⁰⁻²³

The specificity of oxaliplatin as a nucleolar stress inducer is intriguing when considered alongside other data indicating a relationship between Pt(II) compounds and the nucleolus.⁸ Post-treatment fluorescent labeling of clickable Pt(II) drug analogs has shown localization of these compounds to the nucleolus,^{24,25} and there is significant evidence that Pt(II) compounds associate with ribosomes and ribosomal RNA (rRNA).²⁶⁻³² The structural determinants and molecular mechanisms by which only specific Pt(II) compounds may cause a nucleolar stress response are not understood.

Detection of platinum using pre-tethered fluorophores

Methods of tracking platinum compounds in cells are important tools for understanding molecular targets. Atom-based methods such as installation of a radioactive platinum atom, X-ray fluorescence, electron microscopy, NMR, and mass spectrometry can provide information on platinum location and binding partners and have been reviewed previously.³³ These methods, while useful for in vitro and non-cellular

work, are difficult to apply to live cells. One approach for potential live-cell imaging is the tethering of a fluorophore directly onto the platinum compound.

Cisplatin, oxaliplatin, and carboplatin are small, low or no- carbon molecules, in contrast to most fluorophores. The attachment of a fluorophore to platinum compounds can give rise to differences in charge, lipophilicity, solubility, polarity, or reactivity from the parent platinum compounds, as noted previously by Wexselblatt et al.³⁴ For platinum compounds, small changes can result in large differences to toxicity. For example, the addition of a methyl or ethyl to the cyclohexane ring changes the toxicity of oxaliplatin derivatives.³⁵ Another example demonstrated by Rijal et al. showed altered binding specificities of different amino-acid modified platinum compounds towards 16S rRNA.³⁶ If such small changes can make large impacts in these examples, it would stand to reason that larger deviations, such as an added fluorophore, could significantly affect activity. Also of concern may be the assumption that the fluorescent ligand remains tethered to the platinum in the cell. Fluorescence detection only gives information on the location and presence of the fluorophore and not the platinum itself. Fluorophores tethered through a monodentate ligand could be susceptible to trans-labilization.³⁴

Despite these limitations, platinum-tethered fluorophores have proved valuable to research of platinum compounds in cells and continue to be developed. There have been many new compounds that incorporate a fluorophore reported within the last few years. Kitteringham et al. have created a carboplatin mimic with an incorporated BODIPY fluorophore and have imaged it in both cisplatin-sensitive and resistant cells.³⁷ Kalayda et al. created an oxaliplatin mimic which has been functionalized with a fluorescein and used to study oxaliplatin resistance.³⁸ A glucose and BODIPY conjugate has also been

synthesized that shows enhanced uptake into cells.³⁹ Xue et al. created a BODIPY-incorporated platinum compound modified with a photosensitizer to induce reactive oxygen species.⁴⁰ Yao et al. have also produced a maleimide-modified derivative for cysteine conjugation using their click enabled, acridine-tethered Pt(II) compound **7** (Table 1.1).⁴¹ Additionally, platinum(IV) has been derivatized to release fluorophores from the axial positions to investigate payload release upon reduction. Some recent Pt(IV) derivatives utilize aggregation-induced emission for visualization⁴² and also include an EGFR-targeted platinum compound tethered to a fluorescein.⁴³

Fluorescent platinum probes have been valuable to the field and continue to be used to further study platinum accumulation and targets; however, it is clear that small changes to the platinum scaffold change many aspects of the platinum complexes including the mechanism of action. There is concern that the addition of such large and hydrophobic fluorophores to the platinum could significantly alter the derivative's activity inside cells compared to the unmodified parent compound for which it supposed to provide a proxy. A more direct method, such as selectively tethering fluorophores to platinum compounds after native activity has already occurred, is highly desirable.

Click chemistry for post-treatment tethering to platinum compounds

Click chemistry refers to reactions that are distinguished as being modular and high yielding.⁴⁴ A widely used bioorthogonal click reaction is azide-alkyne cycloaddition, either Cu-catalyzed (CuAAC) or strain-promoted (SPAAC). An azide group is relatively easy to incorporate via a substitution reaction into many molecules of interest. The small size, biological inertness, and overall neutral charge have made it an enticing option for incorporation into platinum ligands. The installation of an azide as opposed to a

fluorophore limits the addition of steric bulk and hydrophobicity in this approach. The selectivity of the CuAAC and SPAAC reactions for post-treatment labeling enable direct detection of the platinum compound in permeabilized cells. Post-treatment labeling with biotin also enables enrichment and identification of Pt-bound targets.⁴⁵

There are currently a handful of available click-capable platinum compounds (Table **1.1**). All of the compounds have been used for cellular work and for a variety of other applications. Kitteringham et al. determined the IC₅₀ of the azide-modified compound **2**, which had similar toxicity to the parent carboplatin and much higher toxicity than the pre-tethered BODIPY conjugate mentioned above.^{37,46} Compound **1**, originally synthesized by Urankar et al.,⁴⁶ has been used to label DNA as well as characterize cellular RNA targets in *S. cerevisiae* by Moghaddam et al.⁴⁷ It was also used for in vitro fluorescent protein labeling and an enzymatic assay.⁴⁸ Compound **3** has been used to enrich for Pt-bound proteins for target identification in *S. cerevisiae*,⁴⁸ in addition to its application to enrich for and fluorescently label Pt-bound DNA in vitro.^{25,45} For a more comprehensive look at Pt binding in a cellular context, compound **3** and compound **4**, its alkyne derivative, were used in cellular imaging studies.²⁵ Compound **5**, another click chemistry-enabled compound developed in the DeRose lab, was used to fluorescently label

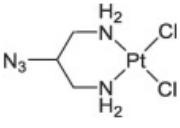
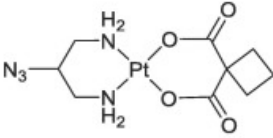
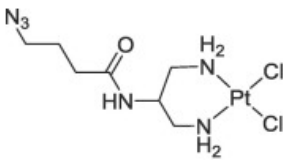
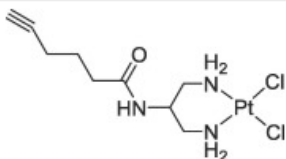
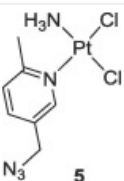
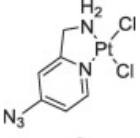
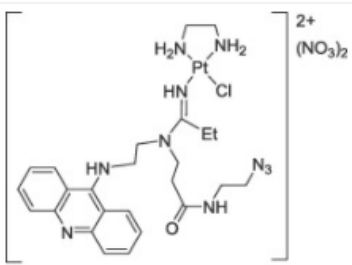
Structure	Use
 <p style="text-align: center;">1</p>	<p>Library synthesis of carboplatin derivatives</p> <p>Fluorescent labeling of DNA and ribosome</p> <p>Protein target identification</p>
 <p style="text-align: center;">2</p>	<p>Synthesis of carboplatin derivatives</p> <p>Toxicity</p>
 <p style="text-align: center;">3</p>	<p>Protein target identification</p> <p>DNA pulldown</p> <p>Cellular imaging</p> <p>Fluorescent labeling of DNA</p>
 <p style="text-align: center;">4</p>	<p>Cellular Imaging</p>
 <p style="text-align: center;">5</p>	<p>Fluorescent labeling of RNA, ribosomal RNA and tRNA</p>
 <p style="text-align: center;">6</p>	<p>Cellular imaging, gene expression, DNA binding</p>
 <p style="text-align: center;">7</p>	<p>Synthesis of acridine derivatives</p> <p>Cellular imaging</p> <p>DNA labeling</p> <p>Investigation of DNA and RNA synthesis, Cell cycle investigation</p>

Table 1.1 Currently available click-containing platinum derivatives and the context which they have been used and studied.

ribosomal RNA and tRNA from treated *S. cerevisiae*.⁴⁹ Zacharioudakis et al. synthesized compound **6** in order to determine localization of Pt-DNA adducts upon treatment with a histone deacetylase inhibitor and to investigate the effect of platinum on gene expression.⁵⁰ Lastly, compound **7** was used by Qiao et al. to determine the cellular distribution of a Pt-acridine compound.⁵¹ It has since been used to synthesize new derivatives that incorporate cysteine-directed moieties as described above. Compound **7** has been used to label proteins, investigate DNA and RNA synthesis after platinum introduction, and to fluorescently label DNA.^{41,51,52}

The click chemistry-enabled compounds described above have been used to further understanding of Pt interactions in cells through the direct detection of the Pt(II)-bound ligand post-treatment, allowing for Pt localization that is theoretically unbiased from the influence of fluorophore properties. However, these compounds have all been restricted to the CuAAC reaction which requires a cytotoxic Cu(I) catalyst, or to SPAAC reactions that require a non-cell permeable DIBO.⁵³ Further work into diversifying the click-capable platinum compounds to other types of bioorthogonal reactions may allow expansion into live-cell imaging and other types of investigations based on post-treatment derivatization.

In this document, the influence of small changes to the platinum ligands will be explored. These studies will examine the ligand of oxaliplatin 1,2-diaminocyclohexane and the mechanism of action exhibited by oxaliplatin. The mechanism of action of oxaliplatin, nucleolar stress, is sensitive to small changes to the platinum compounds. This drastic change in platinum activity further illustrates the need for post-treatment clickable derivatives which share similarities to the parent platinum species.

Bridge to chapter II

Chapter I described the discovery and history of platinum compounds that have been used in the United States. It discussed current chemical biology approaches to studying the activity of platinum compounds by either directly tethering a fluorophore or chemical reporting group to the platinum species or by installing an alkyne or azide for post-treatment labelling of the platinum. Modifications for post-treatment labeling create compounds that are much closer in structure to the parent compound and derivatives are more likely to have more similar activity with less perturbation of their structure. Chapter II explores the structural characteristics necessary for oxaliplatin to cause nucleolar stress. It explores how small changes to the oxaliplatin structure cause derivatives to no longer employ the same cell death mechanism.

CHAPTER II: NUCLEOLAR STRESS INDUCTION BY OXALIPLATIN AND DERIVATIVES

This chapter contains published, co-authored material. This communication was co-authored by Emily Sutton, Jack Prochnau, Matthew Yglesias, Austin Mroz, Min Chieh Yang, Rachael Cunningham, Christopher Hendon, and Victoria DeRose. CEM and ECS share co-first authorship.

Nucleolar Stress Induction by Oxaliplatin and Derivatives

The chemotherapeutic agent cisplatin has inspired the synthesis and investigation of thousands of Pt(II) analogs.⁵⁴ Of these, only two other compounds — carboplatin and oxaliplatin — have met FDA standards for medical use. Until recently, it was believed that the cytotoxicity of these compounds could be attributed solely to their DNA crosslinking abilities and subsequent induction of the DNA Damage Response (DDR), a known trigger of apoptotic pathways.⁵⁵ As the body of research on Pt(II) reagents has grown, a more complex picture has emerged of the mechanisms of action behind these ubiquitous drugs.¹⁷ A striking recent discovery is that oxaliplatin, but not cisplatin or carboplatin, causes cytotoxicity via disruptions in ribosome biogenesis rather than DDR.¹⁸ Ribosome biogenesis occurs in the nucleolus, a conserved and highly structured organelle in eukaryotes. Disruptions of the nucleolus or ribosome biogenesis trigger the nucleolar stress response, which leads to cell death or senescence via activation of the tumor suppressor p53. Because its molecular mechanisms are not yet fully understood, and due to its potential role as a chemotherapeutic target, this fascinating stress process is an area of intense interest in the fields of molecular biology and medicine.^{20–23}

The specificity of oxaliplatin as a nucleolar stress inducer is intriguing when considered alongside other data indicating a relationship between Pt(II) compounds and the nucleolus.⁸ Post-treatment fluorescent labeling of clickable Pt(II) drug analogs has shown localization of these compounds to the nucleolus^{24,25}, and there is significant evidence that Pt(II) compounds associate with ribosomes and ribosomal RNA (rRNA)^{26–32}. The structural determinants and molecular mechanisms by which only specific Pt(II) compounds may cause a nucleolar stress response are not understood. Here, we explore properties of oxaliplatin and other Pt(II) compounds and find that a narrow window of derivatives is able to induce nucleolar stress. The results define a set of constraints for Pt(II) compounds to induce this unique cell death pathway.

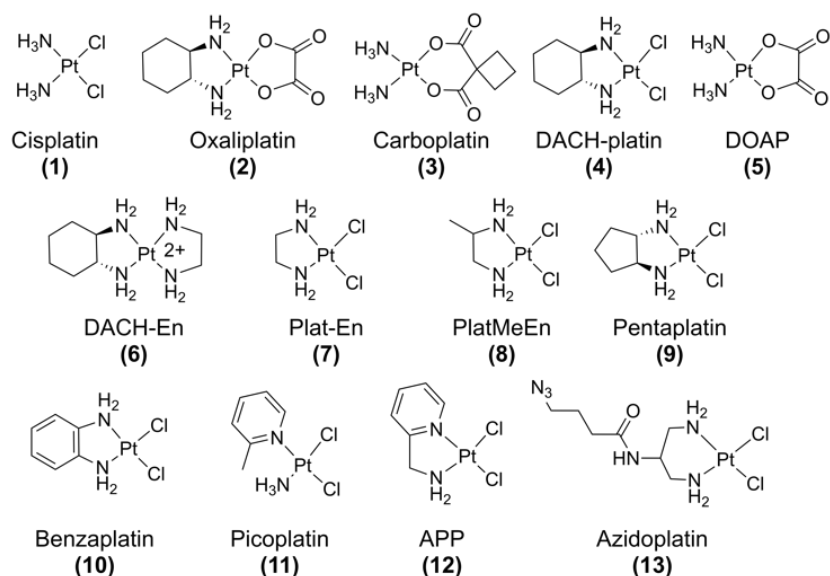


Figure 2.1: Compounds tested for inducing nucleolar stress via NPM1 relocalization in mammalian cells.

We selected Pt(II) compounds to test a variety of properties including steric bulk, hydrophobicity, crosslinking ability, and ligand orientation (**Figure 2.1**). The extent of

nucleolar stress was measured by nucleophosmin (NPM1) imaging (**Figure 2** and **Figure A.1**). Translocation of NPM1 from the granular component (GC) of the nucleolus to the nucleoplasm is a hallmark of the nucleolar stress response^{56,57}. This translocation has been shown to be a necessary, but not sufficient, feature of p53-mediated cell death upon nucleolar stress⁵⁷, and thus is a robust and appropriate marker for nucleolar stress. A549 cells were selected for this study as they are well established to have a characteristic nucleolar stress response resulting in p53-mediated apoptosis^{58,59}.

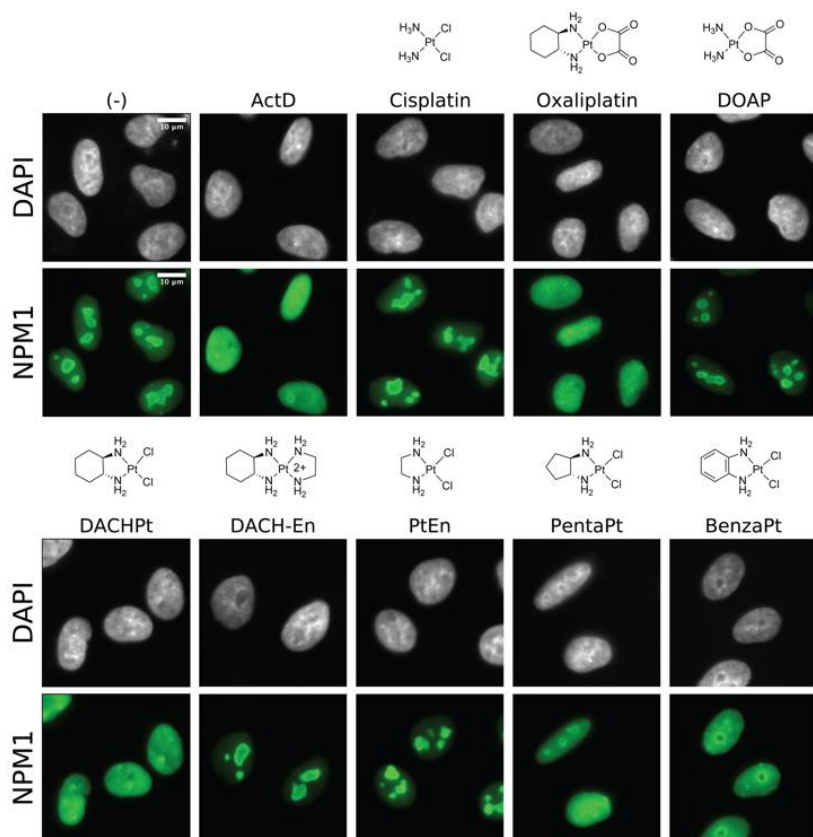


Figure 2.2: Nucleolar stress induced by Pt(II) compounds. NPM1 (green) relocalization following 24-hr treatment in A549 cells. Treatment concentrations are 10 μ M except for Actinomycin D (5 nM). Scale bar = 10 μ m.

Cells were treated for 24 hours with a given compound prior to fixation and secondary immunofluorescence to detect NPM1 (**Figure 2** and **A.1**). The extent of NPM1

redistribution was quantified using an image analysis pipeline (**Figure A.1**) to calculate the coefficient of variation (CV) of NPM1 intensity in each cell (**Figure 2.3**). The uniform distribution of NPM1 in cells undergoing nucleolar stress yields a low CV, as seen in positive control samples treated with known stress-inducer Actinomycin D (**Figure 2.3**). In addition to the observation of NPM1 redistribution, we noted a change in the shape of nucleoli from eccentrically shaped aggregates to round, sphere-like structures upon stress induction (**Figure 2.2**). As predicted^{18,60}, oxaliplatin (**2**) induces robust redistribution of NPM1, similar to the positive control, while NPM1 distribution in cisplatin (**1**) and carboplatin (**3**) treated cells more closely resembles that of the no-treatment control (**Figure 2.2, Figure 2.3**).

We note that for cisplatin-treated cells, a small amount of NPM1 redistribution was observed at this treatment concentration. This is likely because the 24-hour IC-50 value of cisplatin (12.8 μ M, Table **A.1**) is close to the treatment concentration, which may result in a subset of cisplatin-treated cells experiencing abnormal NPM1 distribution downstream of other cell death pathways, such as those mediated by the DDR (see footnote¹). Oxaliplatin, by contrast, shows robust NPM1 relocation at treatment concentrations well below the IC-50 value (81.5 μ M, Table **A.1**), suggesting that nucleolar stress significantly precedes cell death pathways¹⁸. The observation of NPM1 relocation well below IC-50 values was consistent with other stress-inducing

¹ Footnote: This model is supported by previously published data demonstrating that cisplatin causes significantly more DNA damage than oxaliplatin^{16,61} and that DDR-mediated cell death occurs upon cisplatin treatment, but not oxaliplatin treatment¹⁸. Additionally, data from our lab shows that DNA damage occurs at early time points in cisplatin-treated cells, prior to any putative NPM1 relocation, whereas no such damage occurs prior to observed NPM1 distribution in oxaliplatin-treated cells (unpublished).

compounds, including some compounds showing no toxicity at 24 hours despite extensive nucleolar stress (Table A.1). Thus, observation of nucleolar stress does not necessarily predict toxicity at 24 hours. In cases where no toxicity was observed at 24 hours, 48-hour IC-50 values were achieved. For this subset of compounds that was not sufficiently cytotoxic at 24 hours, stress induction did correlate with lower IC-50 values (Table A.2).

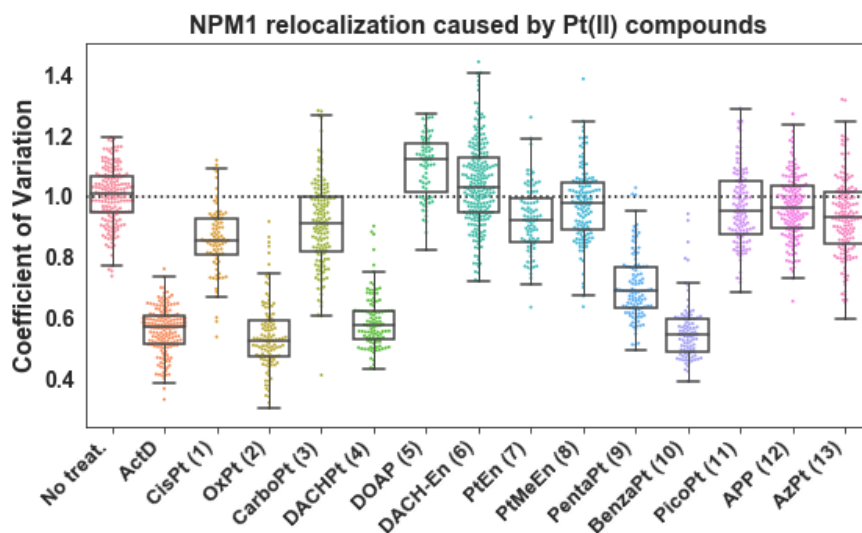


Figure 2.3: Quantification of NPM1 relocalization induced by Pt(II) compounds. Treatment conditions as in Figure 2.2; replicates and CV calculations as described in SI. For each treatment data set, boxes represent median, first, and third quartiles, and vertical lines are the range of data with outliers defined in the SI.

Oxaliplatin is distinct from cisplatin and carboplatin in both labile and non-labile Pt(II) ligands. The labile, chelating oxalate ligand of oxaliplatin delays aquation and therefore biomolecule crosslinking⁶² in comparison with cisplatin. We exchanged the labile and non-labile ligands of oxaliplatin and cisplatin with compounds 4 and 5. We found that compound 4, DACHPt, which has the non-labile DACH ligand of oxaliplatin and labile chloride groups of cisplatin, induces robust nucleolar stress. By comparison, 5,

or DOAP, which possesses the non-labile ammine ligands of cisplatin and the labile oxalic acid ligand of oxaliplatin, does not induce stress (**Figures 2.2 and 2.3**). The oxalic acid ligand alone also had no influence on NPM1 redistribution, nor did the DACH ligand by itself (**Figure A.2, Figure A.3**). From this, we concluded that the non-labile DACH ligand of oxaliplatin is responsible for the nucleolar stress response.

We next considered whether crosslinking of biomolecules by the Pt(II) compound is necessary for the induction of nucleolar stress. An alternate hypothesis is that the charged Pt(II) acts as a targeting agent to facilitate transport of the DACH moiety to the nucleolus where it disrupts nucleolar processes without forming a Pt(II)-DACH lesion on a biomolecule. Compound **6**, DACH-En, retains the DACH ligand but is unable to form crosslinks with biomolecules due to replacement of the oxalic acid with an ethylenediamine ligand (**Figure 2.1**). This positively charged compound did not induce stress (**Figure 2.2, Figure 2.3**), suggesting that crosslinking of Pt(II) to cellular targets is necessary to induce a nucleolar stress response.

To refine requirements of the non-labile Pt(II) ligand that cause nucleolar stress, we examined the effects of steric bulk by testing **7, 8 and 9**. Pt-En (**7**) possesses a non-labile ethylenediamine ligand. This small molecule did not induce stress in A549 cells (**Figures 2.2 and 2.3**), indicating that a chelating diamine ligand, a common feature between PtEn, DACHPt, and oxaliplatin, is not sufficient to induce stress. The addition of a methyl group to generate the bulkier PtMeEn (**8**), was also not sufficient to induce stress (**Figure 2.3, Figure A.2, Figure A.3**). Compound **9**, pentaplatin, possesses a five-membered ring that places its volume between the non-stress inducing PtMeEn and the stress-inducing six-membered DACHPt. Pentaplatin was found to induce nucleolar stress

(**Figure 2.1**), although with a slightly higher resultant CV than positive controls or oxaliplatin (Fig. **2.3**). These results suggest that bulk may be an important metric lending towards the ability of Pt(II) compounds to induce nucleolar stress. Using computed values for volume, we conclude that as a general trend, Pt(II) compounds with more steric bulk are more likely to induce nucleolar stress (**Figure 2.4a**, Y axis). Compound length, or steric reach, also generally appears to correlate with stress induction (**Figure 2.4a**, X axis). Some exceptions to this trend are discussed below.

The chair confirmation of the DACH ligand is not essential for stress induction. BenzaPt (**10**), in which the DACH cyclohexane is replaced with a planar aromatic ring (**Figure 2.5B**), also induces robust NPM1 redistribution (**Figure 2.2** and **Figure 2.3**). Like DACHPt, BenzaPt is more hydrophobic than the simpler diam(m)ine compounds. To estimate the relatively hydrophobicity of our compounds of interest, we measured their water/octanol partition coefficients (Supplementary materials and methods). All of the stress-inducing compounds were found to be relatively hydrophobic (**Figure 2.4b**), leading to the conclusion that hydrophobicity, like steric bulk, positively correlates with stress induction. Similarly to steric bulk, however, exceptions to this trend were observed.

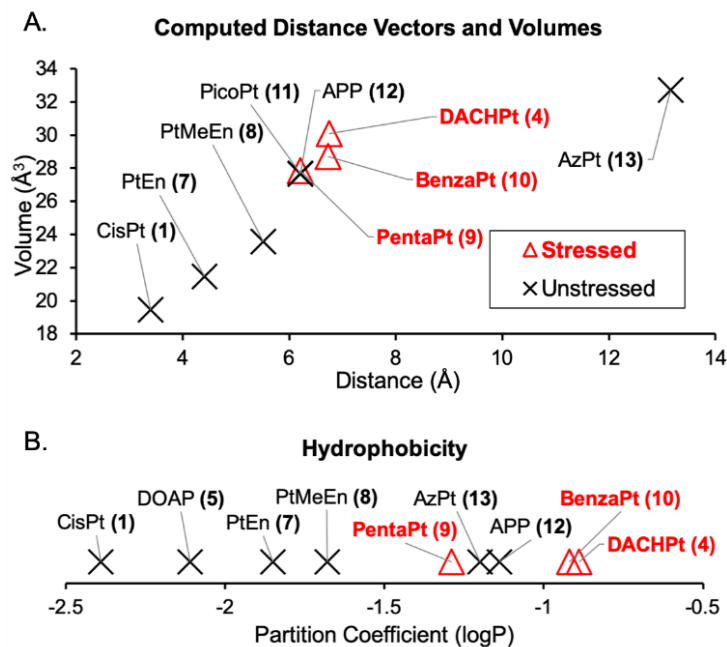


Figure 2.4: Size and hydrophobicity correlate with stress induction, with some exceptions. Compounds with a higher (less negative) partition coefficient are more hydrophobic than those with a lower (more negative) partition coefficient. Measurements and calculations are described in SI.

Compounds **11**, **12**, and **13** do not cause NPM1 relocalization despite being similar or higher in terms of size and hydrophobicity to compounds that do cause nucleolar stress (**Figure 2.4**). These exceptions may provide insight into the elements responsible for causing stress.

One particularly interesting comparison is between APP (**12**)^{63,64} and BenzaPt (**10**) (**Figure 2.5A**). These two Pt(II) compounds both have an aromatic ring, but differ in the orientation of the ring relative to the Pt(II), and by extension ring orientation relative to a biomolecule to which the compound is bound. While BenzaPt causes nucleolar stress, APP does not. Similarly, picoplatin (**11**) does not cause nucleolar stress despite having volume and reach similar to other compounds (**Figure 2.4** and **Figure 2.5**). These

results demonstrate a critical role for ring orientation in the ability of Pt(II) compounds to induce nucleolar stress.

The observation that azidoplatin (**13**) does not cause stress is of interest as this compound has extended volume and has previously been shown to localize to the nucleolus²⁵. Thus, nucleolar localization, even when combined with relatively high hydrophobicity and larger bulk and length, is not sufficient to induce nucleolar stress.

Taken together, the results described provide significant insight into the structural determinants of nucleolar stress induction among Pt(II) compounds. We conclude that there is an important role for ligand orientation and a general correlation between steric bulk and stress induction (**Figure 2.5**).

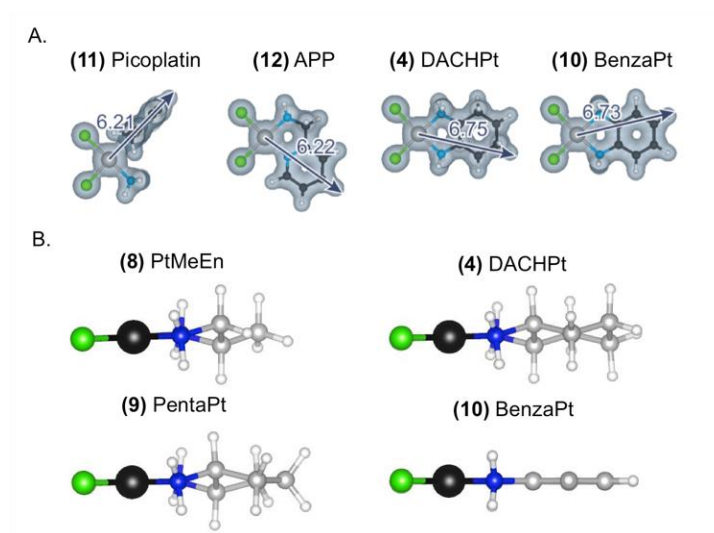


Figure 2.5: (A) Computed volume and distance measurements for non stress-inducing compounds 11 and 12 alongside stress-inducing compounds 4 and 10. (B) Ball and stick drawings of non stress-inducing compound 8 alongside stress-inducing 4, 9, and 10.

The differential responses induced by these compounds have clinical implications as the three currently FDA-approved Pt(II) chemotherapeutics are known to have

different treatment and side effect profiles. Other important differences between these compounds have been observed in the literature. For example, oxaliplatin is noted to cause immunogenic cell death (ICD), while cisplatin does not⁶⁵⁻⁶⁷. Although this contrast is also observed in nucleolar stress, connections between ICD and nucleolar stress are not well-studied. Oxaliplatin has also been shown to cause changes in the size of neuronal nucleoli correlating with peripheral neuropathy⁶⁸, a common side effect associated with oxaliplatin chemotherapy regimens. The relationship between nucleolar stress and platinum-induced neurotoxicity has not been explored. Additionally, there is some evidence that p53 mutations in colon cancer cell lines result in resistance to oxaliplatin-mediated cell death⁶⁹. This may be of interest given oxaliplatin's use in colon cancer treatments and p53's role in nucleolar stress-induced cell death.

Further study is warranted to provide clarification on the molecular mechanisms by which these compounds induce such different responses in the cell. For example, the stress-inducers may be interfering with progression of ribosome biogenesis^{56,58}, disrupting an intermolecular interaction of NPM1 that sequesters it in the nucleolus⁵⁷, altering biophysical properties of nucleic acids^{70,71}, or globally perturbing the biomolecular interactions that maintain nucleolar integrity. More work is needed to understand this fascinating biological stress process and to define the specific properties of Pt(II) compounds that cause it.

Bridge to Chapter III

In chapter II we explored the structural requirements of oxaliplatin to cause nucleolar stress instead of a DNA damage response. We found that compounds that caused nucleolar stress in general exhibited higher hydrophobicity and steric bulk, but

there were important exceptions indicating that these are not the only factors involved. In addition to oxaliplatin being reported to cause nucleolar stress, another platinum compound phenanthriplatin was reported to induce this cell death pathway. In chapter III we explore the structural properties of phenanthriplatin that are important to causing nucleolar stress and look for a structural connection between oxaliplatin and phenanthriplatin that could explain why both platinum compounds cause nucleolar stress.

CHAPTER III: MONOFUNCTIONAL PLATINUM(II) COMPOUNDS AND NUCLEOLAR STRESS: IS PHENANTHRIPLATIN UNIQUE?

This chapter contains published, co-authored material. This communication was co-authored by Matthew Yglesias, Austin Mroz, Emily Sutton, Min Chieh Yang, Christopher Hendon, and Victoria DeRose.

Introduction

Platinum-based drugs are an important class of chemotherapeutics. After the initial discovery of the antiproliferative capabilities of cisplatin, the drug was FDA-approved in 1978 and continues to be in significant use over 40 years later.² Two additional Pt(II) compounds were subsequently approved by the FDA, carboplatin in 1989 and oxaliplatin in 1996. Improvements upon these three drugs have been attempted and some new compounds even entered into clinical trials, but none have been approved by the FDA.⁵⁴

The three FDA-approved drugs are all considered classical platinum compounds. The characteristics of classical compounds are a result of early structure–activity relationship (SAR) studies that determined the necessary properties for platinum compounds to exhibit anti-proliferation activity.⁹ These required components are that the platinum compound be square planar, have a neutral overall charge, and contain two non-labile *cis*-am(m)ines and two labile *cis* anionic ligands. Although these rules led to the drugs that are used today, research into compounds that would not be within a traditional SAR study have produced non-classical platinum drugs with anti-proliferative activity. These non-classical compounds include Pt(IV) prodrugs, monofunctional, trans-platinum, polyplatinum, and tethered platinum complexes.^{9,32} One of the most effective and well-

studied non-classical compounds is the monofunctional Pt(II) phenanthriplatin^{9,72} (**Figure 3.1**). In addition to having only a single exchangeable anionic ligand, the *N*-heterocyclic ligand of phenanthriplatin and others of this class, such as pyriplatin (**Fig. 3.1**), is rotated perpendicular to the square-planar Pt ligand plane.

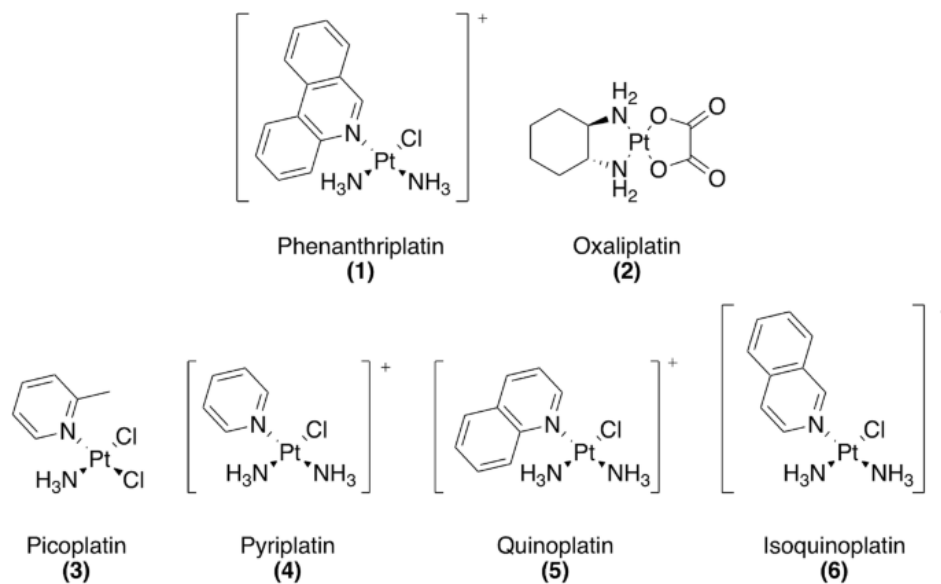


Figure 3.1 Platinum compounds used in this study

Phenanthriplatin has exhibited unique activity in the NCI-60 cell line screen when compared to other platinum chemotherapeutics.⁷² Phenanthriplatin is significantly more potent with a 7–40× higher toxicity than cisplatin.^{9,72} It has higher cellular uptake than cisplatin or pyriplatin.⁷² In addition, the phenanthridine ligand of phenanthriplatin may facilitate rapid DNA binding through reversible intercalation between nucleobases before platinum binding occurs.⁷³ Studies have also revealed some of the biological targets of phenanthriplatin. It has been shown to act as a topoisomerase II poison.⁷⁴ Phenanthriplatin also was demonstrated to inhibit RNA polymerase II,⁷⁵ but allows

efficient DNA polymerase η bypass.⁷⁶ Overall, these studies have shown that phenanthriplatin can affect biological processes in a variety of ways, and this has led researchers to suggest that the effectiveness of the compound is through multiple cellular pathways.⁷⁷

In a recent study, the classical platinum compound oxaliplatin and non-classical phenanthriplatin were both shown to induce ribosome biogenesis stress as the primary pathway to cell death.¹⁸ This surprising observation is in contrast with cisplatin and carboplatin, which were shown to cause cell death through DNA damage as is expected for classical compounds. The ability to induce nucleolar stress shared between oxaliplatin and phenanthriplatin is perplexing considering the major structural differences between the two compounds. We endeavored to determine whether there were structural similarities between these two molecules which would explain this similar activity, and determine whether the ability to induce nucleolar stress was inherent to the family of non-classical monofunctional platinum(II) compounds. To do this, we synthesized a suite of monofunctional and related platinum compounds (**Figure 3.1**) and analyzed their ability to cause nucleolar stress by measuring nucleophosmin (NPM1) relocalization. We further compared structural and electronic properties of these compounds based on DFT calculations. We find that phenanthriplatin, but not related quinoplatin or isoquinoplatin, induces nucleolar stress as measured by NPM1 relocalization in human lung carcinoma A549 cells. Although phenanthriplatin has the largest total volume and hydrophobicity of the compounds tested, quinoplatin and isoquinoplatin may have similar potential to disrupt intermolecular interactions based on Pt-ligand distances. We conclude that the unique ability of phenanthriplatin to induce nucleolar stress is conferred by the third

aromatic ring. The ligand disposition of these monofunctional *N*-heterocyclic Pt(II) compounds is sufficiently different from oxaliplatin to suggest that separate properties of oxaliplatin and phenanthriplatin lead to their abilities to both cause nucleolar stress.

Results and Discussion

Oxaliplatin and phenanthriplatin cause NPM1 relocalization

A previous study examining cell death mechanisms of phenanthriplatin (**1**) and oxaliplatin (**2**) has shown that both compounds cause cell death through ribosome biogenesis stress.¹⁸ For the current studies, we monitored NPM1 relocalization from the nucleolus to the nucleoplasm, which is a hallmark of nucleolar stress resulting from the disruption of ribosome biogenesis.⁷⁸ Under non-stressed conditions, NPM1 is localized to the nucleolus; however, NPM1 is distributed throughout the nucleoplasm following nucleolar stress. We set out to measure the extent of NPM1 relocalization when cells were treated with a series of platinum compounds with cyclic ligands and either monofunctional or bifunctional substitution properties.

We first examined NPM1 relocalization following treatment with oxaliplatin and phenanthriplatin. As expected, known ribosome biogenesis stress inducer actinomycin D caused NPM1 relocalization to the nucleoplasm while the negative no-treatment control showed NPM1 localized in the nucleoli (**Figure 3.2a**). Both oxaliplatin and phenanthriplatin caused relocalization of NPM1 throughout the nucleus, confirming their ability to cause nucleolar stress as previously reported.⁵⁸

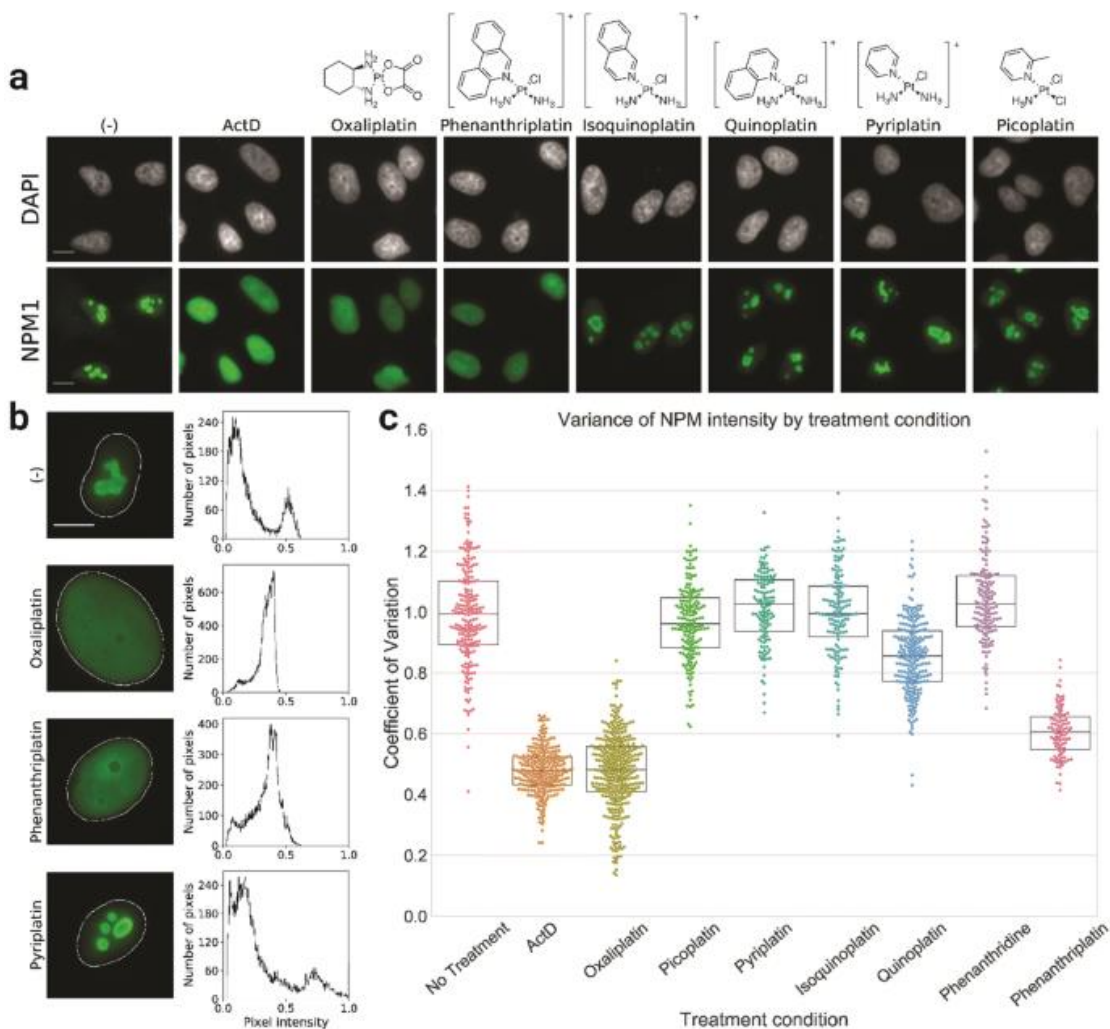


Figure 2.2 NPM1 relocalization. **A** Representative images for each platinum treatment. DAPI (grey) shows the nucleus of A549 cells. NPM1 (green) is evenly distributed in positive control actinomycin D (ActD), and also in cells treated with oxaliplatin, and phenanthriplatin, indicating nucleolar stress. NPM1 is localized to the nucleolus in untreated cells, and cells treated with isoquinoplatin, 27uinoplatin, pyriplatin, and picoplatin. Scale bar is 10 μ m. Cells were treated with 10 μ M platinum at 24 h with the exception of phenanthriplatin and phenanthridine which were used at 0.5 μ M. **b** Representative histograms for individual cells. In untreated negative control and pyriplatin-treated cells, large populations of pixels are found at low and high intensity. NPM1 localization throughout the nucleoplasm is seen following oxaliplatin and phenanthriplatin treatment with pixel intensity centered around 0.4. **c** Coefficient of variation for platinum treatments. CV values for individual nuclei are plotted for each treatment group. Box plot center line represents the median, and the bottom and top limits represent the first and third quartile, respectively. The CV from each cell is normalized to the mean CV from the no-treatment control sample. Populations that have NPM1 relocalized have a median CV of around 0.6 while populations without NPM1 relocalization are around 1

To determine the extent of nucleolar stress, we quantified the heterogeneity of nuclear NPM1 intensity distribution by its coefficient of variation (CV). The CV is the standard deviation of the pixel intensity populations corresponding to NPM1-based immunofluorescence normalized by the mean intensity of each nucleus. In cells that are undergoing nucleolar stress, NPM1 is relatively evenly diffused throughout the nucleus, leading to homogeneous intensities and a small CV. Histograms of representative cells show a large population of medium intensity pixels across the cell for compounds that cause NPM1 relocalization (**Figure 3.2b**). For cells that are not undergoing stress, NPM1 is concentrated in the periphery of the nucleolus while being absent in the nucleoplasm, resulting in a heterogeneous population of pixel intensities and a high CV. Histograms of cell images from compounds that do not cause NPM1 relocalization show large populations at the two extremes of the pixel intensity which would result in a large CV (**Figure 3.2b**). CVs were calculated for each cell in a population and the distribution of these CVs was evaluated for each treatment condition. Corresponding to our representative NPM1 images (**Figure 3.1a**), compounds that caused no NPM1 redistribution had median CVs around 1 (when normalized to the no-treatment control) while compounds that caused NPM1 relocalization had medians at or lower than 0.6 (normalized to the no-treatment control). NPM1 relocalization was observed upon treatment with oxaliplatin, phenanthriplatin and actinomycin D (**Figure 3.2c**). Additionally, treatment with the phenanthridine ligand alone is not sufficient to induce nucleolar stress (**Figure 3.2c**).

Picoplatin does not cause NPM1 relocalization

There are large structural differences between oxaliplatin and phenanthriplatin; however, these disparate compounds are both able to activate nucleolar stress pathways whereas cisplatin does not. Both the DACH ligand of oxaliplatin and the phenanthridine ligand of phenanthriplatin add significant steric bulk in comparison with cisplatin. However, phenanthriplatin is a monofunctional compound. In addition, unlike the case of oxaliplatin, in phenanthriplatin, the phenanthridine rings are oriented perpendicular to the square-planar Pt ligand plane.⁷⁶ Picoplatin (**3**) is one compound that bridges these differences in that the picoline ring is oriented perpendicular to the platinum plane.⁷⁹ Picoplatin is also a classical bifunctional platinum compound and enabled us to determine whether the added ligand bulk regardless of orientation was sufficient to induce NPM1 relocalization. In A549 cells treated with picoplatin, NPM1 did not relocalize to the nucleoplasm (**Figure 3.2a**) as quantified by a median CV of around 1 (**Figure 3.2c**), indicating that picoplatin does not cause nucleolar stress.

NPM1 relocalization is not a general property of monofunctional platinum compounds

After determining that the classical compound picoplatin did not cause NPM1 relocalization despite having some similarities to oxaliplatin in terms of added ring and steric bulk, we next examined the properties of non-classical monofunctional platinum compounds. We synthesized three additional monofunctional compounds that have one or two aromatic rings to test whether nucleolar stress was inherent to ring-containing monofunctional platinum(II) compounds as a whole or whether it was a phenomenon only exhibited by phenanthriplatin.

We had tested picoplatin and determined that the perpendicular orientation of the picoline ligand is not sufficient to cause NPM1 relocalization. To further explore the influence of ligand orientation and the binding mode of platinum, we next tested pyriplatin (**4**). Similar to picoplatin, pyriplatin contains a single aromatic ring. However, unlike picoplatin, pyriplatin has more possible orientations of the aromatic ring due to lack of steric interference involving the methyl of the picoline.⁸⁰ In addition, pyriplatin is more similar to phenanthriplatin in being a monofunctional compound with an overall positive charge. Following a 24 h treatment at 10 μ M, pyriplatin did not cause NPM1 relocalization and samples had a median CV of around 1 (**Figure 3.2**). From this, we concluded that the ability to cause NPM1 relocalization was not inherent to the class of monofunctional platinum(II) compounds containing *N*-heterocyclic ligands.

We next considered whether steric bulk was a factor in NPM1 relocalization by examining the influence of the addition of a second ring. We synthesized the structural isomers quinoplatin (**5**) and isoquinoplatin (**6**) (**Figure 3.3**), to test whether a second aromatic ring would be sufficient to cause NPM1 relocalization. We tested these compounds and determined that neither quinoplatin nor isoquinoplatin caused increased NPM1 relocalization, with NPM1 intensities from cells treated with both compounds having a median CV of around 1 (**Figure 3.2**). From this we concluded that for monofunctional Pt(II) compounds, the steric bulk from a second ring alone does not induce NPM1 relocalization regardless of ring orientation. This added further evidence that NPM1 relocalization was not an inherent property of this non-classical class of platinum compounds and was unique to phenanthriplatin under these conditions.

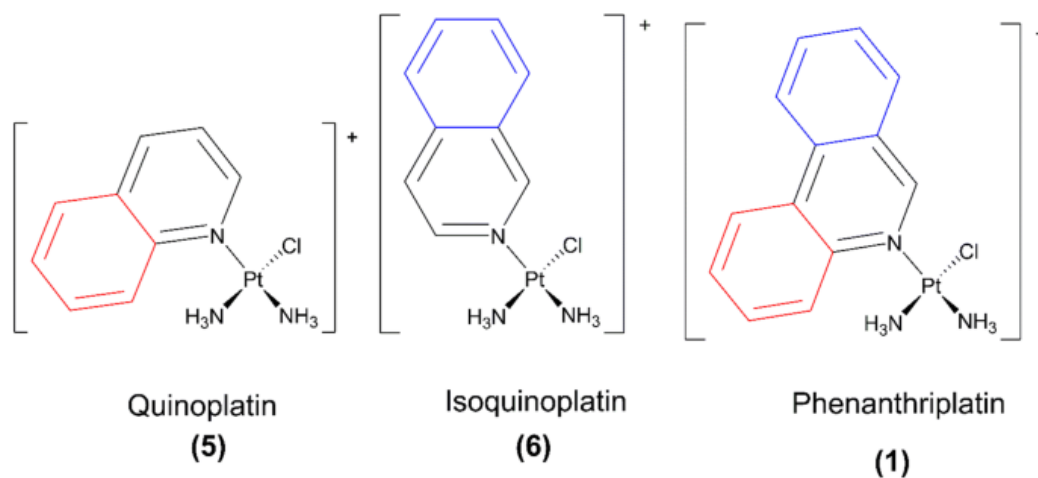


Figure 3.3 Two-ring structural isomers related to phenanthriplatin

Steric bulk is not sufficient to predict NPM1 relocation

From our data, we have determined that phenanthriplatin and oxaliplatin are unique to our suite of compounds. We next examined whether there are any trends present in steric bulk that could explain whether compounds caused NPM1 relocation. All platinum(II) compounds were optimized using DFT (**Figure 3.4**) and two variables were calculated to assess steric bulk. First, the volume of the optimized, non-hydrolyzed structure is obtained by sampling the respective electrostatic potential (Table **3.1**). Oxaliplatin and phenanthriplatin were the compounds with the largest volume; however, this included the aquation-labile ligands which accounts for a large portion of oxaliplatin's volume.

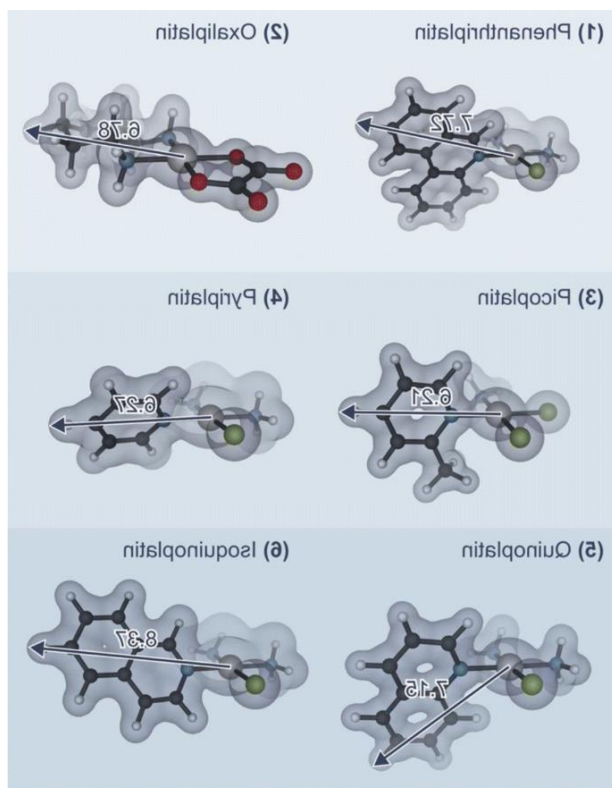


Figure 3.4 Optimized structures of the platinum(II) compounds are displayed at an isosurface level of $0.25 \text{ e}/\text{\AA}^{-3}$ for each compound, as implemented in VESTA. This illustrates the volume of the molecule that is reported. The distances between the platinum atom and the surface of each compound are shown with the corresponding vector. All measurements are reported in angstrom (\AA)

Table 3.1 Steric bulk measurements for platinum compounds in order of increasing volume

Compound	Volume (\AA^3)	Maximum Pt-to-surface distance (\AA)
Pyriplatin (4)	24.91	6.27
Picoplatin (3)	27.69	6.21
Isoquinoplatin (6)	31.21	8.37
Quinoplatin (5)	33.89	7.15
Oxaliplatin (2)	34.13	6.78
Phenanthriplatin (1)	37.25	7.72

Second, the magnitude of the maximum vector between platinum and the surface of the compound, where the surface of the compound is defined as the extent to which the electrostatic potential permeates in space (Table 3.1), was calculated. No trend was found with these distance measurements. Oxaliplatin, which caused NPM1 relocalization, had a similar maximum distance as that of quinoplatin, which did not cause NPM1 relocalization. Additionally, phenanthriplatin, which caused NPM1 relocalization had a similar distance to that of isoquinoplatin which did not cause NPM1 relocalization (Table 3.1). Thus, while phenanthriplatin exhibits the largest steric bulk, it does not have the maximum steric reach from platinum to the surface of the compound.

Hydrophobicity is not sufficient for predicting NPM1 relocalization

Hydrophobicity of the non-labile ligand may be an important factor in interrupting biomolecular interactions, or in partitioning into cellular compartments or regions of the nucleolus. We examined if there was a trend in hydrophobicity that would explain why oxaliplatin and phenanthriplatin caused NPM1 relocalization while all other compounds in our library did not. We used our optimized structures to calculate $\Delta G_{\text{water-octanol}}/\Delta G_{\text{water-octanol}}$ (Table 3.2). As expected, compounds with more aromatic rings were more hydrophobic and had more positive differences in $\Delta G_{\text{water-octanol}}/\Delta G_{\text{water-octanol}}$, while compounds with less rings showed the opposite trend. Phenanthriplatin is more hydrophobic than all other compounds except picoplatin, which does not cause NPM1 relocalization and is the most hydrophobic compound tested with a Gibbs solvation energy of 2.54 kcal/mol. Overall, this measure of hydrophobicity was not able to produce a trend that provides a satisfactory explanation for why oxaliplatin and phenanthriplatin cause NPM1 relocalization while others did not.

Therefore, we conclude that hydrophobicity alone is not sufficient for causing NPM1 relocalization.

Table 2 Gibbs free energy of transfer between octanol and water

Compound	$\Delta G_{\text{water-octanol}}$ (Kcal/mol)
Oxaliplatin (2)	-4.92
Pyriplatin (4)	-1.92
Isoquinoplatin (6)	-0.607
Quinoplatin (5)	-0.34
Phenanthriplatin (1)	0.94
Picoplatin (3)	2.54

Conclusions

This work aimed to find a structural relationship between oxaliplatin and phenanthriplatin which would provide information on necessary and sufficient structural components required for these platinum compounds to induce cell death via nucleolar stress. In comparison with cisplatin, which does not cause nucleolar stress, oxaliplatin and phenanthriplatin both have significantly larger ring-containing ligands.

Phenanthriplatin is also a monofunctional Pt(II) compound. To explore this question, we synthesized a library of ring-containing platinum compounds, most being monofunctional Pt(II) compounds. This library was tested for the ability to induce nucleolar stress by monitoring NPM1 relocalization, and quantifying the resulting images. First, we tested oxaliplatin and phenanthriplatin to confirm that they caused NPM1 relocalization in agreement with previous literature proposing that they cause nucleolar stress.¹⁸ We then tested whether a heterocyclic ligand oriented perpendicular to the square-planar

platinum(II) ligand plane would be sufficient by testing picoplatin, and found that picoplatin did not cause nucleolar stress as measured by NPM1 relocalization. Thus, for bifunctional platinum compounds, a ligand ring is insufficient to cause nucleolar stress.

We investigated the importance of ligand ring number and distribution in other compounds of the monofunctional platinum(II) class by testing pyriplatin, quinoplatin and isoquinoplatin. None of these compounds caused NPM1 relocalization, indicating that phenanthriplatin was unique in this class of monofunctional compounds. We note that this limited study has been performed at a single concentration and treatment time for all compounds. It is possible that longer treatment time or higher concentrations might lead to different effects, and this is being explored in further studies. None of the non-phenanthriplatin compounds cause significant levels nucleolar stress at relatively high (10 μM) treatment concentrations compared to phenanthriplatin (0.5 μM), indicating that they are in a different class than phenanthriplatin in terms of activities.

We performed DFT calculations to optimize structures and calculate the solvent-dependent difference in Gibbs free energy between water and *n*-octanol, a measure of hydrophobicity. To further investigate structural characteristics, we calculated the maximum distance from the platinum atom to the surface of each structure and volume from the DFT-optimized structures. We found no correlation between this distance and the ability to cause NPM1 relocalization. Further, there was no strong correlation between the solvent-dependent difference in Gibbs free energy between water and octanol for compounds that were able to induce NPM1 relocalization.

In view of these results, we suggest that phenanthriplatin is a unique compound in the monofunctional platinum(II) compound class in its ability to cause NPM1

relocalization. We suggest that the addition of a third aromatic ring in phenanthriplatin may play a large role in differentiating phenanthriplatin from other monofunctional platinum(II) compounds we tested for inducing nucleolar stress. The presence of a third aromatic ring increases steric bulk both above and below the square-planar platinum ligand plane. Additionally, a third ring increases hydrophobicity and provides intercalation potential to phenanthriplatin in comparison to quinoplatin and isoquinoplatin.⁷³ Phenanthriplatin exhibited the largest volume and was the most hydrophobic compound of the monofunctional platinum(II) compounds but did not exhibit the longest distance from platinum atom to the edge of the non-labile ligand. Consequently, spatial orientation and/or hydrophobicity caused by the presence of a third aromatic ring may be significant factors in differentiating phenanthriplatin from the rest of its family. Derivatization of phenanthriplatin could further elucidate the structural components of this third aromatic ring that are responsible for causing NPM1 relocalization. We also note that the fast kinetics of DNA binding exhibited by phenanthriplatin may play a role in why phenanthriplatin is unique in the class of monofunctional platinum(II) compounds.⁷³

While oxaliplatin and phenanthriplatin both contain extended ligand structures around platinum(II), we find that steric properties alone are insufficient to explain the shared ability of these compounds to cause nucleolar stress. It is possible that monofunctional and bifunctional platinum(II) compounds may induce NPM1 relocalization through differential binding effects or mechanisms.

Bridge to Chapter IV

In chapter III we explored the structural characteristics of phenanthriplatin that are necessary for this platinum compound to cause nucleolar stress. We found that phenanthriplatin-related compounds containing 2-membered rings did not cause nucleolar stress, indicating that the third ring of the phenanthridine ligand is important for nucleolar stress. We also found that phenanthriplatin and oxaliplatin do not share a structural property that can explain why both cause nucleolar stress. This could indicate that the biomolecular interactions phenanthriplatin and oxaliplatin are involved in are different and that they are causing nucleolar stress through different interactions. In chapter IV we will further examine derivatives of oxaliplatin to determine the tolerance for derivatization at the 3,4 position of the 1,2-diaminocyclohexane ring found on DACH-Pt and oxaliplatin.

CHAPTER IV: STRUCTURE -FUNCTION INVESTIGATION OF THE 4,5 POSITION ON 1,2-DIAMINOCYCLOHEXANE OF OXALIPLATIN

This chapter contains unpublished, co-authored material. This communication was coauthored by Andres S Guerrero and Haley Smith.

Introduction

Platinum chemotherapeutic drugs are included in 10-20% of cancer therapies today.¹ The oldest FDA-approved platinum drug in the United States, cisplatin, has been in use for over 40 years while the newest, oxaliplatin, has been in use for over 20 years.² Oxaliplatin is widely used to treat colorectal cancers and lung cancers while cisplatin is used to treat bladder, testicular, cervical and ovarian cancer.³ Despite their extensive use, significant differences between the mechanism of action of cisplatin and oxaliplatin have only recently been determined.⁴⁻⁶ Oxaliplatin causes cell death via induction of the nucleolar stress pathway, as opposed to the DNA damage response pathway induced by cisplatin. Oxaliplatin and cisplatin have very different structures. Both compounds have two types of ligands, aquation labile and non-labile. The aquation labile ligand of oxaliplatin is oxalic acid while cisplatin has two chloride ions. The non-labile ligand for oxaliplatin is also different than cisplatin. Oxaliplatin's non-labile ligand is 1,2-diaminocyclohexane (DACH) while cisplatin's non-labile ligands are two amines.⁷

The differences in the mechanism of action between these two compounds led us to perform a limited structure-function study to determine which characteristics of oxaliplatin were necessary to cause nucleolar stress.⁴ We found that increase in steric bulk and hydrophobicity of ligands positively correlated with nucleolar stress induction; however, notable exceptions were also found, including examples indicating that ligand orientation was an important factor in why compounds caused nucleolar stress. One

notable example of the importance of ligand orientation was comparison of benzaplatin and APP. Both compounds include a six membered, aromatic ring situated similarly to the DACH ligand of oxaliplatin. In benzaplatin, which causes nucleolar stress, the benzene ring's steric bulk is located in the same orientation as the DACH ligand. For APP, however, the ligand, 2-picolylamine, shifts the direction of the steric bulk of the aromatic ring and this compound does not cause nucleolar stress. This strong dependence on orientation of the non-labile platinum ligand is interesting and could point toward a specific interaction that is being disrupted by these platinum compounds.

We have investigated the compounds previously found to cause nucleolar stress in chapter II further with time-dependent studies.⁸ Pentaplatin, a compound that caused less NPM1 redistribution than other compounds studied, also had a delayed NPM1 relocalization response. This was not caused by lowered platinum uptake compared to other stress inducing compounds. Additionally, pentaplatin is less hydrophobic than APP, a compound that does not cause stress, indicating that there is a more complex interaction occurring that is not explained by bulk chemical characteristics.⁴

Our previous studies have examined derivatives that were similar in steric bulk or smaller than oxaliplatin. In this study we examine structures that increase the size of the DACH ring found on oxaliplatin to probe the specificity requirements of oxaliplatin (**1**). We determine whether larger and more hydrophobic structures cause nucleolar stress and probe 4,5- substitutions in both the axial and equatorial positions of DACH to determine whether stereochemistry of the oxaliplatin ring is a driving factor of nucleolar stress.

Derivatives of Pt(II)-DACH compounds have been studied by introducing various alkyl groups to the 4-position.⁹⁻¹³ These groups included methyl, ethyl, propyl, isopropyl,

and benzene.⁹ Interestingly, methyl and ethyl derivatives show similar IC₅₀ values to oxaliplatin in normal cells, but show lowered IC₅₀ values than oxaliplatin in cell lines that are platinum resistant.^{10,11} Additionally, while installation of methyl and ethyl groups at the 4-position show similar IC₅₀ values to each other, the addition of larger, more hydrophobic groups lowers the toxicity of the platinum compounds significantly indicating that the compound's overall cytotoxic effects are sensitive to changes to the DACH ring.⁹

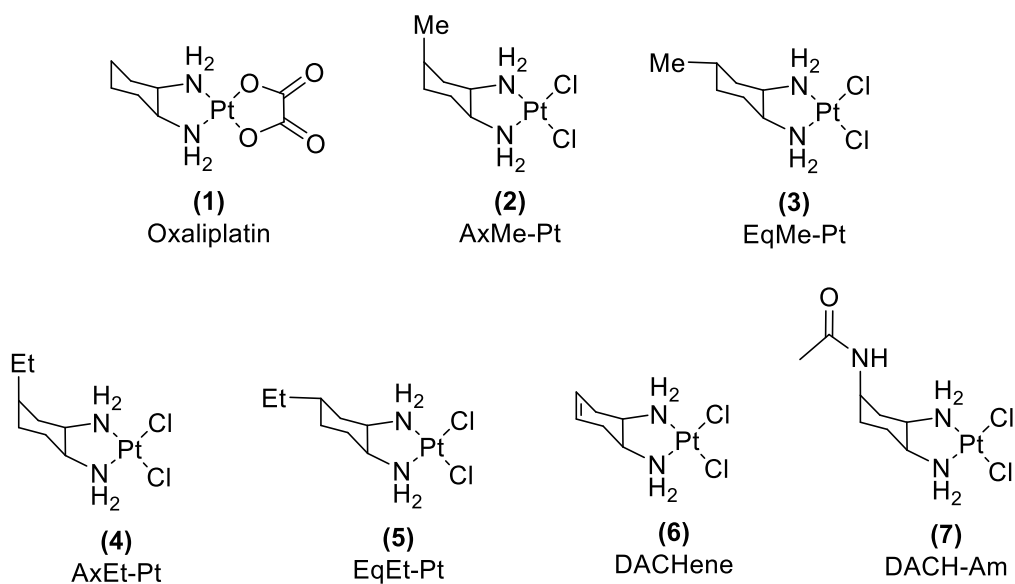


Figure 4.1 Compounds used in this study.

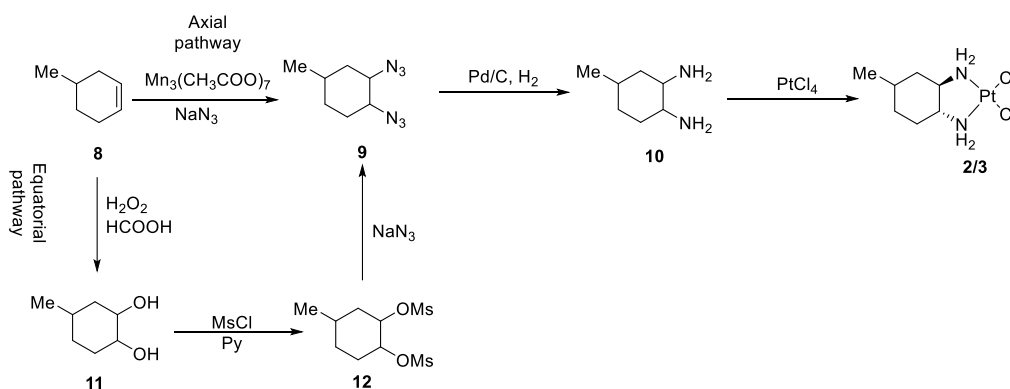
Here we synthesized seven compounds to probe the 4,5 positions on the DACH ligand and how these changes affect whether compounds cause nucleolar stress (**Figure 4.1**). We tested a methyl (**2,3**) and ethyl (**4,5**) group in the axial and equatorial positions. Additionally, we investigate DACHene (**6**), a compound with a double bond at the 4,5 position and DACH-Am (**7**) which includes an acetamide in the axial position. We found that while both methyl derivatives are still able to cause nucleolar stress as marked by NPM1 redistribution, preliminary evidence suggests that the ethyl derivatives no longer

caused nucleolar stress. DACHene (**6**) did cause nucleolar stress while the addition of an acetamide in the axial position as in compound **7** did not cause nucleolar stress. Despite increased steric bulk and hydrophobicity that could further drive non-specific interactions, these limitations suggest an interaction with a much higher specificity and selectivity.

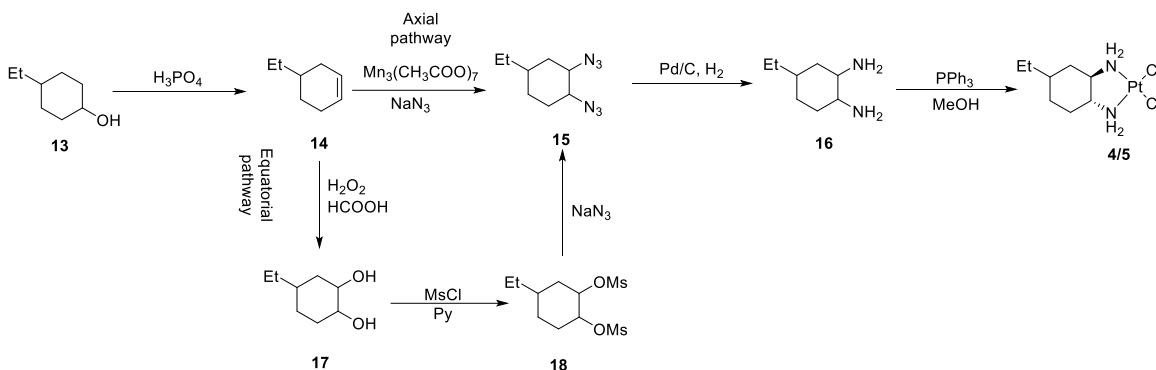
Results

Limited tolerance for substitutions at the DACH 4-position

In order to investigate the effects of modifications to the DACH ring of oxaliplatin we created a small library of derivatives that increased steric bulk at the 4-position in a stepwise manner. These derivatives also explored the increase of steric bulk in both the axial and equatorial positions at carbon 4. Derivatives were synthesized according to previously published procedures starting from either the cyclohexene or alcohol derivatives. The pathways used to synthesize the methyl axial and equatorial derivative is shown in scheme **4.1**.^{10,13} The synthesis of ethyl derivatives is shown in scheme **4.2**.^{12,13} DACH-Am was synthesized according to previously reported methods (and described in chapter V).¹⁴ DACHene was synthesized using general procedures for coordination of platinum compounds (see appendix C).¹⁵



Scheme 4.1 Synthetic schemes used to synthesize the axial and equatorial methyl derivatives used in this study. Axial derivative **2** was created using pathway (8→9→10→2). The equatorial derivative **3** used pathways (8→11→12→10→3).



Scheme 4.2 Synthetic scheme used for ethyl axial and equatorial derivatives. The axial derivative **4** was created using pathway (13→14→15→16→4). The equatorial derivative used pathway (13→14→17→18→15→16→5).

Once compounds were in hand, an NPM1 relocation assay was used to determine whether tested compounds caused nucleolar stress.⁴ Methyl derivatives (**2**, **3**), and DACH-Am (**7**) were dissolved in DMF to form a 5 mM stock solution while ethyl derivative (**4**, **5**) stock solutions were made in DMSO due to limited solubility in DMF. Based on these results, both methyl derivatives caused nucleolar stress. In preliminary trials, neither ethyl derivative caused nucleolar stress (**Figure 4.2**). These preliminary results are complicated by potential effects of the solvent used for the stock solutions, as discussed below. Additionally, we tested the addition of an acetamide in the axial position to further increase the bulk in the 4-position. DACH-Am (**7**), similar to the ethyl derivatives, did not cause nucleolar stress (**Figure 4.3**).

The observation that both methyl derivatives cause NPM1 relocation, but not DACH-Am (**7**), demonstrates a small window of tolerance for substitutions at the 4-position of DACH-Pt derivatives for inducing nucleolar stress. While the addition of a single carbon at the 4-position is tolerated, increasing the steric bulk at this location to a

second carbon caused the derivative may no longer cause nucleolar stress. The effects of the ethyl derivative are discussed in subsequent sections and need to be investigated further. The comparison of the methyl derivatives and DACH-Am derivative could indicate that these compounds are involved in a specific interaction with a biomolecule which could be more sensitive to alkyl groups being added in the axial vs equatorial position.

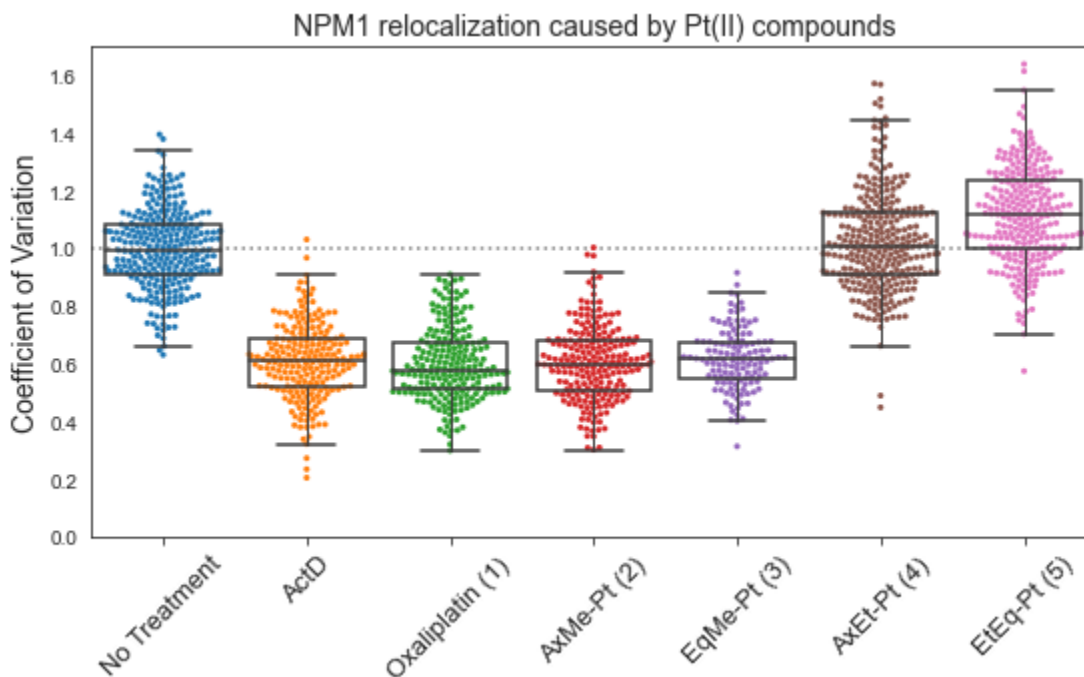


Figure 4.2 NPM1 relocalization of axial and equatorial oxaliplatin derivatives. The CV values for individual nuclei are plotted for each treatment. Center line within the box plot represents the median, and the bottom and top limits are represented the first and third quartiles. Compounds that induce stress show a CV around 0.6 while compounds that do not cause stress show a CV around 1. A549 cells were treated with 10 μ M platinum compound for 24 hours.

Axial vs equatorial substitutions to the DACH ring do not change mechanism of action

When considering the possibility that oxaliplatin is able to block a very specific interaction, we wondered whether there would be different tolerance for substitutions in the axial and equatorial positions.

Both axial and equatorial derivatives were synthesized separately and tested to determine whether they caused nucleolar stress. Compounds were enantiomerically pure by NMR analysis (see appendix C). For the methyl derivatives, both compounds caused nucleolar stress with no differentiation between the axial and equatorial position. Similarly, neither ethyl derivatives (in DMSO) caused nucleolar stress no matter whether the ethyl was in the axial or equatorial position (**Figure 4.2**). Although the small window of tolerance for substitutions at the 4-position previously discussed suggests that nucleolar stress is induced by a specific interaction involving the Pt ligand, the interaction appears to be sensitive to steric bulk but not to disposition.

DMSO may inactivate platinum compound's abilities to cause nucleolar stress

Platinum can coordinate to a variety of atoms including nitrogen, oxygen, and sulfur with sulfur being one of the strongest ligands available for platinum coordination. DMSO is known to coordinate to platinum compounds very quickly and this coordination can be identified via NMR spectroscopy. DMSO is also known to limit side effects but also to deactivate effectiveness of platinum drugs in clinical trials. We wanted to ensure that the lack of nucleolar stress exhibited by both ethyl derivatives was not caused by inactivation due to coordination with DMSO. Since previous studies had shown the identity of the non-labile ligand was not important in causing nucleolar stress we expected the possible DMSO coordination to cause no effect on NPM1 relocalization. We performed the NPM1 relocalization assay on both methyl derivatives as well as DACH-platin (Cis-[1,2-diaminocyclohexane]dichloride platinum(II)) which was first shown to cause nucleolar stress in chapter II.

When these platinum compounds were dissolved in DMSO as opposed to DMF, the compounds no longer caused nucleolar stress to occur (**Figure 4.3**). This indicates that for these compounds, DMSO inhibits the relocalization of NPM1. Interestingly,

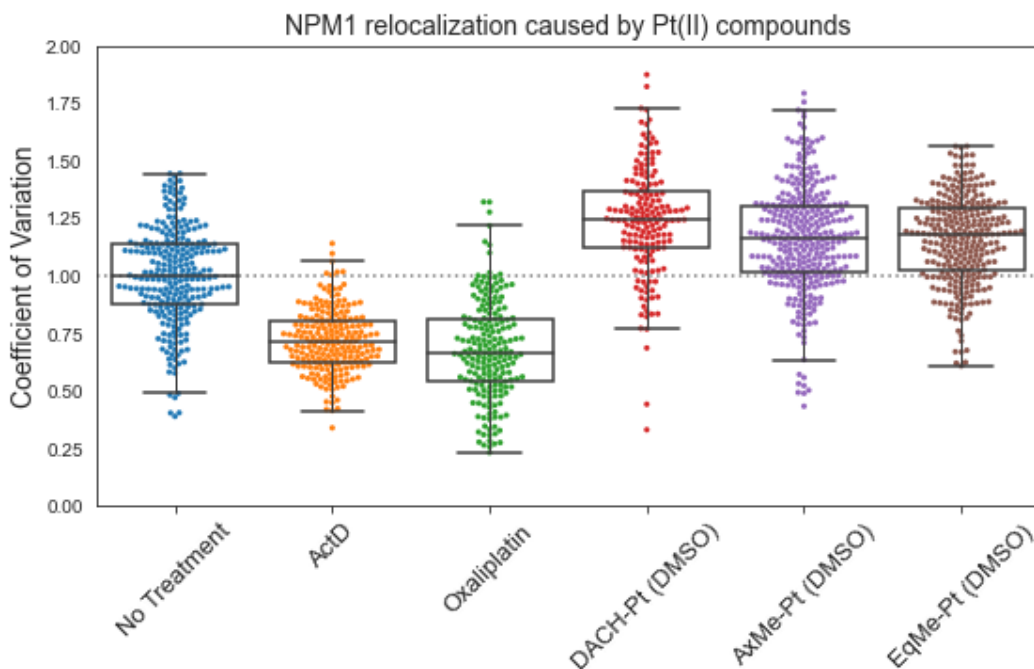


Figure 4.3 NPM1 relocalization of DACH-Pt and Methyl Oxaliplatin Derivatives in DMSO. The CV values for individual nuclei are plotted for each treatment. Center line within the box plot represents the median, and the bottom and top limits are represented the first and third quartiles. Compounds that induce stress show a CV around 0.6 while compounds that do not cause stress show a CV around 1. A549 cells were treated with 10 μ M platinum compound for 24 hours.

DACHene, which is dissolved in DMSO as well, continues to cause nucleolar stress despite likely coordination to DMSO (**Figure 4.3**). This indicates that not all platinum compounds are inhibited by DMSO but that care needs to be taken to ensure that results are not being caused by the introduction of DMSO.

The inhibition of some platinum compounds when coordinated to DMSO could be an indicator of the strength of the coordination at the target biomolecule that is occurring to cause nucleolar stress. Sulfur is one of the strongest ligands available to

coordinate to platinum and the lack of NPM1 redistribution could point towards a weaker coordination event occurring at the biomolecule. The coordination that causes nucleolar stress could involve oxygen or nitrogen ligands, both of which are weaker coordination partners for platinum. It could also indicate that the biomolecular target is coordinating in a mono adduct to the platinum compound which would also be a weaker interaction that might not be able to displace DMSO from the platinum compounds. The identification of DMSO as inhibiting NPM1 redistribution of platinum compounds that otherwise cause robust nucleolar stress, could inform us of the biomolecular coordination that is occurring to cause nucleolar stress.

Installation of a double bond at the 4,5 position is tolerated

In addition to methyl, ethyl, and acetamide derivatives, which increase the size and hydrophobicity of the DACH ligand of oxaliplatin, we also tested eliminating the protons at the 4- and 5-position by introducing a double bond using DACHene (**6**). When this compound was used to treat cells, NPM1 relocalized to the nucleoplasm indicating that the compound caused nucleolar stress (**Figure 4.4**). DACHene (**6**) causing nucleolar stress indicates that the protons at the 4,5-positions are not necessary to cause nucleolar stress and that some changes to this position can be tolerated as long as the steric bulk is not increased too much. To investigate the orientation of the ligand when the protons are not present, we modeled this compound using Avogadro (**Figure 4.5**). The chair conformation found in the DACH ligand is also present in DACHene (**6**), while the protons in 4,5-axial positions are no longer present.

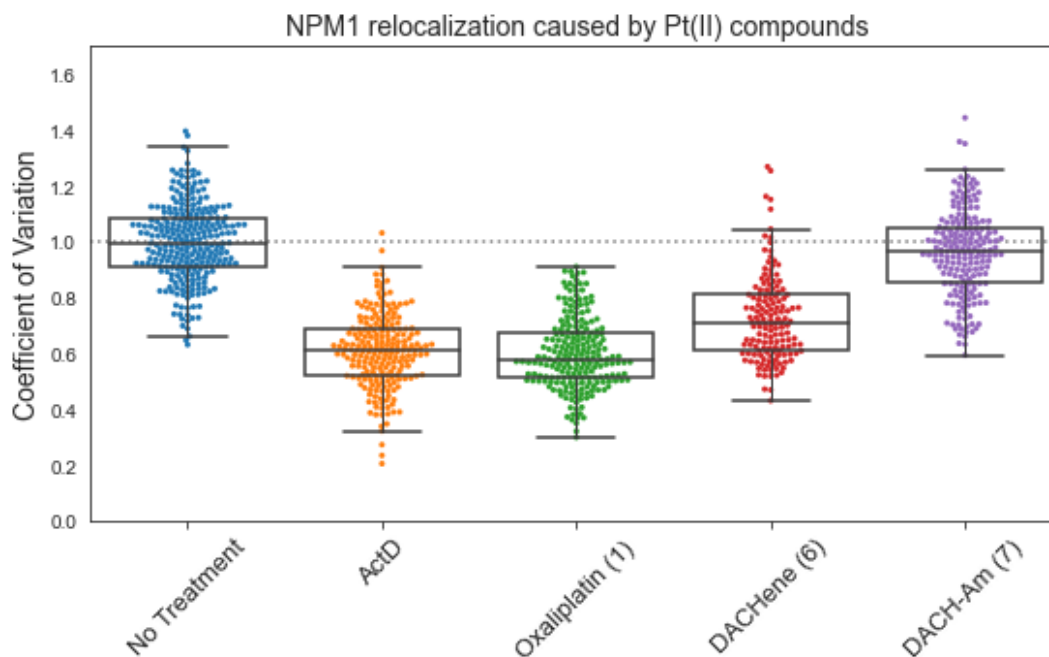


Figure 4.4 NPM1 relocation caused by compounds DACHene (6) and DACH-Am (7) are plotted. The median is represented by the middle line. The top and bottom of the box are the first and third quartiles. The whiskers represent the range of data excluding outliers (the highest and lowest 10% of the sample). Each nuclei is represented as one dot. The compounds that caused NPM1 relocation have a CV around 0.6 while compounds that did not cause stress have a median CV around 1. A549 cells were treated with 10 μ M platinum compound for 24 hours.

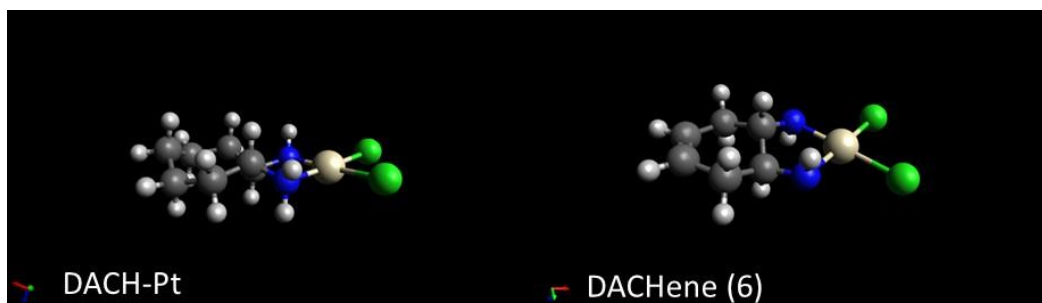


Figure 4.5 Computational model of DACHene (6) showing the location of protons at the double bond.

Changes to hydrophobicity do not explain why compounds no longer cause nucleolar stress

It is possible that oxaliplatin and similar derivatives exert their effects through non-specific hydrophobic interactions with biomolecules. Both the methyl and ethyl

derivatives add hydrophobicity to the ligand along with steric bulk. However, DACH-Am (7) includes an amide bond which is less hydrophobic than the other derivatives. In order to determine the hydrophobicity of DACH-Am (7), we determined a logP value. The preliminary logP value of DACH-Am (7) was found to be -1.03. Previously reported DACH-Pt, which includes the DACH ligand of oxaliplatin and two chloride ligands, had a logP of -0.89 while pentaplatin which contains a 5-membered ring had a logP value of -1.29.⁴ The hydrophobicity of DACH-Am (7), as measured by logP, is between that of stress-inducing compounds penta-Pt and DACH-Pt indicating that hydrophobicity is not a driving factor in why DACH-Am does not cause nucleolar stress.

Discussion

In this work we sought to explore the tolerance for deviation at the 4,5 position on oxaliplatin for inducing nucleolar stress. We synthesized and tested the addition of a methyl or ethyl at the 4-position of the DACH ligand (compounds 2, 3, 4, and 5). We also tested compound 7, which has an acetamide in the axial position, to test the effects steric bulk in the 4-position while changing the hydrophobicity of the ligand. Additionally, we probed the elimination of protons at the 4,5-position of oxaliplatin through incorporation of a double bond (6). We used an NPM1 redistribution assay to determine whether compounds caused nucleolar stress in A549 cells when treated with 10 μ M platinum at 24 hours.

Our results showed that while the addition of a methyl was tolerated, the addition of an acetamide in the axial position no longer caused nucleolar stress. It is possible that the ethyl derivatives also may not cause nucleolar stress, but this needs to be investigated further. This, along with our previous work, illuminates a very small window of

derivatives that cause nucleolar stress and highlights the unique structural requirements that oxaliplatin satisfies in order to cause a different mechanism of action than cisplatin.

The inhibition of some platinum compounds (both methyl derivatives and DACH-platin) by the coordination of DMSO also indicates some properties of the site where the coordination is occurring. DMSO coordinates through the sulfur atom which is a strong coordination partner to platinum. The inhibition of NPM1 relocalization when some compounds are coordinated to DMSO could indicate that the coordination is weaker than coordinating through a sulfur. It could mean that the coordination is through a nitrogen or oxygen, both of which are weaker ligands for platinum or it could indicate that there is a monoadduct forming which might not be able to displace DMSO.

The chair conformation of the DACH ligand of oxaliplatin provides interesting positioning of functional groups that remain rigid after coordination to the platinum atom. The observation that the ability to cause nucleolar stress appears to be insensitive to changes in both the axial and equatorial positions points towards similar constraints at both locations. If both ethyl derivatives do not cause stress when not in the presence of DMSO, one possibility could be the presence of steric interactions with another biomolecule that surrounds the 4-position. If the ethyl derivatives are shown to cause nucleolar stress when not in the presence of DMSO, the steric interaction may be further from the platinum atom but still surrounding the 4- position because DACH-Am (**7**) does not cause nucleolar stress. The specific spatial arrangement of the axial and equatorial positions on these compounds is further discussed in Chapter VI.

This could indicate that the interaction involving platinum-bound biomolecules following oxaliplatin treatment that induces nucleolar stress is relatively rigid, and the

interaction is only able to accommodate minor changes to the DACH ligand. One possible mechanism could be similar to a lock and key type mechanism for a nucleolar stress-inducing interaction in which the DACH ligand of oxaliplatin is uniquely situated as the “best fit” and where smaller ligands, such as 1,2-diaminocyclopentane found in pentaplatin which shows delayed and diminished NPM1 relocalization, and larger ligands, such as DACH-Am (**7**) discussed here, are no longer able to function similarly and their binding results in diminished nucleolar stress response.⁸

Although initial interaction between oxaliplatin and the derivatives presented here could be specific, more work is needed to determine whether non-specific activity is important to the process of nucleolar stress caused by platinum compounds. It is possible that initial inhibition of rRNA transcription, demonstrated with previously reported nucleolar stress inducing compounds^{5,8}, could lead to changes in the nucleolar structure allowing non-specific, hydrophobic interactions between the DACH ring of oxaliplatin and previously inaccessible compartments of the nucleolus leading to more widespread changes to the nucleolus. One observation that could indicate a more widespread effect on the nucleolus after the initial specific disruption is the change in nucleolar morphology from eccentrically shaped nucleoli to round structures when NPM1 is relocalized. The change in morphology has been noted by many previous studies, yet the source of the change is currently unknown.^{4,6,17}

Here we present a more stringent set of structural requirements required for oxaliplatin derivatives to cause nucleolar stress and potential insight into how these compounds could be causing stress. More research is needed to determine the exact mechanism and biomolecule target by which platinum induces nucleolar stress, including

both initial effects of platinum binding as well as the results of such disruption. This understanding can help to better hone a new generation of platinum compounds that exploit the nucleolar stress pathway.

Bridge to chapter V

In chapter IV we explored the window of tolerance of the 1,2-diaminocyclohexane ring found on oxaliplatin. We found that there is very little tolerance for changes at the 4,5 position. The specific requirements at the 4,5 position along with additional requirements discussed in chapter II indicate that the interaction between oxaliplatin and a biomolecule has very high specificity. We are now aware of the structural requirements of oxaliplatin needed to cause nucleolar stress. In chapter V I will discuss work towards the synthesis of two click capable platinum compounds, one that would be compatible with live cell imaging and another that mimics the oxaliplatin structure. The compound that mimics the oxaliplatin structure could be used to isolate and determine the identity of the biomolecules that are involved in the specific interaction with oxaliplatin.

CHAPTER V: SYNTHESIS OF A CLICK CAPABLE PLATINUM DERIVATIVES

Introduction

Bioorthogonal chemistry and click chemistry have been utilized to study specific targets within cells. Compounds designed for studies inside cells provide a myriad of chemical challenges. These reagents must react quickly and selectively with only their partner inside a cellular environment rich in reactive functional groups.⁹³ One bioorthogonal reaction in particular, the copper-catalyzed azide-alkyne cycloaddition (CuAAC) reaction, has been introduced for application to cisplatin derivatives.^{33,81} These derivatives allow researchers to track localization of Pt(II) compounds as well as purify their targets.

The CuAAC reaction is one of many bioorthogonal reactions. These must take advantage of unnaturally occurring functional groups that react selectively and quickly with their reacting partner.⁹⁴ In traditional bioorthogonal studies, one partner is incorporated into a known biomolecule of interest through a metabolic pathway such as a modified sugar, amino acid or through introduction of DNA and RNA nucleotides. The biomolecule of interest is then tagged and can be tracked through a cell through the introduction of the reacting partner which will only interact with the moiety introduced on the modified biomolecule. This can be a fluorophore or moieties for a pulldown system such as biotin.

The strategy employed by the DeRose lab differs from traditional bioorthogonal studies in that a modified Pt(II) compound is used as the targeting moiety and the target of interest is unknown (Figure 5.1). The strategy allows us to answer more general questions related to what biomolecules interact with Pt(II) compounds. Once the Pt(II)

reagent has reacted with its targeted biomolecules in the cell, the CuAAC moiety is used to selectively react with reporting compounds to image the localization of the Pt(II) compound or purify its targets for identification and further study.

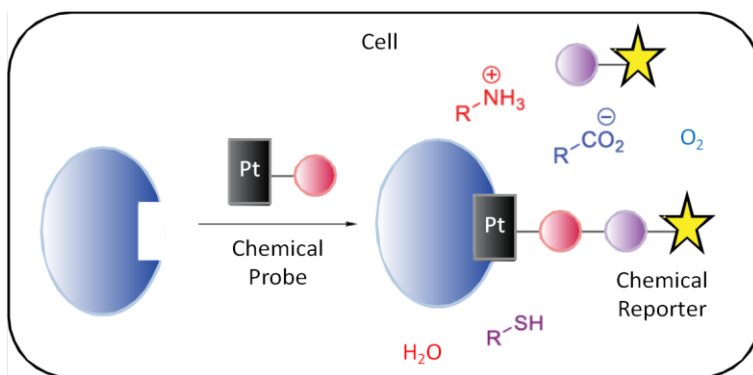


Figure 5.1 Platinum compound incorporation into biomolecules and subsequent click reactions

Previously, the DeRose lab has created multiple cisplatin-like molecules with incorporated CuAAC moieties (**Figure 5.2**). These compounds include a short or long chain linkage to azide or alkyne substituents^{33,95} and have been used to demonstrate interaction of the cisplatin derivatives with various proteins in the endoplasmic reticulum (ER) as well as interactions with DNA, RNA and localization to the nucleolus. The CuAAC reaction requires catalytic Cu(I) to be present in the solution, however, which is cytotoxic to cells. In vivo studies, as well as in vitro and ex vivo, use an excess of copper reagent as opposed to a catalytic amount. This is a significant challenge for *in vivo*

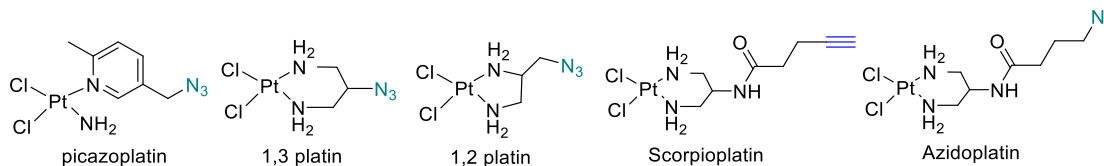


Figure 5.2 CuAAC platinum derivatives created by the DeRose lab

studies, which require the cells to be viable through all treatment conditions. A lowered copper concentration can be used for live cell imaging using CuAAC reactions. The reaction proceeds much slower at lower copper concentrations. Under excess copper conditions, the reaction rate is dependent on the azide and alkyne concentrations; however, under catalytic conditions, the reaction rate becomes dependent on the concentration of copper present in the solution. Thus, under low copper concentrations, the copper catalyst becomes the rate limiting reagent leading to lowered reaction rates under conditions used for live cell imaging.⁹⁶ In addition, copper has been proposed to localize alkyne-substituted fluorophores to the nucleolus.⁹⁷ Recent studies have brought up concerns with biased imaging with G quadruplexes when using the CuAAC reaction in fluorescent imaging.⁹⁷ With concerns from other research as well as our desire to explore live cell imaging, it is worthwhile to explore the incorporation of alternative bioorthogonal moieties in our Pt(II) compounds that do not require a copper catalyst.

Second generation click-capable platinum compounds for live cell imaging

Many different bioorthogonal reagents are available that react selectively and quickly within a cellular environment, and each reaction exhibits strengths and weaknesses. CuAAC is the fastest of the click reactions but requires a copper catalyst, the limitations of which have been outlined above.⁹⁸ One of the first reagents to be used for click chemistry was the traceless Staudinger reagent.⁹⁹ This reagent used a modified triphenyl phosphine reacting with an azide. The reaction transfers a fluorophore or other moiety from the triphenyl phosphine to the biomolecule that initially included an azide. This reaction is considerably slower than other bioorthogonal reactions discovered later and requires permeabilization for the triphenyl phosphine reagent to be introduced into

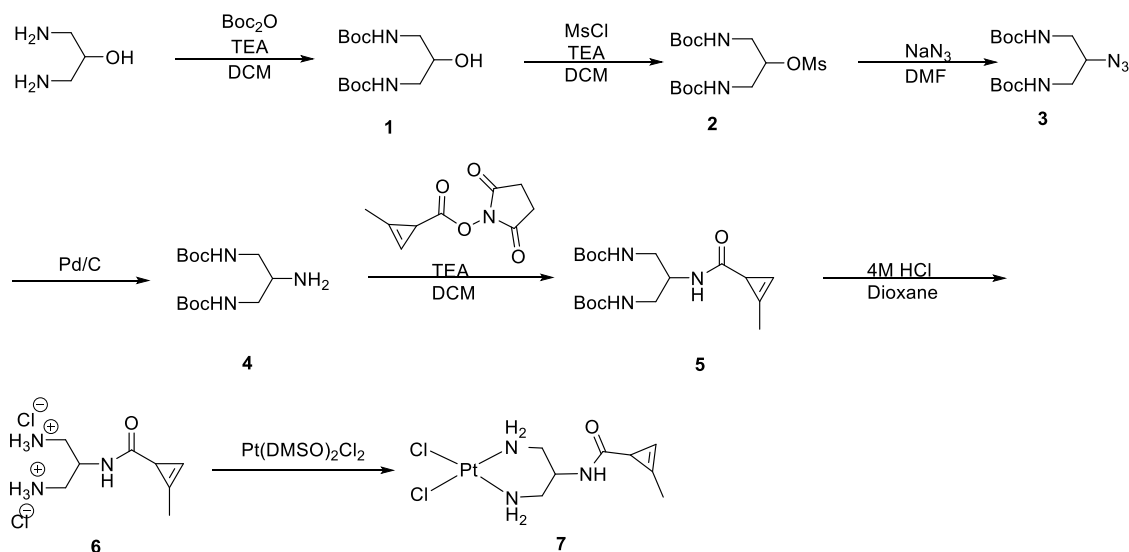
cells. Another common bioorthogonal reaction is the cycloaddition of strained cyclooctynes with azides.¹⁰⁰ This reaction does not require a copper catalyst, so it can be used in live cell imaging but has five-fold slower kinetics compared to a CuAAC. The cyclooctynes are in general large hydrophobic molecules with limited water solubility. Their large size can also interfere with some cellular mechanisms which require the recognition of the unmodified parent compound. The most popular alternative to CuAAC reactions uses a trans-cyclooctene.¹⁰¹ This reaction is the fastest bioorthogonal reaction available and trans-cyclooctene derivatives are commercially available to incorporate into parent molecules. However, these reagents need to be handled carefully and away from light to ensure that the reagent does not isomerize to the less reactive cis isomer. Additionally, while the cyclooctene is smaller than other reagents, it is still much larger than azides and alkynes.

An alternative—cyclopropenes—are small in size, and react slower than CuAAC but significantly faster than strained cyclooctynes.^{94,102} Cyclopropenes take advantage of the large amount of strain found in their three-membered ring (54 kcal/mol) and react with a derivatized tetrazine.¹⁰³

Our already synthesized CuAAC-enabled platinum compounds provide a convenient synthetic route to the inclusion of a cyclopropene moiety rather than an azide. In addition, the small size of the cyclopropene should limit effects from modifying the platinum scaffold. Conveniently, the proposed synthetic schemes for cyclopropene-modified platinum compounds use many steps already well documented in the DeRose lab.⁹⁵ The synthesis of azidoplatin includes a free amine intermediate and subsequent

amide ligation to the azide substituent. The formation of an amide bond to desired functional groups can be modified to incorporate an amide-linked cyclopropene.

To test the properties of a cyclopropene-Pt(II) derivative **7**, an initial synthetic route started with 1,3-platin (**1**). Synthesis of that ligand concludes with installation of an azide at the 2- position. We initially sought to harness the amine derivative to form an amide bond to a cyclopropene, followed by coordination to Pt(II) (Scheme **5.1**).



Scheme 5.1 Synthetic scheme 1 to create a cyclopropene Pt(II) derivative.

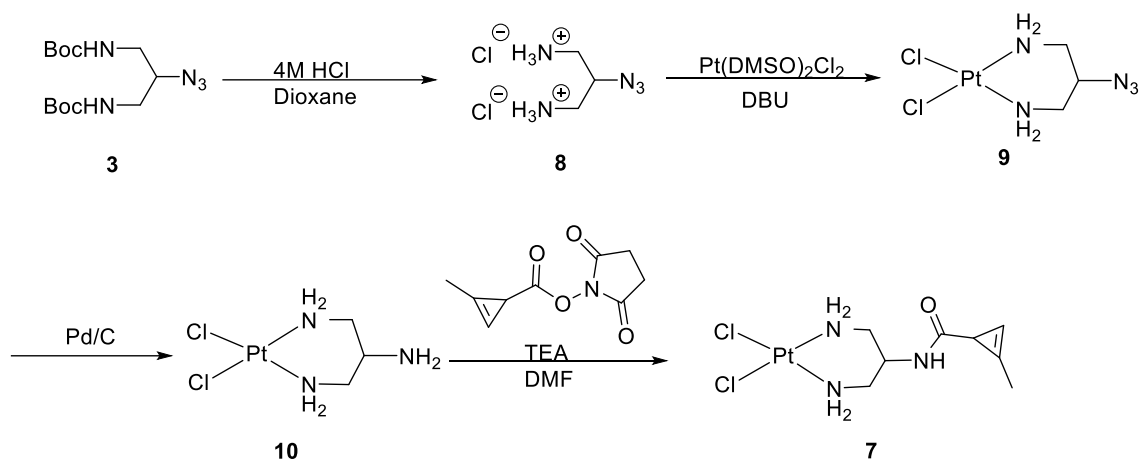
Scheme **5.1** follows a similar synthesis as that used to form 1,3-platin and azidoplatin.^{46,95} Following scheme **5.1** 1,3-diamino 2-propanol is reacted with di-tert-butyl carbonate to form the boc-protected compound **1**. This compound is converted from the alcohol to a methanesulfonyl group by reacting with methanesulfonyl chloride and triethylamine. The methanesulfonyl group on compound **2** is then displaced by azide using a substitution reaction with sodium azide to form compound **3**. Compound **4** is formed by converting the azide to an amine using Pd/C and hydrogen. This product is

then reacted with NHS ester cyclopropene and triethyl amine to form an amide bond (compound **5**) and separated using an extraction. The NHS-ester is used to form the amide bond because of the ease of separating biproducts of the reaction. NHS-esters can be cleaved by the addition of acid and both products from the reaction are water soluble. This allows the biproducts of an amide bond formed using an NHS-ester to be separated using an extraction with water. The ligand (compound **5**) is then deprotected by reaction with 4M HCl in dioxane and coordinated to Pt(DMSO)₂Cl₂ to form the final compound **7**.

Cyclopropenes are known to be sensitive to acid; however, carbon NMR deprotected compound **6** before coordination showed the presence of the double bond of cyclopropene. However, following coordination to Pt(II) using tetrachloroplatinate(II), these cyclopropene-associated carbon NMR peaks at 114 ppm and 97 ppm were no longer present (see appendix D). It was unclear what reaction was happening at the electron-rich double bond. It is possible that a ring-opening occurred and a normal double bond was present or that the double bond was converted into a cyclopropane. Certain platinum species are known to ring-open cyclopropenes.¹⁰⁴ Additionally, Pt(II) can react with very electron rich groups to transition between ionization states. After determining that the reaction conditions were degrading or reacting with the cyclopropene, we replaced tetrachloroplatinate with Pt(DMSO)₂Cl₂ which is generally used to ensure that additions to the platinum are in the cis conformation as the DMSO ligands are preferentially displaced. This, however, did not change the reactivity of cyclopropene with platinum under these reaction conditions.

Due to the presumed reactivity of the cyclopropene on the ligand with platinum in the solution, we decided to attempt an alternative route (scheme **5.2**) that pre-coordinated

Pt(II) to a chelating diamine before installation of the cyclopropene. In order to perform initial tests we allowed 1,3-platin and our ligand and DBU to interact for multiple days in solution. After a few days we dried the solution and resuspended in deuterated DMF. NMR analysis showed the presence of the characteristic strained double bond of the cyclopropene at 114 ppm and 97 ppm indicating that at least some of the cyclopropene was still present. This preliminary evidence indicated that coordinating platinum to a chelating diamino ligand would stop the platinum from interacting with the double bond of the cyclopropene.



Scheme 5.2 Synthetic scheme 2 to create a cyclopropene Pt(II) derivative.

We took advantage of the stability of cyclopropene to pre-coordinated diamino ligands in scheme **5.2**. The formation of 1,3-platin has been previously described.^{33,46} Following scheme **5.2** boc-protected compound **3** is deprotected by reaction with 4M HCl in dioxane. To ensure successful coordination, the deprotected ligand **8** is dried thoroughly in vacuo and tested for acidity. The ligand **8** is then coordinated to platinum by reaction with Pt(DMSO)₂Cl₂ and DBU to produce a yellow solid which is separated through filtration or pelleting the solid using a centrifuge. The azide of 1,3-platin (compound **9**) is

converted to an amine through a hydrogenation reaction with Pd/C and hydrogen. Compound **10** is reacted with NHS-ester cyclopropene to form the final amide bond between cyclopropene and the platinum compound (compound **7**). Purification of this compound is ongoing.

As proof of concept we used the crude mixture to confirm the presence of Pt(II)-tethered cyclopropene and subsequent ability to perform click ligation to a tetrazine-modified fluorophore. We first reacted the crude mixture of **7** with a DNA hairpin containing one GG basepair for 24 hours at room temperature. The DNA was then purified using a G20 column and reacted with tetrazine rhodamine without further purification. The resulting dPAGE analysis showed bands indicating DNA that is both shifted to lower mobility and exhibits fluorescence (shown in pink, **Figure 5.3**). Bands for DNA containing both one and two Pt(II)-fluorophore

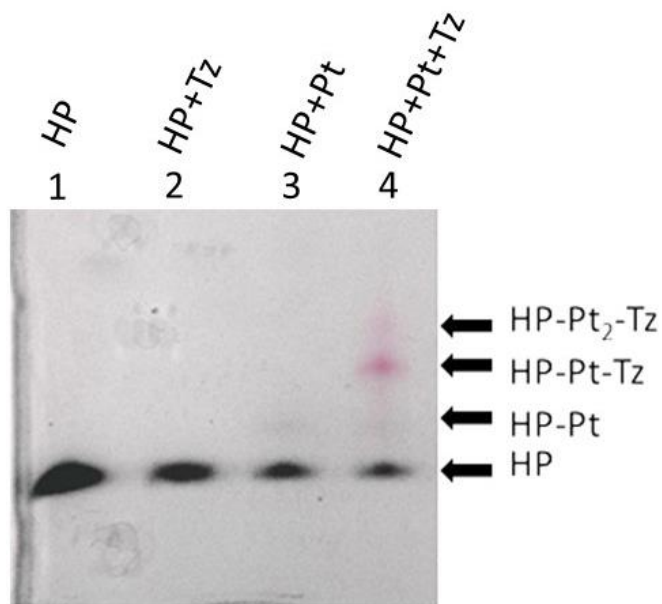


Figure 5.3 dPAGE analysis of Pt(II)-cyclopropene derivative bound to DNA. The crude mixture of **7** was used to platinate a small hairpin DNA (HP) then incubated with tetrazine rhodamine. Rhodamine fluorescence imaging can be seen in pink. DNA was Coomassie stained (black).

conjugate are shown, consistent with previous results.⁴⁷ These results demonstrate that the desired Pt(II)-cyclopropene compound was present in our crude mixture and able to undergo click ligation to tetrazine fluorophores following coordination to DNA. After purification of the compound is complete, this compound should be able to be used for live cell imaging and for comparison with its azide-containing derivative.

Synthesis and characterization of click capable oxaliplatin mimic

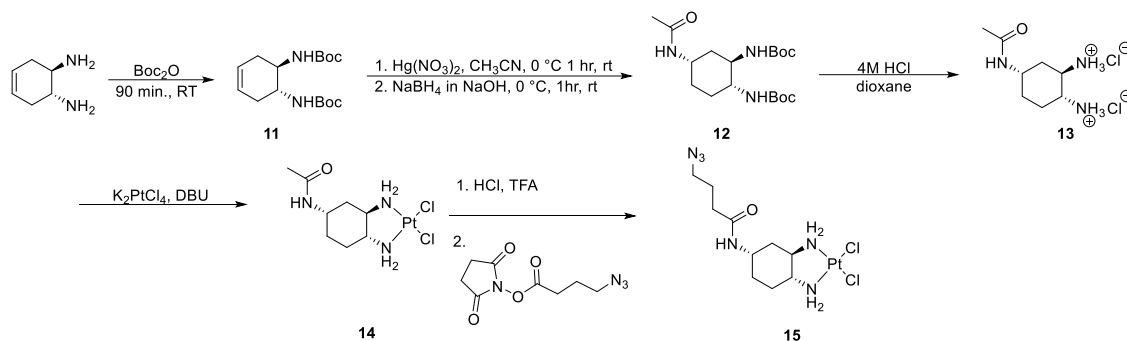
In previous chapters, we investigated the structural components of platinum compounds that were required to cause nucleolar stress.^{82,105} In these studies, we uncovered a series of structural requirements that indicate that a specific interaction may be influenced by oxaliplatin and other stress inducing compounds. Determination of the structural characteristics necessary to cause nucleolar stress can indicate a certain type of mechanism; however, it cannot identify what biomolecule is interacting with platinum to cause nucleolar stress. We have investigated some pathways which could be responsible for causing nucleolar stress using biochemical and biological methods and uncovered that our stress inducing compounds all affect the transcription of rRNA.^{83,85} This is a promising lead since inhibition of RNA polymerase I (Pol I) can lead to transcription inhibition. These methods, however, cannot be used to track whether the platinum could be interacting with rDNA and causing the inhibition of Pol I or if it could be directly interacting with Pol I itself. Similar limitations with other techniques exist because we are not able to probe the platinum compounds directly after binding within the cell.

A helpful addition to the repertoire of techniques already established and used would be a platinum compound that mimics the structure of oxaliplatin and that includes

an azide. The incorporation of an azide to the oxaliplatin (or DACH-Pt) scaffold would allow for further identification of platinum targets in cells that influence nucleolar stress. This derivatized compound would be required to not only have a similar structure to oxaliplatin but also cause the same mechanism of action in cells. Chapter IV described the limitations of modifying the 4- and 5- positions of DACH. This limits the locations on the scaffold that could be used to synthesize an azide-containing oxaliplatin derivative; however a mimic that shared similar structural characteristics could help distinguish effects from overall targeting differences vs effects due to a different mechanism of action. The DeRose lab has used azide-containing cisplatin mimics (1,3 platin, scorpioplatin, and azidoplatin) to investigate off-target effects that did not directly contribute to the mechanism of action for cisplatin.^{106,107} An oxaliplatin mimic that does not cause nucleolar stress could prove useful in this kind of investigation as well. While investigations of the DACH scaffold are ongoing and suitable modification at a position that still causes nucleolar stress has not been determined, an oxaliplatin-like scaffold would increase the toolbox available for investigating the overall effects of oxaliplatin on cells.

To this end we sought to create an oxaliplatin mimic that contained the DACH ligand that was modified with an azide-containing group. Kalayda and coworkers reported an oxaliplatin mimic which was tethered to a fluorophore through an amide linkage.³⁸ We thought we could use the synthetic method published by Kalayda and coworkers to create an amide bond to 4-azidobutyric acid. In this synthesis, the amide bond is always formed in the axial position. We were able to use the synthetic procedure

to synthesize intermediate **14** (DACH-Am) which we tested previously in chapter IV and found that the acetamide derivative did not cause a nucleolar stress response.



Scheme 5.3 Oxaliplatin mimic synthetic scheme.

Scheme **5.3** closely follows synthesis by Kalayda and coworkers.³⁸ Following scheme **5.3**, 1,2-diaminocyclohexene is reacted with di-tert-butyl carbonate to form the boc-protected compound **11**. The double bond of compound **11** is then reacted with $\text{Hg}(\text{NO}_3)_2$ in a solvo-mercuration reaction followed by displacement of mercury by reduction with NaBH_4 to form elemental mercury. Compound **12** is separated by extraction followed by column chromatography (20:1 DCM:methanol). The ligand is then deprotected by reaction with 4M HCl in dioxane to form compound **13** which is then coordinated to platinum using tetrachloroplatinate and DBU. This platinum compound intermediate then undergoes acid-catalyzed hydrolysis of the acetamide to form an amine. This is followed by introduction of the NHS ester of 4-azido butanoic acid to form compound **15**. The purification of this compound is ongoing; however, good separation between two products can be achieved using silica and water as the mobile phase.

Although we do not expect this derivative **15** to mimic oxaliplatin or other nucleolar stress-inducing compounds because the acetamide intermediate **14** does not cause nucleolar stress, it can still be used to study off-target effects of oxaliplatin and

compare the effects of targeting based off the changes in ligands between cisplatin and oxaliplatin. Our lab has used our cisplatin mimics to identify new proteins that were previously unknown to interact with platinum.¹⁰⁶ These cisplatin mimics could be used to compare to the biomolecules identified using the oxaliplatin mimic. Additionally, tagging the oxaliplatin mimic with a fluorophore could show differential localization of the oxaliplatin mimic compared to our cisplatin mimics that could further understandings about how oxaliplatin's ligand is important to its activity.¹⁰⁸ This could also give insight into why oxaliplatin exhibits different side effects than cisplatin an ongoing and unexplained phenomenon of these FDA approved drugs. The off-target effects are thought to be one possible reason for side effect profiles of the different chemotherapy drugs.⁶

An alternative oxaliplatin mimic than what is described here will be necessary to directly measure the activity of oxaliplatin that causes nucleolar stress. Instead, the derivative described here could work in conjunction with a nucleolar stress-inducing compound to differentiate biomolecules that are affected because of the change in ligand to the DACH ring and the specific interactions that might be causing nucleolar stress.

Bridge to Chapter VI

Chapter V described the work towards synthesizing new platinum compounds that included bioorthogonal groups which could be used to directly investigate the platinum compound targets. These click-capable compounds can help to provide targets that are interacting with platinum and explain what might be occurring in cells. One compound included a new bioorthogonal group, a cyclopropene, which has not been incorporated into platinum compounds for use in a click reaction before. This derivative can be used

for live cell imaging which provides opportunities to study the changes in platinum localization throughout a cell cycle.

The other derivative described was an oxaliplatin mimic which could be used in conjunction with cisplatin mimics already previously synthesized. An oxaliplatin mimic could help to illuminate differential binding caused by the DACH ring found on oxaliplatin. Although measurements with an intermediate suggest that our initial proposed oxaliplatin mimic may not induce nucleolar stress, it may still give insight into off-target effects of oxaliplatin. Chapter VI includes computational studies of the nucleolar stress inducing compounds that could explain why some structures cause nucleolar stress while others do not. We investigate potential interactions with NPM1 that could cause nucleolar stress. The oxaliplatin mimic described could provide potential targets for computational work while modeling could provide a molecular level explanation for why platinum causes nucleolar stress once targets of oxaliplatin are identified.

CHAPTER VI: MODELING AND VISUALIZING STRESS-INDUCING PLATINUM COMPOUNDS

Introduction

In previous chapters, the structural requirements of platinum compounds have been explored in order to determine characteristics that are required for compounds to cause nucleolar stress. The results described in chapters II, III, and IV show that seemingly small changes to non-labile Pt(II) ligands result in large differences in their ability to cause nucleolar stress.^{82,85,105} This suggests that a specific interaction is being affected by the coordinating platinum. Results from Sutton and DeRose suggest that RNA Pol I synthesis of rRNA from rDNA is inhibited in early stages of nucleolar stress induction by Pt(II) compounds.⁸³ The inhibition of Pol I transcription is also present with other stress inducing compounds described in previous chapters.⁸⁵ This work suggests that this process could be a cause of nucleolar stress caused by platinum compounds. Alternatively, the nucleolar protein NPM1 is a potential direct target of Pt(II) compounds that could also cause nucleolar stress. NPM1 interacts with DNA and RNA in the nucleolus. In a study of nucleolar stress induction by oxidative stress, Yang and coworkers found that a reactive cysteine in NPM1 (cysteine 275) is ubiquitinated.⁷⁸ Modifications at cysteine 275 causes NPM1 to relocate into the nucleoplasm regardless of whether there are stress-inducing conditions present.

While efforts to identify the target of platinum compounds that could be causing this differential mechanism of action compared to cisplatin are ongoing, investigating the way in which the different derivatives behave at molecular interfaces can be illuminating. In this chapter we explore two potential binding partners, DNA and NPM1, that could

bind with platinum to cause nucleolar stress. We investigate the coordination of our platinum compounds at two adjacent guanines on a DNA oligonucleotide which exemplifies a bidentate adduct to a nucleic acid. Additionally, we use the C-terminus of NPM1 as a model for a monoadduct at a cysteine present on a protein. The different models help to explore possible influences of different ligands on stress inducing and non-stress inducing Pt(II) compounds on biomolecular interactions.

Modeling platinum compounds binding to DNA

Previous studies have found that cisplatin and oxaliplatin preferentially bind to the N7 of guanine. Pt(II)-amine compounds preferentially form diadducts with adjacent guanines due to the ability to form a hydrogen bond between the -NH₂ protons and the 5' guanine carbonyl. Due to the selectivity of platinum at this binding position, we began modeling our compounds on a double strand of DNA using previously published NMR structures of oxaliplatin binding to a 24-nucleotide double-stranded DNA (pdb id: 1PG9).¹⁰⁹ We wished to compare the different structures in order to explore possible molecular bases for their different effects at biomolecular interfaces.

Avogadro was used to model compounds. Crystal structures were used as the starting point for modeling. Neither DNA nor platinum were held constant but the oligonucleotide had minimal structure changes during the simulation due to being in an already low energy conformation in the crystal structure as the starting point. Structures were optimized using UFF force field following the steepest descent until dE measured under 0.01.¹¹⁰ This method does not identify or take into account hydrogen bonding or other factors outside of bond length, angle, and steric clashes; however, these structures could be used for further optimization using density functional theory to elucidate these

types of interactions using previously described methods as in chapter II. To ensure planar ligand geometry around Pt(II), the structures were corrected if needed and optimized a second time. The visualizations were created in Pymol version 2.4.¹¹¹ The difference in binding between cisplatin and oxaliplatin at two adjacent guanines in a double stranded helix can be seen in **Figure 6.1**

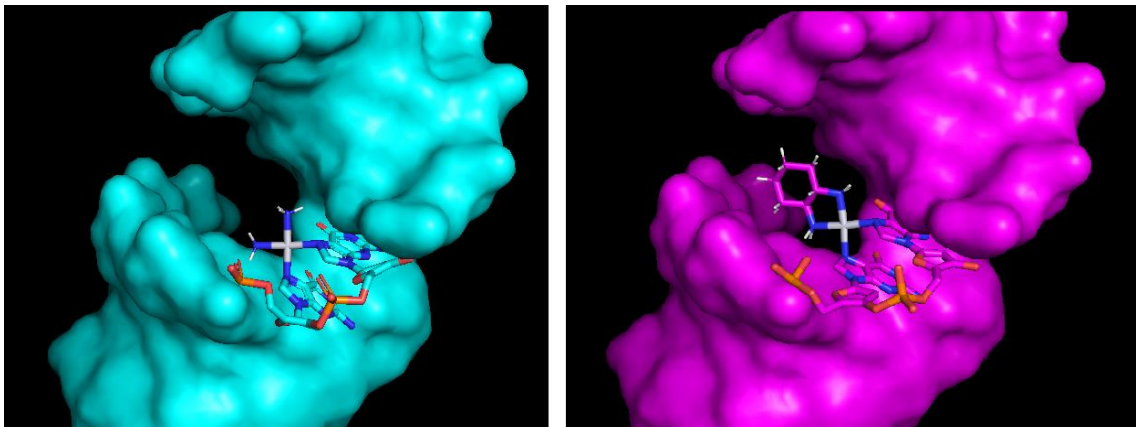


Figure 6.1 Computed DNA structures showing cisplatin binding to double stranded DNA (cyan) and oxaliplatin binding to double stranded DNA (magenta).

We were particularly interested in the differentiation between non-stress inducing compound APP (cyan) and nucleolar stress-inducing compound benzaplatin (green) (compounds **10** and **12** in chapter II) (**Figure 6.2**). APP and benzaplatin have nearly identical steric bulk and hydrophobicity but caused different effects on NPM1 redistribution. It is possible that the ability of Pt(II) compounds to cause nucleolar stress is dependent on the orientation of the ring that is coordinated to platinum. Modeling the compounds gave us further insight into how the directionality of the Pt(II) ligand could play a role in how relatively similar Pt(II) compounds could change the effects at biomolecular interfaces.

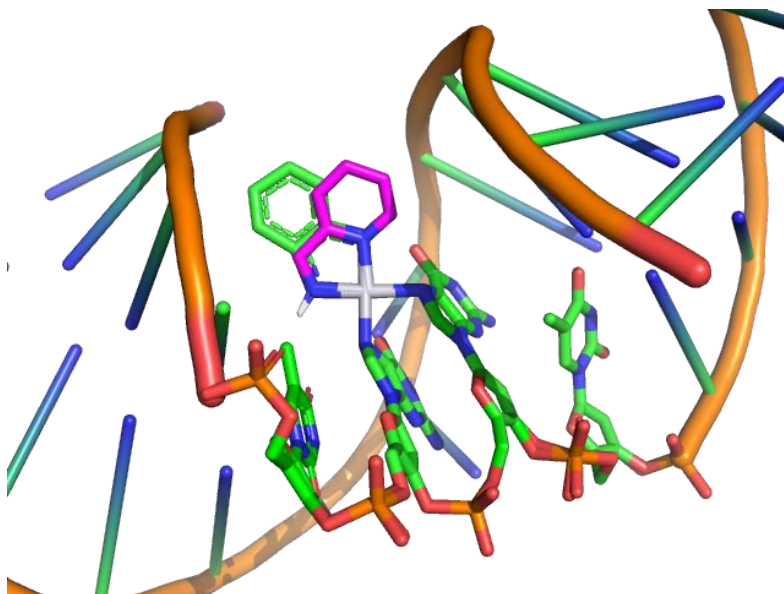


Figure 6.2 Computed structure of platinum compounds bound to double stranded DNA. APP (magenta) is overlaid with benzaplatain (green).

The first major difference between benzaplatain and APP was that APP had multiple orientations available when binding to adjacent guanines on DNA (**Figure 6.3**). While benzaplatain's symmetry only produced one structure, APP could bind in a way that the picolylamine ligand's steric bulk could be towards either the 5' or 3' direction of the coordinated DNA strand. The other major distinction is how the steric bulk from the Pt(II) ligands is located within the major groove. For benzaplatain, the steric bulk protrudes towards the center of the major groove. APP's asymmetry pushes the bulk of the ligand towards one side of the major groove. This orientation may still allow potential access to the 5' or 3' side of the major groove depending on the binding orientation. This property of APP could allow some recognition at the major groove for biomolecule interactions although the strength of the resulting interactions would likely be diminished.

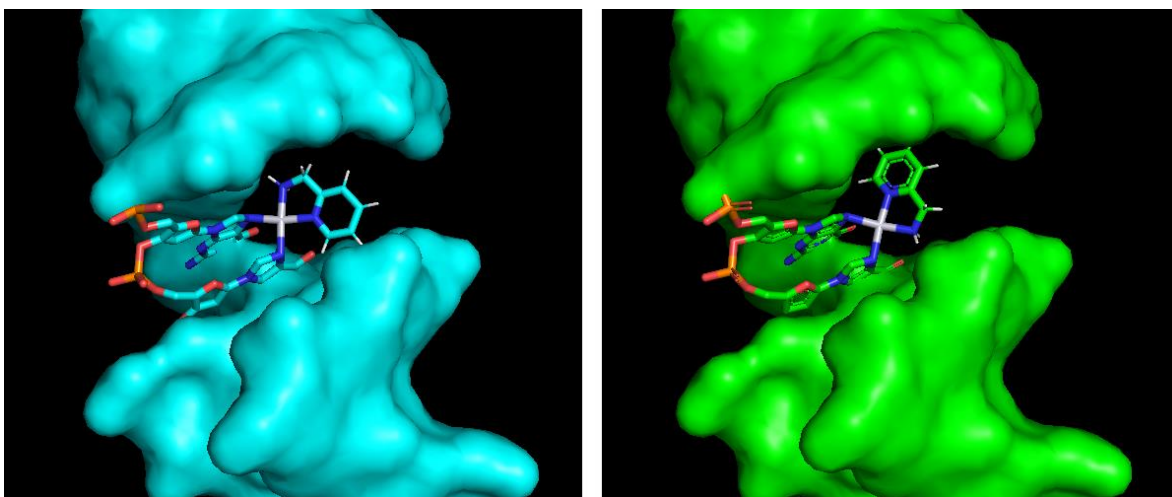


Figure 6.3 Computed structure of APP bound to DNA. Two bound confirmations of APP are presented (cyan and green).

We also investigated the structural differences between PlatMeEn ([give chemical structure here], blue) and pentaplatin ([chemical structure], green) (**Figure 6.4**) bound to DNA. When probing the size-dependence of compounds that could cause nucleolar stress, pentaplatin was the smallest compound we found that still caused stress. PlatMeEn, the next smallest compound, no longer caused stress. When comparing these two structures in the context of binding to adjacent guanines (**Figure 6.4**), we could clearly illustrate how the change in ligand size could affect a biomolecular interface. When pentaplatin is bound to DNA the steric bulk resembles that of benzaplatin, blocking potential interactions on either side of the ligand while also protruding towards the center of the major groove. Binding to PlatMeEn still results in some steric blocks to the major groove, but significantly less than the effects of pentaplatin. It is possible that the driving factor for why pentaplatin but not PlatMeEn causes nucleolar stress is driven by the increase in steric bulk between the two compounds.

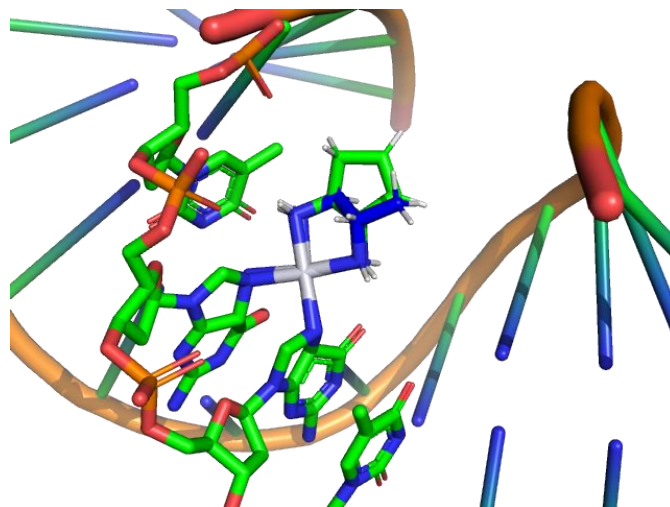


Figure 6.4 Computed structure of DNA bound to platMeEn (dark blue) and pentaplatin (green).

Another set of compounds of interest was the DACH derivatives with axial and equatorial substituents described in Chapter IV. The chair confirmation of DACH provides an interesting directional component that affects the orientation of substitutions. This was very interesting to consider because of the strong directionality component we found when considering different effects of APP and benzaplatin. Viewing the derivatives with 4-methyl substitutions in the equatorial and axial positions, we can clearly see how the disposition of the methyl group could affect the binding in the major groove (**Figure 6.5**). In the equatorial methyl derivative (yellow) the methyl protrudes into the middle of the major groove away from the DNA. In the axial methyl derivative (magenta), the methyl is pushed into the major groove following the helical turn. These differences illustrate how a potential biomolecular interface could be affected based on the orientations of ligand substituents on the Pt(II)-coordinated DACH ring.

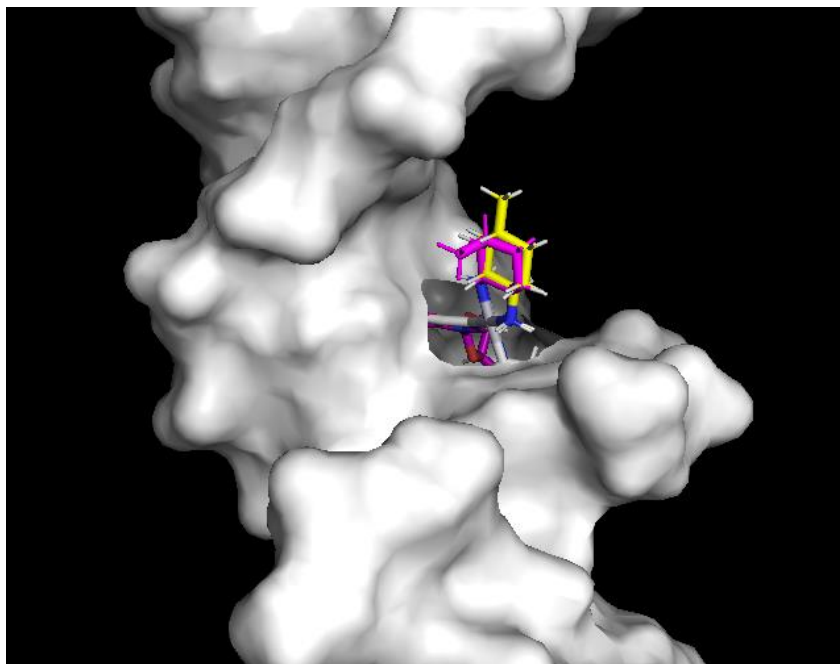


Figure 6.5 Computed structure of methyl oxaliplatin derivatives binding to DNA. Equatorial derivative is in yellow. Axial derivative is in magenta.

Platinum compounds interacting with NPM1

Binding to genomic DNA and subsequent DNA damage response is believed to be the mechanism by which cisplatin causes cell death. Oxaliplatin, however, is known to cause much less DNA damage than cisplatin and was recently found to cause cell death through ribosome biogenesis stress (referred to here as nucleolar stress). There are many biomolecules that are involved in the nucleolar stress response pathway including RNA Pol I and NPM1 which have been discussed in previous chapters. When considering how our platinum compounds could affect nucleolar stress and bind at a biomolecular interface we chose to examine NPM1 as a potential target that could be affected by platinum compounds and cause nucleolar stress.

The C terminal tail of NPM1 contains a cysteine 275 which is glutathionylated under oxidative stress conditions. When it is glutathionylated, NPM1 relocates to the nucleoplasm regardless of whether there is nucleolar stress occurring. We imagined cysteine 275 could be coordinating with our platinum species and the Pt(II) adducts causing steric hinderance similar to the glutathionylation. Pt(II) compounds are known to bind avidly to cysteine, forming a monoadduct with the thiolate ligand. This model also allowed us to investigate the influence of positioning in Pt(II) monoadducts.

We modeled our compounds using Avogadro onto the C terminus of NPM1, using crystal structure PDB ID 2VXD.¹¹² The structure of NPM1 was not held constant but only shifted minimally due to the starting point being the already low- energy crystal structure. The compounds were optimized using the same method as in the previous section. The optimization was performed using UFF force field following the steepest descent until dE measured under 0.01.¹¹⁰ If the Pt(II) ligand geometry was not planar after the first round of optimization, the structure was corrected and optimized again. This computational method takes into account bond lengths, angles, and steric clashes and structures produced can be used for higher level computational analysis to determine other characteristics such as electron density or hydrogen bonding. The optimized structures were then visualized in Pymol version 2.4.¹¹¹

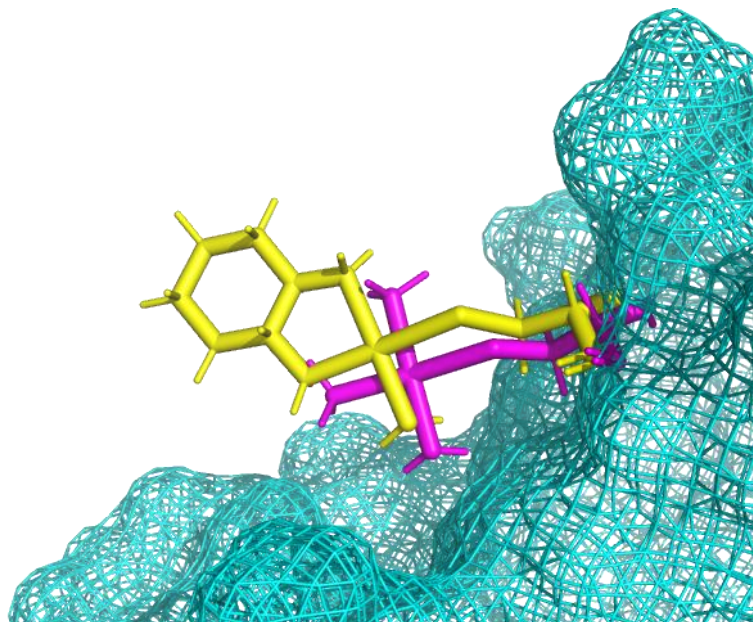


Figure 6.6 Computed structure of Pt(II) compounds modeled bound to the C terminus of NPM1. Cysteine 275 is bound to cisplatin (magenta) or oxaliplatin (yellow).

When viewing the coordination of oxaliplatin and cisplatin to this cysteine it is clear that oxaliplatin's ligand creates a much larger steric hinderance at this position (**Figure 6.6**). Cystine 275 exists in the center of the DNA/RNA-NPM1 interface where DNA or RNA would bind to NPM1. The ligand of oxaliplatin providing a steric block at that region could interact similarly to glutathionylation of NPM1 which blocks the binding of RNA and DNA to the c-terminus tail of NPM1 and causes NPM1 to relocate to the nucleoplasm.⁷⁸ Oxaliplatin could interact similarly as well as the other stress inducing platinum compounds.

If NPM1 is the target of platinum, then any compound that could provide enough steric bulk could stop NPM1 binding to RNA and DNA. This is not consistent with our observations in chapter II that steric bulk alone is not sufficient to cause NPM1 redistribution. Instead, there is a strong directionality component between compounds

that exhibit similar steric bulk but do not cause the same outcome regarding NPM1 redistribution.⁸² We examined benzaplatin and APP again to determine whether our models could highlight why benzaplatin but not APP could cause nucleolar stress. In our models we found that the asymmetry of APP allowed the ligand to encompass a much larger space but also the flexibility to potentially be moved out of the way of an RNA or DNA binding partner (**Figure 6.7a**). In comparison, benzaplatin's possible lower-energy conformations were fewer, only changing minimally compared to the differences in conformations available to APP (**Figure 6.7b**). The flexibility of available

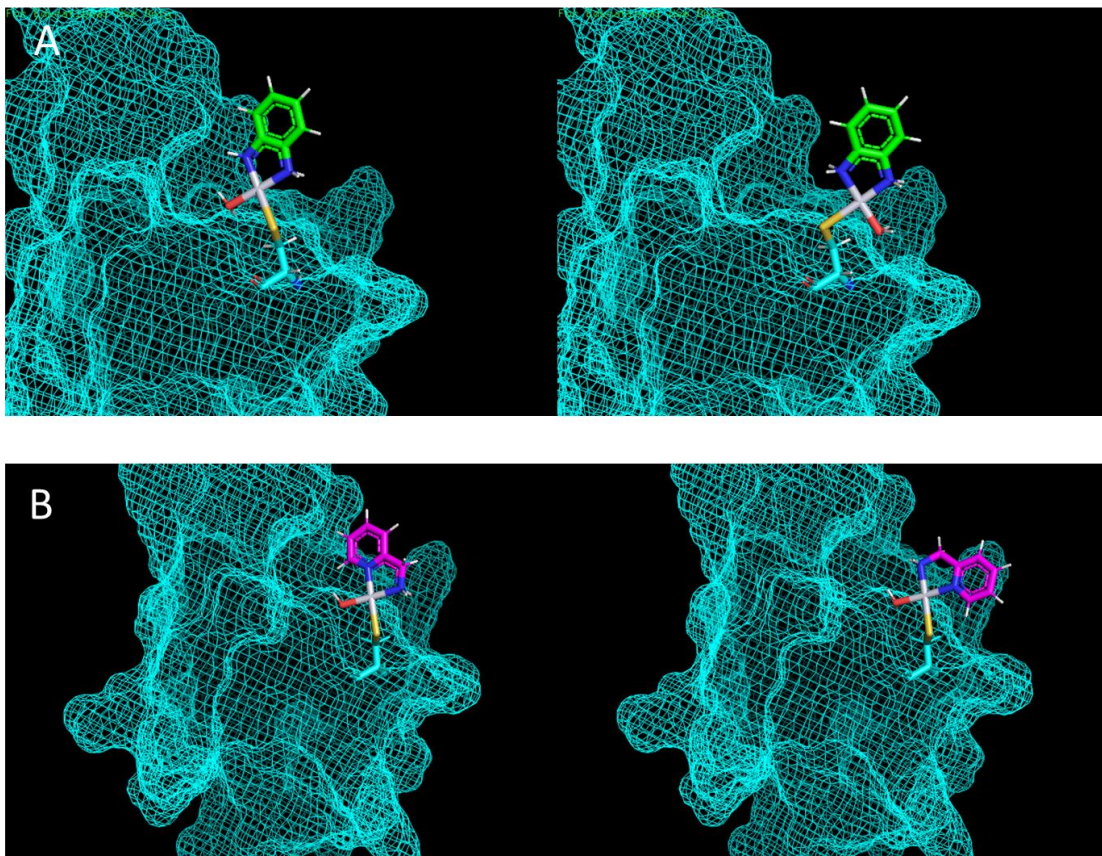


Figure 6.7 Computed structures of platinum binding to cysteine 275 of NPM. Two possible conformations are shown. APP is shown in magenta. Benzaplatin is shown in green.

conformations of APP could allow APP the ability to move out of the way of an interacting biomolecule at other interfaces. While APP had two low-energy conformations available when binding to double stranded DNA with a bidentate adduct, APP has many more available when forming only a monoadduct with a biomolecule. This was determined by modifying the platinum structure to alternate configurations and optimizing the structures. Due to no steric interactions around the platinum compounds for these models, the lowest energy structures found were varied and depended on the original orientation of the platinum introduced, as opposed to settling into one structure despite any manipulation as was the case for models using DNA. Two orientations are presented in **Figure 6.7** for two compounds. If another biomolecule were to bind to this interface, it is possible that more steric constraints would be present and limit the orientations available to the platinum molecules.

Our platinum compounds could be interacting to form both monoadducts and bidentate adducts on biomolecules to cause nucleolar stress. It is interesting to consider asymmetry as a source of flexibility at these interfaces and as a potential molecular reason why these compounds act dissimilarly. The asymmetry may allow compounds to be moved away from interfaces needed to bind to other biomolecules allowing for the biomolecules to bypass or ignore the effects of these platinum compounds. This is in comparison with symmetric, rigid molecules which would not allow the bulk of the platinum ligand to be shifted away from potentially important interfaces. The identification of proteins and other biomolecules that interact with oxaliplatin derivatives would help guide computational analysis and better refine why oxaliplatin and similar derivatives cause nucleolar stress at a molecular level.

CHAPTER VII: CONCLUDING REMARKS

Summary

Chapter I introduces Pt(II) anticancer drugs. The background and discovery of cisplatin and the two FDA-approved platinum drugs that followed are described. The mechanism of action for cisplatin and oxaliplatin is described with the current state of knowledge being that cisplatin's cell death mechanism is through the DNA damage response, whereas oxaliplatin's appears to cause cell death through the nucleolar stress response. The use of modified platinum compounds for mechanistic studies is discussed including compounds that are pre-tethered to fluorophores as well as compounds that are modified after the platinum has bound to biomolecules through the use of azides and alkynes for post-treatment conjugation.

In Chapter II, we began our study into what structural components of oxaliplatin were necessary to cause nucleolar stress. We confirmed that oxaliplatin caused nucleolar stress and that a small window of modifications to the DACH scaffold could be tolerated. We synthesized a variety of compounds in a limited structure-activity study. We found that the DACH ligand of oxaliplatin was responsible for causing nucleolar stress and that the identity of the aquation labile ligands was not a factor as long as the compound could bind to biomolecules. We examined hydrophobicity and steric bulk in our compounds and determined that these properties were not sufficient to explain why compounds caused nucleolar stress. We also found that the orientation of the ring of the ligand with respect to the Pt(II) was very important in determining whether compounds caused stress. Through this limited structure-activity study, we found a small window of derivatives

that could cause nucleolar stress indicating that the interaction that causes nucleolar stress could be a specific interaction.

We then examined the structural characteristics of phenanthriplatin in Chapter III. It had previously been reported that phenanthriplatin as well as oxaliplatin caused nucleolar stress as its mechanism of action. We studied other monofunctional platinum derivatives of phenanthriplatin that contained one or two fused rings, and found no other compounds that caused nucleolar stress. The addition of the third ring of phenanthriplatin apparently is important for how phenanthriplatin caused nucleolar stress. This could be because of the orientation the ligand enforced by the addition of the third fused ring or could be because of the enhanced ability of the phenanthridine ligand to intercalate between nucleobases. We found no structural connection between phenanthriplatin and oxaliplatin that explained why both compounds caused nucleolar stress. It is possible that oxaliplatin and phenanthriplatin cause nucleolar stress through different biomolecular interactions.

Chapter IV continued our structural investigation into why oxaliplatin caused nucleolar stress. We investigated substitutions at the 4,5 position of the DACH ligand of oxaliplatin. Our compounds included a methyl or ethyl substituent at the 4- position in the axial or equatorial position. We found that with respect to causing nucleolar stress, a methyl group was tolerated in both the axial and equatorial position while a larger acetamide substitution in the axial position was not. This sensitivity further demonstrated the possibility of a specific biomolecular interaction occurring with oxaliplatin that could cause nucleolar stress. We also tested a compound with a 4-5 double bond in the DACH ring and determined that the lack of protons in the axial positions is tolerated with respect

to causing nucleolar stress. To extend our findings, we further tested a platinum compound with an acetamide at the 4- position, in the axial orientation. This compound did not cause nucleolar stress despite having hydrophobicity that was between DACH-Pt and pentaplatin, which both were determined to cause nucleolar stress as described in Chapter II. From these additional structure studies we have explored compounds that included ligands that are larger than the DACH ligand of oxaliplatin. We have also determined that the 4 position is unsuitable as a location for installing a bioorthogonal handle in either the axial or equatorial positions of the ring.

In chapter V I detailed efforts to synthesize two new platinum derivatives that included a bioorthogonal handle. The first compound, a cyclopropene derivative, could be used for live cell imaging. I discussed approaches to maintain the reactive cyclopropene during synthesis. The initial synthetic procedure installed the cyclopropene onto the protected diamine ligand before coordinating to Pt(II). However, I found that the cyclopropene-containing ligand was unstable in the presence of ligand-exchangeable Pt(II) species, perhaps through a reaction with the Pt(II). I found that a cyclopropene-containing precursor was stable in the presence of diamine-coordinated platinum species, suggesting a new synthetic pathway in which the cyclopropene was installed on pre-coordinated Pt(II) ligand. I used the crude mixture obtained from this second synthetic procedure to demonstrate Pt-cyclopropene adduct formation on a hairpin DNA and successful click conjugation to tetrazine rhodamine.

Chapter V also describes the synthetic steps that have been taken to create an oxaliplatin mimic that includes an azide for post-treatment CuACC conjugation. This synthesis includes an acetamide at the 4-position as a precursor to installing an amide-

linked azide. In Chapter IV, it was found that the acetamide-modified Pt(II) compound does not cause nucleolar stress, suggesting that the azide product would also be limited as an oxaliplatin mimic. Synthesis of the azide-modified DACH-bound Pt(II) compound was partially successful and requires purification of the final product. This compound could be used to investigate how the DACH ligand of oxaliplatin could affect localization, even though the compound is not expected to cause nucleolar stress due to observations reported in Chapter IV.

We return to our platinum compounds that caused stress in Chapter VI. In this chapter we modelled the structures of stress-inducing and non-stress inducing compounds described in Chapters II and IV as adducts on double-stranded DNA and on a DNA-binding protein, NPM1, to investigate how the structural changes could affect a biomolecular interface involving protein-DNA interactions. Compounds were modeled as bidentate adducts on DNA, and as monoadducts on Cys 275 of the C-terminus of NPM1. From these models we found that the asymmetry of APP, a non-stress inducing compound, could bind in multiple conformations providing flexibility that might be less inhibitory at an important interface. We compared APP to benzaplatin, a stress-inducing compound with almost identical hydrophobicity and steric bulk as well as similar structure, that could not sample different conformations. The potential flexibility at a biomolecular interface of APP was even more pronounced when viewing the potential platination of cysteine 275 of NPM1. We also examined the derivatives explored in chapter IV containing methyl or ethyl substituents in axial or equatorial positions of the DACH 4-position, bound to DNA. We considered the finding that an ethyl in the axial and equatorial position was no longer tolerated with respect to causing nucleolar stress.

This could indicate that an interaction around carbon 4 of DACH ligand is important in causing nucleolar stress.

Future Directions

Throughout this document we have explored work towards uncovering what biomolecules are responsible for cell death via nucleolar stress response that is induced by certain platinum compounds. Our structure studies indicate that this response could be caused by a specific interaction with platinum that is very sensitive to small changes in the platinum ligand structure.^{82,85} It is possible that the mechanism of action could resemble a lock and key type mechanism where the DACH ligand coordinated to platinum is situated as a “best fit” and both small changes to increase the size of DACH to include a ethyl substitution as well as decreases in size such as compounds smaller than pentaplatin no longer cause nucleolar stress. This is an interesting potential mechanism because we have observed that pentaplatin could be acting as a “bridging” compound. Pentaplatin shows decreased NPM1 relocalization as well as delayed NPM1 response compared to other stress-inducing compounds described in chapter II.⁸⁵

The studies described in this document are limited in what can be explored by changing the structure of oxaliplatin derivatives. While useful for uncovering a general mechanism that these compounds could be working through, they do not identify the biomolecules that could be involved in these types of mechanisms. Chapter V describes synthetic work towards an oxaliplatin mimic that could add new tools to our toolbox to explore the mechanism of action by oxaliplatin. However, our work suggests that the derivative currently described might not cause nucleolar stress. Future studies should

further probe the DACH scaffold for locations that could be modified and still cause nucleolar stress.

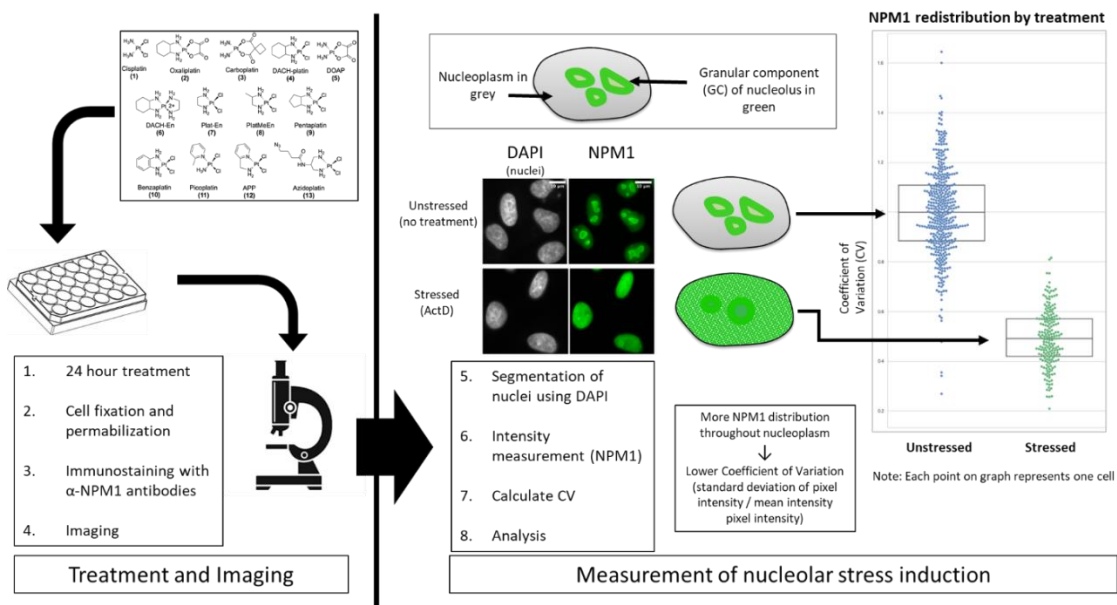
Previous studies using azide-containing cisplatin mimics have uncovered many new effects of cisplatin on cells.^{45,48,81} For instance, these derivatives have been used to determine the localization of cisplatin within cells and shown that azidoplatin, which does not cause nucleolar stress, localizes to the nucleolus.^{33,82,95} Azidoplatin has also been used to pull down and identify proteins that were coordinated to platinum and related to the ability of this compound to cause endoplasmic reticulum stress.⁴⁸ The ability to pull down targets of a compound that causes nucleolar stress could identify potential biomolecules for further study. An azide-containing oxaliplatin mimic that caused nucleolar stress could be used to greatly increase our understanding of how oxaliplatin causes nucleolar stress. Used in conjunction with cisplatin mimics, an oxaliplatin mimic could help to uncover how these two chemotherapy drugs affect different cancerous cell types.⁶

A click-capable oxaliplatin would provide a very useful tool for studying platinum induced nucleolar stress but will take time to both synthesize and to explore the scaffold for an appropriate location for derivatization. While a compound is being synthesized, biochemical and biological approaches can help to explore potential, known targets that could cause nucleolar stress. One potential target of platinum has been reported by Sutton and DeRose indicating that RNA polymerase I is inhibited by oxaliplatin but not cisplatin.⁸³ We have also found that our other stress-inducing compounds also cause the inhibition of rRNA transcription.⁸⁵ This is a promising target that could cause these compounds to employ the nucleolar stress pathway but it is unclear

whether inhibition could be caused by direct binding of platinum to Pol I or whether platinum could be interacting with DNA or other parts of the nucleolus. For these differentiations, being able to identify the platinum targets directly would be beneficial.

Overall, this work has made steps towards exploring the molecular level factors that cause platinum II compounds to cause nucleolar stress. A better understanding of the mechanism of action of oxaliplatin as well as the derivatives discussed here could lead to a better understanding of these chemotherapy drugs at a clinical level. Both identification of what platinum is interacting with as well as downstream effects that perturb the nucleolus would provide opportunities to create a new generation of platinum compounds that exploit the nucleolar stress pathway as their mechanism of action. Additionally, an in depth understanding of this mechanism of action and the platinum compounds that cause it could lead to better predictions about which platinum compounds could be more effective in different types of cancer treatments.

Supplementary Figures



A.1. NPM1 assay and quantification scheme. A549 cells were seeded on coverslips treated for 24 hours with the selected compound. Cells were fixed, permeabilized, and stained with an α -NPM1 antibody as described in Materials and Methods section. After imaging, nuclei were segmented using DAPI staining and pixel intensity from NPM1 imaging was measured. The Coefficient of Variation (CV, standard deviation over mean), was calculated for each nucleus, normalized to the mean CV for the no treatment control on that day, and plotted as above with each nucleus represented by one point on the plot. An average CV of 1.0 indicates no stress, whereas a lower CV (around 0.6) indicates diffusion of NPM1 throughout the nucleoplasm, a positive indicator of nucleolar stress. Treatment data sets are represented by box plots, where the center, top, and bottom lines of boxes represent the median, first and third quartile respectively.

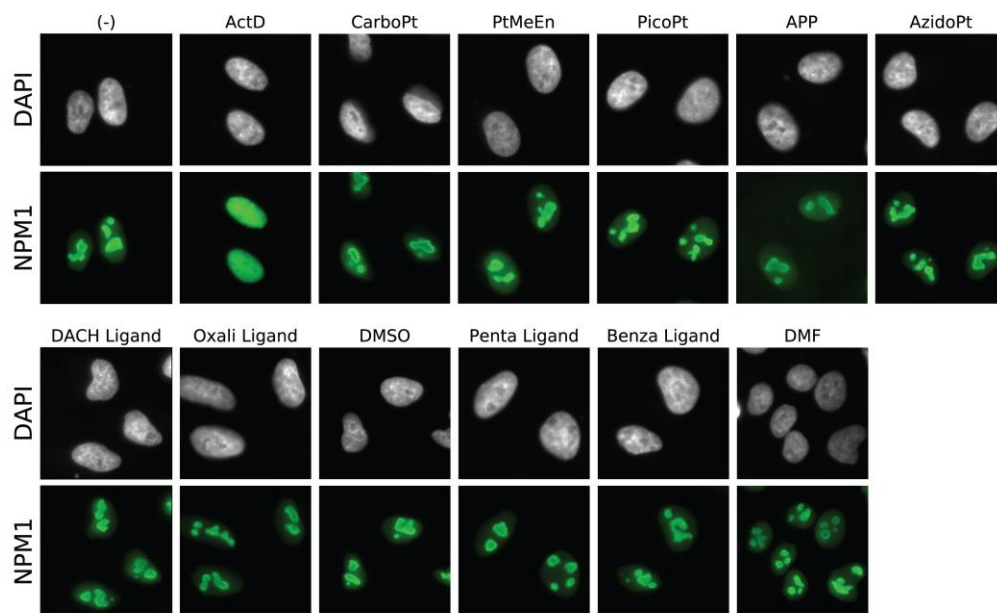


Figure A.2. Additional images for compounds tested. Top row shows negative and positive (Actinomycin D) controls, and Pt(II) compounds **3**, **8**, **11**, **12**, and **13**, — respectively CarboPt, PtMeEn, PicoPt, APP, and AzidoPt— none of which caused nucleolar stress. Bottom row shows Pt(II)-free ligands of stress-inducing Pt(II) compounds and solvents used (DMSO and DMF). Ligands alone do not induce nucleolar stress, and neither do solvents. All treatments were performed for 24 hours. Pt(II) compound and ligand treatments were conducted at 10 μM , with the exception of Actinomycin D, which was 5 nM, and **3** (CarboPt), which was 20 μM .

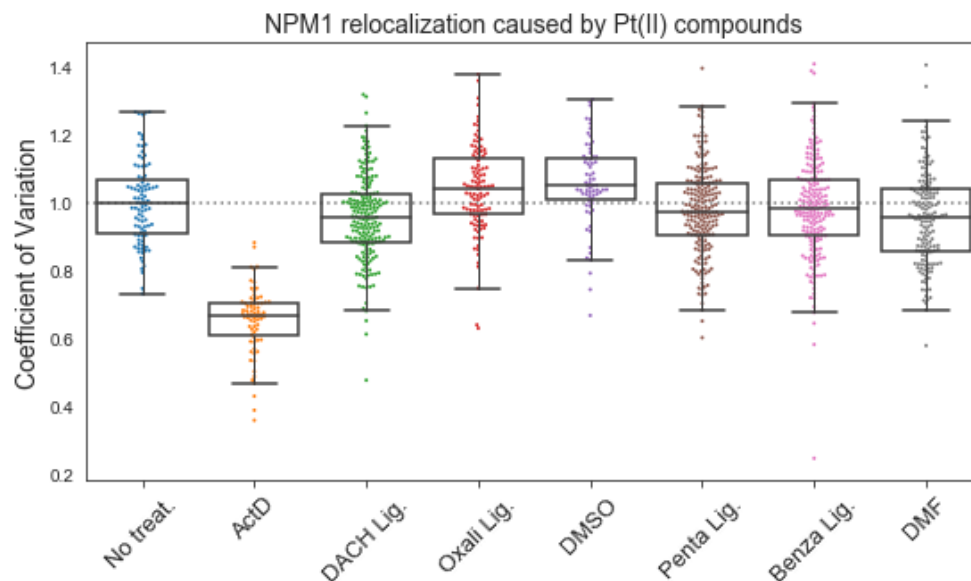


Figure A.3. Quantification of nucleolar stress induction for Pt(II)-free ligands and solvents used. CV quantification confirms that ligands alone do not induce nucleolar stress, and neither do solvents. All treatments were performed for 24 hours. Treatments were conducted at 10 μ M, with the exception of Actinomycin D, which was 5 nM. Treatment data sets are represented by standard box plots, where the center, top, and bottom lines of boxes represent the median, first and third quartile respectively. The vertical lines represent the range of data within 1.5xIQR of the lower and upper quartiles, where IQR is the difference between first and third quartile; points outside this range are considered outliers.

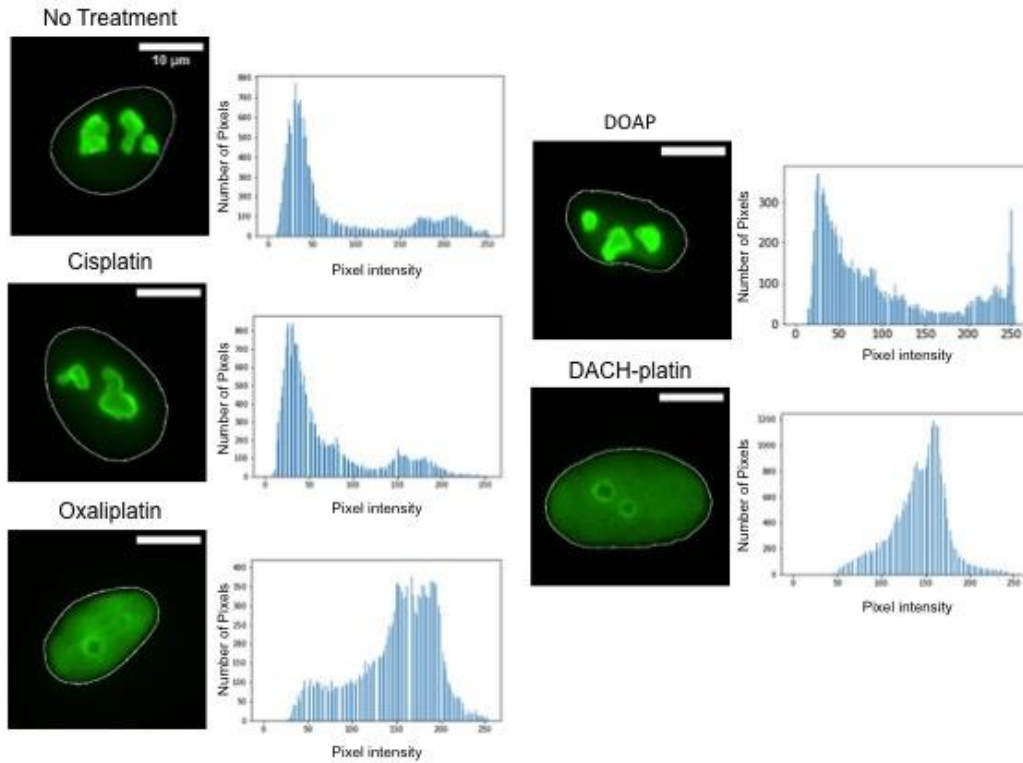


Figure A.4. Histograms showing NPM1 intensity within a single nucleus in stressed and unstressed cells. X axis represents pixel intensity, and Y axis represents the number of pixels within a nucleus of the intensity on the X axis. Cells not undergoing nucleolar stress have a large number of low intensity pixels and a small number of high intensity pixels, indicating NPM1 is concentrated in the granular component of the nucleolus. Cells undergoing stress have a broader distribution of pixel intensities, with the histogram skewing towards high intensity, as NPM1 has redistributed throughout the entire nucleoplasm.

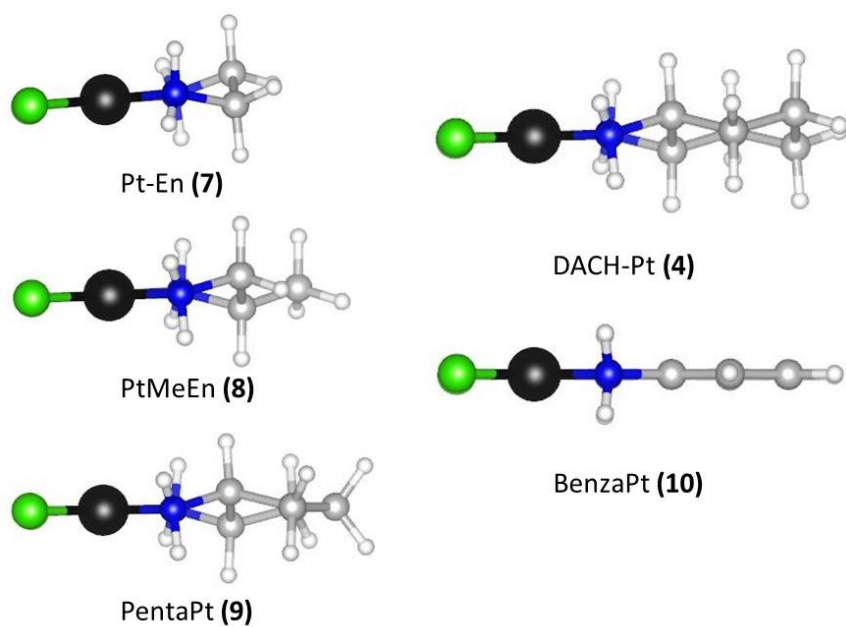


Figure A.5. DFT-optimized structures of compounds illustrating the relative size of compounds and planarity of BenzaPt **10** relative to DACH-Pt **4**

Supplementary Tables

Table A.1. IC₅₀ values in A549 cells for selected compounds at 24 hours^a

Compound	IC ₅₀ (μM)
Oxaliplatin, 2	81.5±7
Cisplatin, 1	12.8±2
DACHplatin, 4	31.9±6
Pentaplatin, 9	37.5±5
Benzaplatin, 10	NR ^b
PlatEn, 7	46.1±6
PlatMeEn, 8	76.1±9
DOAP, 5	36.6±5
APP, 12	NR ^b

^aIC₅₀ values in A549 cells were determined after 24-hour treatment with indicated compound

^bNR=IC₅₀ value not reached, >500 μM

Table A.2. IC₅₀ values in A549 cells for selected compounds at 48 hours^a

Compound	IC ₅₀ (μM)
Oxaliplatin, 2	9.9±3.5
Cisplatin, 1	4.6±0.7
Benzaplatin, 10	6.9±0.7
APP, 12	36.9±4.3

^aIC₅₀ values in A549 cells were determined after 48-hour treatment with indicated compound

Table A.3. Volume and hydrophobicity data

Compound	Volume (Å ³)	Distance (Å)	logP
Cisplatin	19.46	3.40	-2.39±0.005
PlatMeEn	23.56	5.51	-1.68±0.014
PlatEn	21.47	4.41	-1.85±0.013
APP	27.66	6.21	-1.1±0.058
Picoplatin	27.69	6.21	-
Pentaplatin	27.85	6.21	-1.29±0.031
Benzaplatin	28.71	6.73	-0.92±0.038
DACH-platin	30.01	6.75	-0.89±0.011
Carboplatin	30.94	6.30	-
DACH-En	32.41	6.72	-
Azidoplatin	32.71	13.16	-1.2±0.059
Oxaliplatin	34.13	6.78	1.58±0.02

Materials and Methods

1. Cell culture and treatment

A549 human lung carcinoma cells (#CCL-185, American Type Culture Collection) were cultured at 37°C, 5% CO₂ in Dulbecco's Modified Eagle Medium (DMEM) supplemented with 10% Fetal Bovine Serum (FBS) and 1% antibiotic-antimycotic. Treatments were conducted on cells that had been grown for 11-25 passages to 70% confluency. Except where noted otherwise, treatments were conducted for 24 hours at 10 µM. Compounds were made into 5mM stocks on the day of treatment in 0.9% NaCl (cisplatin), DMF (**4, 7, 8, 10, 11, 12, 13, 14**), DMSO (**5**), or water (**1, 2, 3, 6**). Stock solutions were diluted into medium immediately prior to drug treatment.

2. Immunofluorescence

Cells to be imaged were grown on coverslips (Ted Pella product no 260368, Round glass coverslips, 10mm diam, 0.16-0.19mm thick) as described above. After treatment, cells were washed twice with phosphate buffered saline (PBS) and fixed for 20 minutes at room temperature in 4% paraformaldehyde in PBS. PFA was removed via aspiration and cells were then permeabilized with 0.5% Triton-X in PBS for 20 minutes at room temperature. Two ten-minute blocking steps were performed with 1% bovine serum albumin (BSA) in PBST (PBS with 0.1% Tween-20). Cells were incubated for one hour in primary antibody (NPM1 Monoclonal Antibody, FC-61991, from ThermoFisher, 1:200 dilution in PBST with 1% BSA) and 1 hour in secondary antibody (Goat Anti-Mouse IgG H&L Alexa Fluor® 488, ab150113, Abcam, 1:1000 dilution in PBST with 1% BSA), with 3 five minute wash steps using PBST between incubations, and were washed in the same manner again before mounting slides. Coverslips were mounted on slides with ProLong™

Diamond Antifade Mountant with DAPI (Thermo Fisher) according to manufacturer's instructions.

3. Cytotoxicity (MTT assay)

A549 cells were seeded in 24-well plates at a density of 5×10^4 cells/mL. The following day cells were treated with 0-750 μ M of compound in DMEM supplemented with 10% FBS and antibiotic-antimycotic. 24h after treatment, compound-containing medium was removed and cells washed twice with PBS. MTT in DMEM supplemented with 10% FBS and antibiotic-antimycotic was then added to cells and incubated for 3h. DMSO was used to dissolve the formazan crystals and absorbance at 595 nm was then determined using a Tecan microplate reader. Percent viability was determined by comparing to vehicle-treated control for each compound and IC50 concentration calculated from triplicate measurements using the drc package in R ¹¹³.

4. Image processing and quantification

Images were taken using a HC PL Fluotar 63x/1.3 oil objective mounted on a Leica DMi8 fluorescence microscope with Leica Application Suite X software. Quantification of NPM1 relocalization was performed in an automated fashion using a Python 3 script. Images were preprocessed in ImageJ ^{114,115} to convert the DAPI and NPM1 channels into separate 16-bit greyscale images. Between 70 and 225 cells were analyzed for each treatment group. Nuclei segmentation was determined with the DAPI images using Li thresholding functions in the Scikit- Image Python package ¹¹⁶. The coefficient of variation (CV) for individual nuclei, defined as the standard deviation in pixel intensity divided by the mean pixel intensity, was calculated from the NPM1 images using the SciPy Python

package. All data were normalized to the no-treatment control in each experiment. NPM1 imaging results for each compound were observed on a minimum of two separate testing days. Data are represented as boxplots generated using Seaborn within Python.

5. Synthesis

Materials

Cisplatin used for cell treatments was purchased from Strem Chemicals. Cisplatin used as a synthetic precursor was synthesized as described below. Oxaliplatin and carboplatin were purchased from TCI. Unless otherwise noted, all other compounds were purchased from Sigma Aldrich or TCI. Picoplatin and azidoplatin were synthesized as previously reported ²⁵.

Cisplatin (1)

Cisplatin was synthesized according to previously described methods by Dhara ¹¹⁷ and reviewed ¹¹⁸. Briefly, potassium tetrachloroplatinate (62.7 mg, 0.151 mmol, 1 eq) was dissolved in 180 μ L of water and stirred at 40°C. Potassium iodide (300 mg, 1.807 mmol, 12 eq) was dissolved separately in 500 μ L of water and warmed to 40°C. 250 μ L of the potassium iodide solution was added dropwise to the solution containing potassium tetrachloroplatinate. After addition of potassium iodide, the solution was warmed to 70°C. Once the solution reached 70°C it was removed from heat and cooled to room temperature. The solution was then filtered through celite. The filtrate was collected and used for the following reaction. A 2M solution of ammonium hydroxide in water (250 μ L) was added dropwise. The solution was allowed to stand for 30 minutes, filtered, and washed with ethanol (x1) and ether (x2). The solid was collected to yield 56.2 mg *cis*-diamminediiiodoplatinum(II). Silver sulfate (37 mg, 0.119 mmol, 1eq) was added to 5 mL

of water. *Cis*-diamminediiodoplatinum(II) (56.2 mg, 0.116 mmol, 1eq) was added slowly. The solution was heated to 80°C. The solution was stirred overnight. The silver iodide was filtered using celite and the filtrate collected. This solution was concentrated to 1.5 mL. Potassium chloride (174.6 mg, 2.34 mmol, 20 eq) was added to the solution and then heated to 80°C. The solution was stirred at 80°C for another 20 minutes and cooled to room temperature. The solution was filtered and washed with ethanol (x1) and ether (x2) to yield 23.5 mg (52%) *cis*-diamminedichloroplatinum(II). ¹H NMR (500 MHz, DMF-d7) δ 3.99 (s, 6H).

Cis-(*trans*-1,2-diaminocyclohexane)dichloride Platinum(II) (DACH-Pt) (4)

Cis-(*trans*(+/-)-1,2-diaminocyclohexane)dichloride Platinum(II) was prepared using general methods previously described ¹¹⁸. Potassium tetrachloroplatinate (100.3 mg, 0.242 mmol, 1 eq) was dissolved in 4 mL of water. *Trans*(+/-)-1,2-diaminocyclohexane (29.1 mg, 0.255 mmol, 1eq) was added dropwise to the dark red solution and stirred for 7.5 hours. A yellow precipitate formed. The solution was filtered and washed with ice-cold methanol (x1) and acetone (x1). The yellow solid was then collected to yield 70 mg (76 %). ¹H NMR (500 MHz, DMF-d7) δ 5.59 (d, J = 7.4 Hz, 2H), 5.02 (s, 2H), 2.50 (qq, J = 11.2, 5.6, 3.8 Hz, 2H), 2.15 – 2.04 (m, 2H), 1.56 (dd, J = 7.7, 3.3 Hz, 2H), 1.48 (tt, J = 11.9, 5.6 Hz, 2H), 1.15 (qd, J = 11.9, 2.9 Hz, 2H). ¹⁹⁵Pt NMR (107 MHz, DMF-d7) δ -2270.32.

Cis-(diammine)oxalic acid Platinum(II) (DOAP) (5)

Cis-(diammine)oxalic acid Platinum(II) was prepared using general methods previously described ¹¹⁸. Sodium oxalate was prepared by introducing excess sodium hydroxide to oxalic acid and filtering the resulting solid. *Cis*-(diammine)diiodo platinum(II) (92.3 mg, 0.193 mmol, 1 eq) was dissolved in 5 mL water. Silver nitrate

(82mg, 0.4823 mmol, 2.5eq) was added and the reaction stirred overnight protected from light. The reaction was then filtered through celite and the filtrate collected. Sodium oxalate (26 mg, 0.194 mmol, 1 eq) was added to the filtrate and the reaction was stirred overnight and protected from light. The resulting light grey solid was filtered from the solution and washed with water (2x) and methanol (x2). Yield 33.3mg (54%). ^1H NMR (500 MHz, DMSO-d6) δ 4.27 (s, 6H). ^{13}C NMR (126 MHz, DMSO-d6) δ 166.38. ^{195}Pt NMR (107 MHz, DMSO-d6) δ -1743.33.

Cis-(trans-1,2-diaminocyclohexane)1,2-ethylenediamine Platinum(II) (DACH-En) (6)

Cis-(trans(+/-)-1,2-diaminocyclohexane)dichloro platinum(II) (62 mg, 0.163 mmol, 1eq) was dissolved in 5 mL of water. 1,2-diaminoethane (32 mg, 0.533 mmol, 3.2eq) was added to the solution and refluxed for two days. The solution was then cooled room temperature over 24 hours. Solution was then evaporated to yield a yellow solid. ^1H NMR (500 MHz, Deuterium Oxide) δ 3.31 (t, $J = 5.8$ Hz, 1H), 3.05 (t, $J = 5.8$ Hz, 1H), 2.97 (s, 2H), 2.72 – 2.64 (m, 4H), 2.47 – 2.39 (m, 2H), 2.09 (dt, $J = 12.8, 2.0$ Hz, 2H), 1.67 – 1.60 (m, 2H), 1.41 – 1.28 (m, 2H), 1.20 (td, $J = 9.4, 8.9, 4.0$ Hz, 2H). ^{13}C NMR (126 MHz, D₂O) δ 61.17, 46.83, 40.43, 32.14, 23.92. ^{195}Pt NMR (107 MHz, D₂O) δ -3002.42. TOF MS ES+ for m/z [(M)]²⁺ C₈H₂₁Pt calculated: 368.1414 found: 368.1403 ([M]²⁺).

Cis-(1,2-diaminoethylene)dichloride Platinum(II) (Plat-En) (7)

Cis-(1,2-diaminoethylene)dichloride Platinum(II) was prepared using general methods previously described¹¹⁸. Potassium tetrachloroplatinate (66 mg, 0.159 mmol, 1eq) was dissolved in 500 μL of water. 1,2-diaminoethane (9.36 mg, 0.156 mmol, 1eq) was added to the dark red solution and allowed to stir at room temperature for 12 hours. A

yellow precipitate formed. The solution was filtered and washed with ice-cold 0.1M HCl (x1), ethanol (x1), and ether (x1). The yellow solid was collected to yield 27.5 mg (53%). ^1H NMR (500 MHz, DMF- d_7) δ 5.38 (s, 4H), 2.61 (s, 4H). ^{13}C NMR (126 MHz, DMF- d_7) δ 50.52. ^{195}Pt NMR (107 MHz, DMF- d_7) δ -2309.12.

Cis-(2,3-diaminopropane)dichloride Platinum(II) (Plat-MeEn) (8)

Cis-(2,3-diaminopropane)dichloride Platinum(II) was prepared according to previously reported methods and used as a mixture of isomers ¹¹⁹. Potassium tetrachloroplatinate (34 mg, 0.082 mmol, 1eq) was dissolved in 1ml water and heated at 50 °C. Excess potassium iodide (40 mg, 0.24 mmol, 3eq) was dissolved in 0.5 mL water and added dropwise to the platinum. The solution was stirred for 10 minutes and became black. To the stirring solution, 1,2-diamino propane (7 μL , 0.08 mmol, 1 eq) was added and the solution was stirred for 40 minutes. Yellow precipitate formed immediately. The solution was cooled to room temperature and filtered. The solid was washed with ice-cold ethanol (1x) and ether (1x).

The solid was dissolved in 2ml water and silver nitrate (28 mg, 0.16 mmol, 2eq) was added. The reaction was stirred for 2 days protected from light. The solution was filtered through celite and concentrated to 1ml. Excess potassium chloride (120 mg, 1.61 mmol, 20 eq) was added rapidly to the concentrated solution and the mixture was stirred at 50 °C for 1 hour. The resulting yellow solid was filtered and washed with methanol (1x) and ether (1x). ^1H NMR (500 MHz, DMF- d_7) δ 5.74 (s, 1H), 5.55 (d, J = 40.1 Hz, 2H), 5.22 (s, 1H), 3.30 – 3.17 (m, 1H), 2.89 – 2.80 (m, 1H), 2.66 (td, J = 8.2, 6.1, 3.1 Hz, 1H), 1.53 (d, J = 6.5 Hz, 3H). ^{13}C NMR (126 MHz, DMSO) δ 56.00, 52.41, 16.38.

Cis-(trans-1,2-diaminocyclopentane)dichloride Platinum(II) (Penta-Pt) (9)

Cis-(trans-1*S*,2*S*-diaminocyclopentane)dichloride Platinum(II) was synthesized according to previously published methods ¹²⁰. Potassium tetrachloroplatinate (101 mg, 0.243 mmol, 1eq) was dissolved in 2 mL of water. (1*S*, 2*S*)-trans-diaminocyclopentane dihydrochloride (43.1 mg, 0.249 mmol, 1eq) was added and stirring continued. 73 mg of 1,8-Diazabicyclo[5.4.0]undec-7-ene (DBU) (0.482 mmol, 2eq) was added to the solution. A yellow precipitate formed. The solution was filtered and washed with ethanol (x1) and ether (x2). The yellow solid was collected to yield 50.5 mg (57%). ¹H NMR (500 MHz, DMF-*d*₇) δ 5.18 (s, 2H), 5.00 (s, 2H), 3.41 – 3.31 (m, 2H), 2.16 (tdd, *J* = 9.6, 8.0, 5.3 Hz, 2H), 1.78 – 1.64 (m, 2H), 1.63 – 1.48 (m, 1H). ¹³C NMR (126 MHz, DMF-*d*₇) δ 70.21, 26.73, 23.93. ¹⁹⁵Pt NMR (107 MHz, DMF-*d*₇) δ -1987.96.

Cis-(1,2-phenylenediamine)dichloride Platinum(II) (Benza-Pt) (10)

Cis-(1,2-phenylenediamine)dichloride Platinum(II) was prepared using general methods previously described ¹¹⁸. Potassium tetrachloroplatinate (103 mg, 0.248 mmol, 1eq) was dissolved in 1 mL of water. A dark red solution formed. 1,2-phenylenediamine (26.8 mg, 0.248 mmol, 1eq) was added and stirring continued for 6 hours. The solution was filtered and washed with ice-cold ethanol (x1) and ether (x2). The dark yellow/brown solid was collected with a yield of 89.8 mg (96%). ¹H NMR (500 MHz, DMF-*d*₇) δ 7.72 (s, 2H), 7.46 (dd, *J* = 5.9, 3.5 Hz, 1H), 7.28 (dd, *J* = 6.0, 3.4 Hz, 1H). ¹³C NMR (126 MHz, DMF-*d*₇) δ 144.76, 128.85, 127.36. ¹⁹⁵Pt NMR (107 MHz, DMF-*d*₇) δ -2199.18.

Cis-(2-aminomethylpyridine)dichloride Platinum(II) (APP) (12)

Cis-(2-aminomethylpyridine)dichloride Platinum(II) was synthesized according to previously described methods ⁶⁴. A solution of 2-picolyamine (120 μL, 0.075 mmol, 1 eq)

was made in 1.2 mL water. Potassium tetrachloroplatinate (55mg, 0.133 mmol, 2eq) was dissolved in 1.2 mL water. The platinum solution was added to the 2-picolyamine and the pH was adjusted to pH 5 using concentrated HCl. The reaction was stirred for 4 hours. The pH of the solution was adjusted during the reaction to be around pH 5-6 using 1 M NaOH. The resulting yellow solid was filtered and washed with water (2x) to yield 38.7 mg (89%). ^1H NMR (500 MHz, DMF- d_7) δ 9.43 (d, $J = 5.3$ Hz, 1H), 8.37 (t, $J = 7.7$ Hz, 1H), 7.91 (d, $J = 7.8$ Hz, 1H), 7.72 (t, $J = 6.7$ Hz, 1H), 6.42 (s, 2H), 4.55 (t, $J = 5.9$ Hz, 2H).

6. Measurement of partition coefficients

Water was mixed with octanol for 24 hours and left to stand for an additional 24 hours to obtain water-saturated octanol and octanol-saturated water that were used for determining partition coefficients. Measurements of the partition coefficients were performed using classical shake-flask method according to OECD guidelines¹²¹. Platinum complexes were dissolved in octanol-saturated water at concentrations between 0.5 mM and 5 mM. The octanol-saturated water mixtures were mixed with water-saturated octanol in a 1:1 ratio and vortexed for 30 minutes^{121,122}. The mixtures were then centrifuged and 0.5 mL samples of both phases were collected and quantified using RP-HPLC as described by Klose et al¹²⁰. An isocratic method was used for HPLC analysis with water and methanol. Methanol concentrations ranged from 10% to 30% with 30% being used for more hydrophobic compounds. The area of absorbance was used to calculate the ratio (P) of platinum in octanol and water as this area is proportional to the concentration according to the Lambert-Beer law. The column was washed with 95% methanol 5% water between each octanol sample and equilibrated before the next sample was introduced. The stock solution of each platinum compound was compared to the total from octanol and water samples as a check

of this method. This procedure to calculate logP was performed in triplicate and standard deviations were determined.

7. Computations

Computations were performed as previously reported⁶⁰. Briefly, compounds were optimized using density functional theory (DFT) in Gaussian09¹²³. Optimizations to geometry were performed using a RMS force convergence criterion of 10^{-5} hartree. The electronic wavefunction was minimized using GGA functional PBE^{124,125}, with the DEF2TZP basis set. We did not explicitly include relativistic effects as these were not expected to impact the geometries of the compounds significantly¹²⁶.

Two measures of size were used for the compounds: volume and longest vector between the platinum atom and the surface of the molecule. The vector represents the main steric component of the non-labile ligand of each compound to provide a direct comparison especially when comparing compounds that do not share the same aquation-labile ligand identity. In order to quantitatively assess the size of the molecules we used the presence of electric field, as derived from the electrostatic potential, to signify the location of the chemical system. DFT yields the electrostatic potential of the optimized, non-hydrolyzed compound structures and tools previously developed and reported were used to analyze the electrostatic potential of a chemical system¹²⁷. We used the same file format to analyze the electrostatic potential and the result was the electrostatic potentials of the optimized structures were computed by minimizing the electronic wavefunction using 500 eV planewave cutoff, a gamma only k-grid, and a PBE functional utilizing a plane-augmented wave (PAW)^{128,129} basis as implemented in the Vienna Ab Initio Software Package^{129–}

132.

All compounds were calculated in a sufficiently large computational box to minimize self-interaction. The electric field is the gradient of the electrostatic potential; therefore, the electric field includes the direction of the greatest increase in electrostatic potential. DFT calculations return electrostatic potential values on the order of 10^{-6} eV, therefore a change in less than 10^{-5} eV is considered negligible. This approach is based on previous atomic radii calculations which employ negligible change in electron density to assess the size of atoms. We used this measurement of the electric field and definition of the surface of the compound to find the total volume of the compounds as well as the longest vector from the platinum center to the farthest edge of the non-labile ligand.

APPENDIX B: SUPPLEMENTARY INFORMATION FOR CHAPTER III

Materials and methods

Reagents and synthesis

Cisplatin,¹¹⁷ picoplatin,¹³³ and pyriplatin, quinoplatin, isoquinoplatin, and phenanthriplatin⁷² were synthesized as previously reported. Oxaliplatin was purchased from TCI America. Actinomycin D was purchased from Thermo Fisher Scientific. A549 cell line was acquired from the American Type Culture Collection.

Cell culture and treatment

A549 human lung carcinoma cells (#CCL-185, American Type Culture Collection) were cultured at 37 °C, 5% CO₂ in DMEM supplemented with 10% FBS and 1% antibiotic–antimycotic. A549 cells have been used previously to study nucleolar stress pathways.^{58,59} Cells between passage 11–25 and at confluency of 70% were used in the treatments. Cells were treated for 24 h with 10 µM compound, with the exception of phenanthriplatin and phenanthridine which were administered at 0.5 µM and actinomycin D at 5 nM. The counterion for positively-charged compounds is nitrate. Stock solutions of 5 mM compound in DMF were made and used with the exception of oxaliplatin, which was made in water and actinomycin D which was made in DMSO. Immediately prior to treatment, platinum compounds were diluted into media. Final DMF and DMSO concentrations were 0.2% (v/v) in media. We chose to use 0.5 µM phenanthriplatin to account for the higher cellular accumulation of phenanthriplatin and to be more in line with reported 72 h IC₅₀ values which are not exhibited by the other studied compounds.⁷²

Immunofluorescence

Cells to be imaged were grown on coverslips (Ted Pella product no 260368, Round glass coverslips, 10-mm diam, 0.16–0.19-mm thick) as described above. Following treatment, cells were washed twice with PBS. They were then fixed for 20 min at room temperature in 4% paraformaldehyde diluted in PBS. Cells were permeabilized with 0.5% Triton-X in PBS for 20 min at room temperature followed by two 10-min blocking steps with 1% BSA in PBST. The cells were incubated for 2 h using primary antibody (NPM1 Monoclonal Antibody, FC-61991, from Thermo Fisher, 1:200 dilution in PBST with 1% BSA) and 1 h in secondary antibody (Goat Anti-Mouse IgG H&L Alexa Fluor® 488, ab150113, Abcam, 1:1000 dilution in PBST with 1% BSA). Between each incubation and before mounting, slides were washed three times for 5 min each using PBST. Coverslips were mounted on slides with ProLong™ Diamond Antifade Mountant with DAPI (Thermo Fisher) according to manufacturer's instructions.

Imaging and quantification

Images were taken using a HC PL Fluotar 63×/1.3 oil objective mounted on a Leica DMI8 fluorescence microscope with Leica Application Suite X software. Quantification of NPM1 relocalization was performed in an automated fashion using a Python 3 script. Images were preprocessed in ImageJ^{114,115} to convert the DAPI and NPM1 channels into separate 16-bit greyscale images. Between 100 and 250 cells were analyzed for each treatment group. Nuclei segmentation was determined with the DAPI images using Li thresholding functions in the Scikit-Image Python package.¹³⁴ The

coefficient of variation (CV) for individual nuclei, defined as the standard deviation in pixel intensity divided by the mean pixel intensity, was calculated from the NPM1 images using the SciPy Python package. All data were normalized to the no-treatment control in each experiment. NPM1 imaging results for each compound were observed on two separate testing days. Duplicates of treatments were performed and analyzed and are available upon request from the corresponding author.

Computations

Based on the experimental results, we hypothesized that the size, shape or hydrophobicity of the platinum(II) compounds may be instructive in correlating the biological activity with the chemical structure because of biological implications of these structural components in an interaction between two biomolecules that may be disrupted. Thus, we optimized all platinum(II) compounds using density functional theory (DFT) as implemented in Gaussian09¹²³ so that we might quantitatively assess the structural differences and hydrophobicity of the compounds.

Geometry optimizations were performed with an RMS force convergence criterion of 10⁻⁵ hartree. The electronic wavefunction was minimized using the GGA functional PBE,^{124,125} with the DEF2TZP basis set. Relativistic effects were not explicitly included, however, these were not expected to significantly impact the geometries of the platinum(II) complexes.¹²⁶ Solvent was implicitly included using the Solvent Model Density method.¹³⁵

The solvent-dependent difference in Gibbs free energies ($\Delta G_{\text{water-octanol}}$) was calculated using

$$\Delta G_{\text{water-octanol}} = \Delta G_{\text{water}} - \Delta G_{\text{octanol}},$$

where (ΔG_{water}) and ($\Delta G_{\text{octanol}}$) are the change in free energies of the system in water and n-octanol, respectively. (ΔG_{water}) was computed using the structure optimized in the pseudo solvent, water. This optimized structure was kept constant for all subsequent computations, including calculation of the compound in pseudo-solvent, n-octanol, which yielded ($\Delta G_{\text{octanol}}$). This approach minimizes the reorganizational energetic differences. Thus, ($\Delta G_{\text{water-octanol}}$) is a measure of the hydrophobicity for each compound.

Further calculations were required to assess the size and shape of the platinum(II) compounds. Two measures of size were considered, (i) volume, and (ii) the longest vector between the platinum atom and the surface of the molecule. The latter characteristic represents the main steric component of the ligand in each compound.

To quantitatively assess the volume of each compound, a definition of size is necessary. Thus, we will use the presence of electron density to signify the location of the chemical system. Since DFT yields both the electron density and electrostatic potential of the optimized, non-hydrolyzed platinum(II) compound structures and we have previously developed a tool to analyze the electrostatic potential of chemical systems,¹²⁷ we will use the same file format to analyze the electrostatic potential. As a result, the electrostatic potentials of the optimized structures were computed by minimizing the electronic wavefunction using a 500 eV planewave cutoff, a gamma-only k-grid, and the PBE^{124,125} functional utilizing a plane-augmented wave (PAW)^{128,129} basis as implemented in the

Vienna Ab initio Software Package (VASP).^{130–132,136} All compounds were calculated within a sufficiently large computational box to minimize self-interaction.

The electric field is the gradient of the electrostatic potential; thus, the electric field embodies the direction of greatest increase in electrostatic potential. This is significant because the increased slope of the electric field enables us to more clearly define the edge of a chemical system in space. Therefore, deriving the electric field from the electrostatic potential returned by DFT allows us to assess the size of each compound by sampling the electric field. However, to achieve this, definition of a surface needs to be addressed.

We will define the edge of a chemical system as the point where the electric field magnitude no longer changes, which is intuitive considering the definition of the electrostatic potential. Since DFT calculations return electrostatic potential values on the order of 10^{-6} eV, a change in less than 10^{-5} eV is considered negligible. This approach is based on previous atomic radii calculations, which employ negligible change in electron density to assess the size of atoms.^{128,129}

Using the area of each compound defined by sampling the electric field, the longest vector between the platinum atom and the surface was calculated for each compound, capturing the main steric component of each ligand.

APPENDIX C: SUPPLEMENTARY INFORMATION FOR CHAPTER IV

Materials and methods

Materials

Cisplatin used for cell treatment was purchased from Strem Chemicals. Oxaliplatin was purchased from TCI. Unless otherwise state, all other materials were purchased from Millipore Sigma and TCI America. All compounds were synthesized according to previously reported methods with modifications to hydrogenation reactions outlined below. Methyl derivatives (both axial and equatorial) were synthesized according to literature by Abramkin and coworkers. Ethyl derivatives were synthesized according to literature by Galanski and coworkers and Habala and coworkers. The synthesis of DACH-am is described in appendix D.

General procedure for the hydrogenation of methy oxaliplatin derivatives

Diazido starting material (0.8g) was dissolved in 10ml dry methanol. A catalytic amount of Pd/C was added to the solution and the reaction put under hydrogen atmosphere at 1atm. The reaction was allowed to proceed for 2 days. The solution was then filtered over celite and the crude mixture rotovapped to dryness. The crude mixture was then dissolved in water with 2-5 drops of DBU added. 34mg of tetrachloroplatinate was added to the solution. After yellow solid began to precipitate out of solution, the solid was centrifuged to remove the solid. The reaction was continued for up to 6 hours, removing solid via pelleting at various points and air dried. The yield for the axial derivative was 2%. Only 1/6th of the crude mixture was used to coordinate to platinum when forming the equatorial derivative. The yield for the equatorial derivative was approximately 6%.

General procedure for the hydrogenation of ethyl oxaliplatin derivatives

Diazo starting material was dissolved in 5ml methanol. Triphenyl phosphine was added in a 1:1.5 ratio diazide:triphenylphosphine. The reaction was refluxed for 1 hour then allowed to cool. After, 2ml water were added to the reaction mixture and the mixture was filtered through cotton. The solution was then coordinated to 50mg tetrachloroplatinate with 2-5 drops DBU for up to 6 hours to yield a yellow solid as the product. The solid was centrifuged and collected in multiple fractions and air dried. A pink product may also be present which should be separated by pelleting fractions throughout the reaction.

Synthesis of DACHene

1,2diamino 3-cyclohexene (50mg, 0.45mmol) is dissolved in 1ml water with DBU (137mg, 0.9mmol). Tetrachloroplatinate (187mg, 0.45mmol) is added to the reaction and allowed to react for 2 days. The yellow solid is then centrifuged and collected. The solid is allowed to air dry (15% yield).

Cell culture and treatment

A549 human lung carcinoma cells (#CCL-185, American Type Culture Collection) were cultured at 37°C, 5% CO₂ in Dulbecco's Modified Eagle Medium (DMEM) supplemented with 10% Fetal Bovine Serum (FBS) and 1% antibiotic-antimycotic. Treatments were conducted on cells that had been grown for 10-30 passages to 70% confluency. Cells were treated for 24 hours at 10 μM in order to compare to previous literature. 5mM stock solutions of all compounds were made in water (oxaliplatin), DMF (AxMe-Pt, EqMe-Pt), or DMSO (DACH-ene, AxEt-Pt, EqEt-Pt, Actinomycin D). Stock solutions were diluted into media immediately prior to drug treatment.

Immunofluorescence

Cells to be imaged were grown on coverslips (Ted Pella product no 260368, Round glass coverslips, 10mm diam, 0.16-0.19mm thick) as described above. After treatment, cells were washed twice with phosphate buffered saline (PBS) and fixed for 20 minutes at room temperature in 4% paraformaldehyde in PBS. PFA was removed via aspiration and cells were then permeabilized with 0.5% Triton-X in PBS for 20 minutes at room temperature. Two ten minute blocking steps were performed with 1% bovine serum albumin (BSA) in PBST (PBS with 0.1% Tween-20). Cells were incubated for one hour in primary antibody (NPM1 Monoclonal Antibody, FC-61991, from Thermo Fisher, 1:200 dilution in PBST with 1% BSA) and 1 hour in secondary antibody (Goat Anti-Mouse IgG H&L Alexa Fluor® 488, ab150113, Abcam, 1:1000 dilution in PBST with 1% BSA), with 3 five minute wash steps using PBST between incubations, and were washed in the same manner again before mounting slides. Coverslips were mounted on slides with ProLong™ Diamond Antifade Mountant with DAPI (Thermo Fisher) according to manufacturer's instructions.

Image processing and quantification

Images were taken using a HC PL Fluotar 63x/1.3 oil objective mounted on a Leica DMI8 fluorescence microscope with Leica Application Suite X software. Quantification of NPM1 relocalization was performed in an automated fashion using a Python 3 script. Images were preprocessed in ImageJ^{2,3} to convert the DAPI and NPM1 channels into separate 16-bit greyscale images. Between 70 and 225 cells were analyzed for each treatment group. Nuclei segmentation was determined with the DAPI images using Li thresholding functions in the Scikit- Image Python package. The coefficient of variation

(CV) for individual nuclei, defined as the standard deviation in pixel intensity divided by the mean pixel intensity, was calculated from the NPM1 images using the SciPy Python package. All data were normalized to the notreatment control in each experiment. NPM1 imaging results for each compound were observed on a minimum of two separate testing days. Data are represented as boxplots generated using Seaborn within Python.

Log P Measurements

Water was mixed with octanol for 24 hours and left to stand for an additional 24 hours to obtain water-saturated octanol and octanol-saturated water that were used for determining partition coefficients. Measurements of the partition coefficients were performed using classical shake flask method according to OECD guidelines. Saturated solutions were created by dissolving compounds in octanol saturated water. Excess solid was filtered out using a 0.2 μm filter. The octanol-saturated water mixtures were mixed with water-saturated octanol in a 1:1 ratio and vortexed for 30 minutes. The mixtures were then centrifuged for 30 minutes and 0.5 mL samples obtained. The samples were quantified using ICP-MS to determine the concentration of platinum in the mixture. Since octanol solutions are incompatible with some ICP-MS, we quantified the original saturated stock solutions and assumed that the difference between the concentration found in the water solutions and the stock solution represented the platinum present in the octanol solution. LogP was calculated using the concentrations obtained from ICP-MS.

NMR Spectra

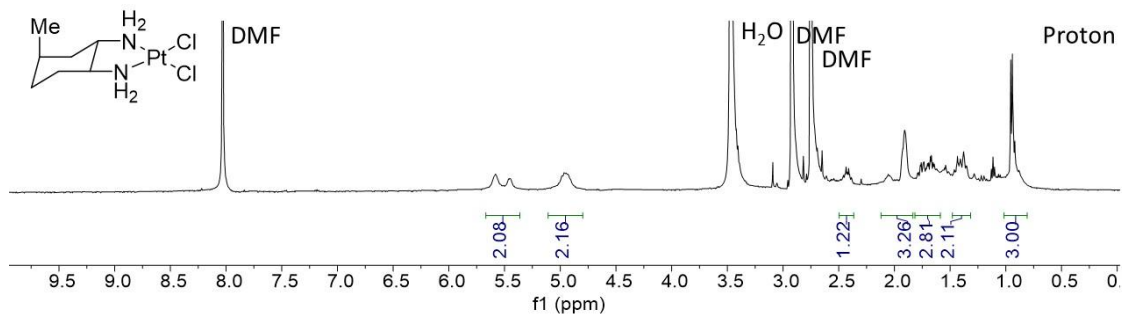


Figure C.1 NMR for EqMe-Pt

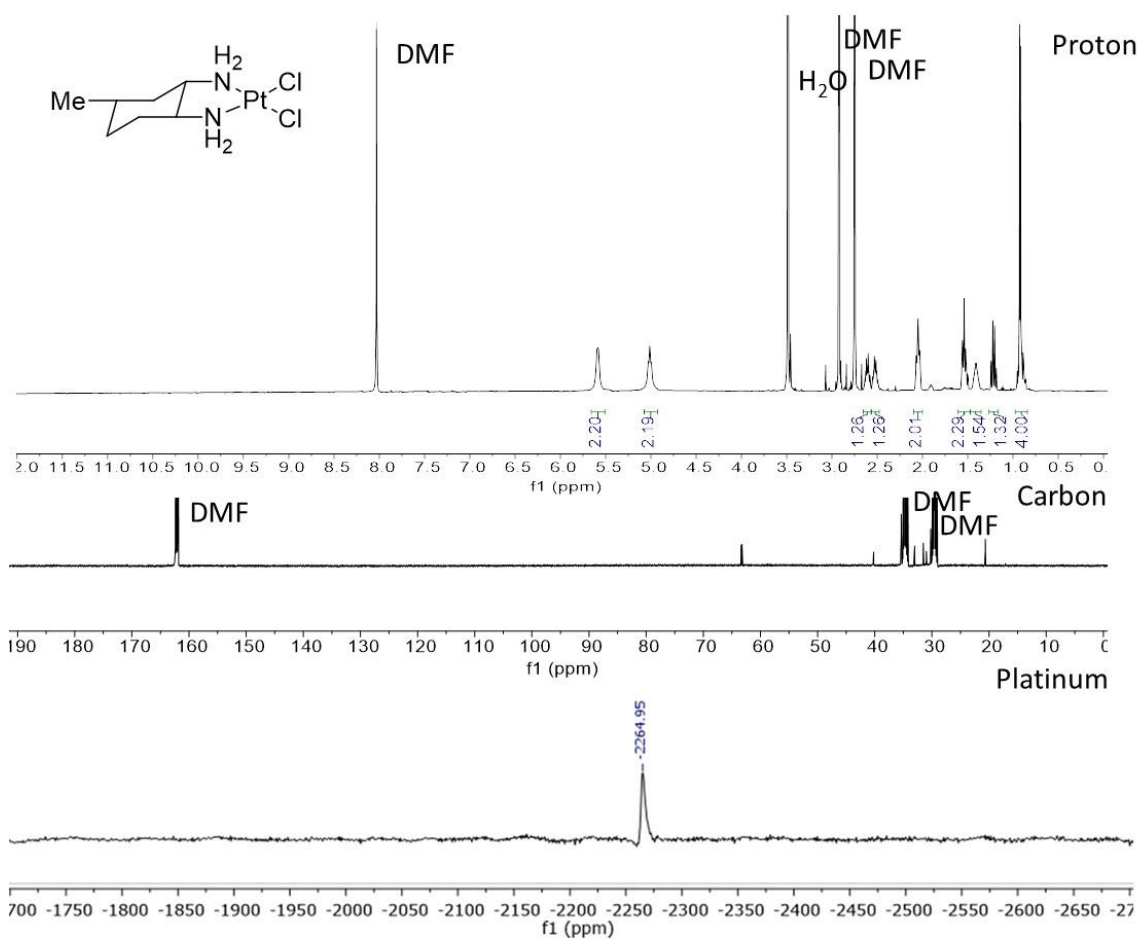


Figure C.2 NMR for AxMe-Pt

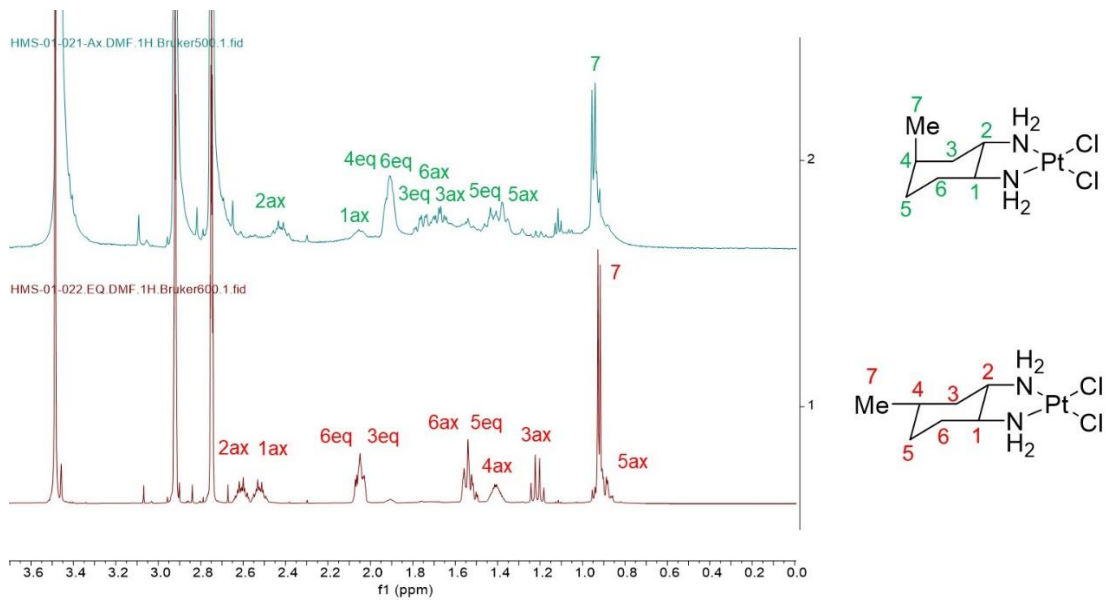


Figure C.3 Stacked NMR showing AxMe-Pt and EqMe-Pt

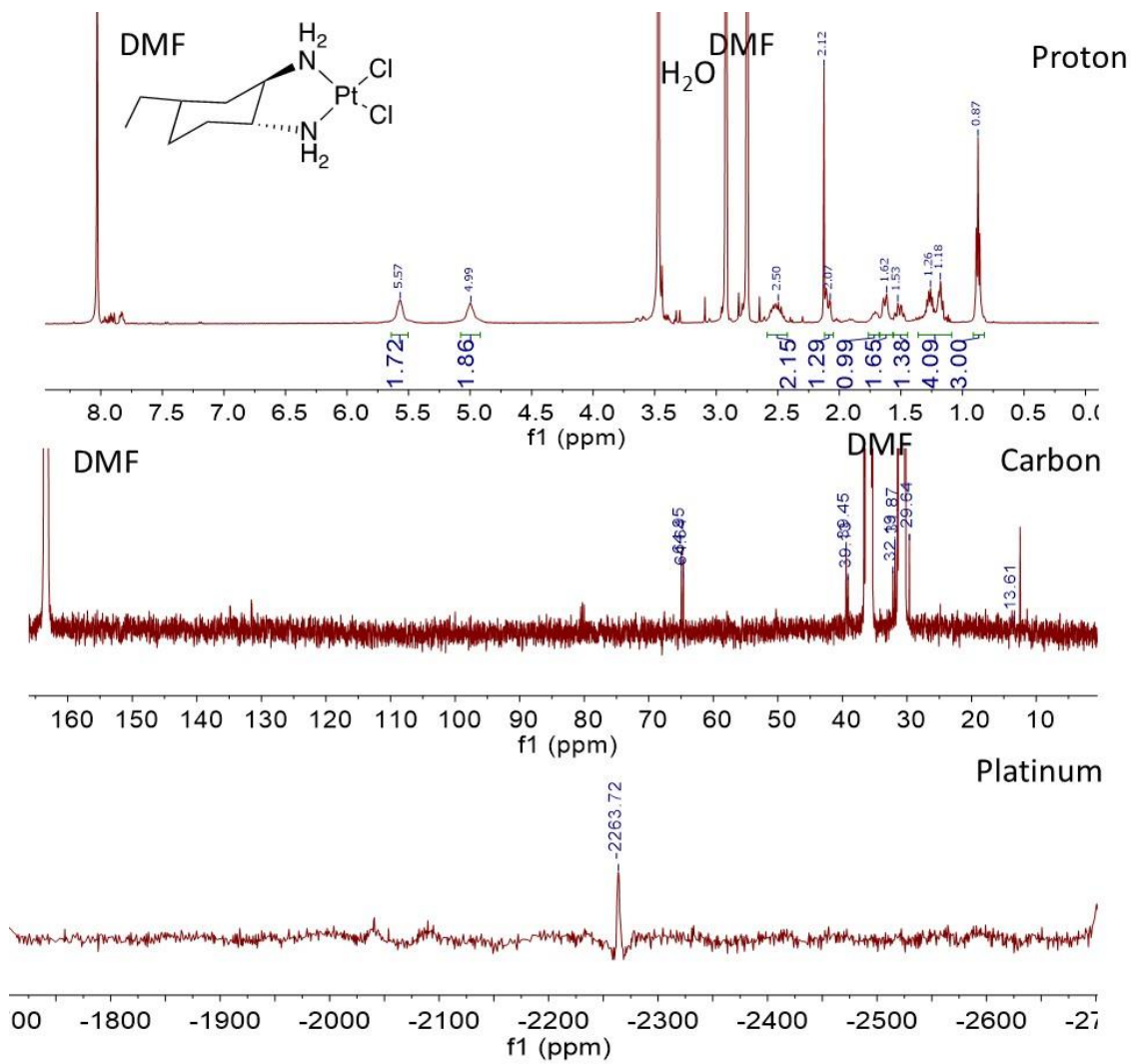


Figure C.3 NMR for EqEt-Pt

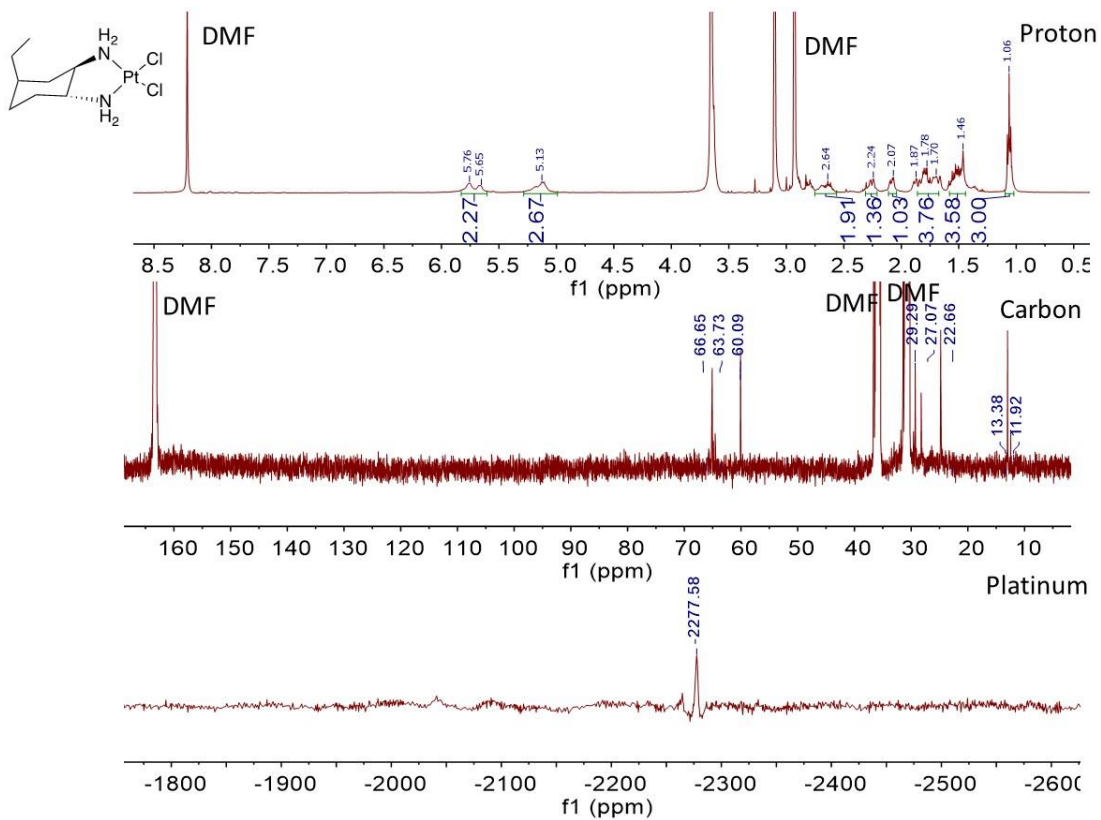


Figure C.4 NMR for AxEt-Pt

Cyclopropene Supplemental material and methods

Materials

Unless otherwise noted, all materials were purchased from Millipore sigma or TCI America.

Synthesis scheme 1

The synthesis of compounds **1, 2, 3 and 4** followed previously reported methods.

NHS ester cyclopropene

A solution of cyclopropene carboxylic acid (152mg, 1.5mmol), NHS (258mg, 2.25mmol), and EDC (278mg, 1.8mmol) in 3ml DCM was stirred overnight at room temperature in the dark. The reaction mixture was washed with saturated ammonium chloride (2x) and brine (1x). The organic phase was dried with sodium sulfate and evaporated to yield 236mg (80%) as a sweet-smelling orange oil.

1,2-(ditert-butyl) 2-cyclopropene propane (5)

1,3-diboc 2-aminepropane (249mg, 0.86mmol), NHS ester cyclopropene (124mg, 0.64mmol) was added to 10ml DCM and 1ml triethyl amine. The solution was reacted overnight and protected from light. The reaction mixture was dried *in vacuo* and recrystallized in ethyl acetate. The filtrate was collected and dried to produce a pale yellow solid. The solid was dissolved in DCM and washed 8 times with 1M HCl. The organic phase was dried with sodium sulfate and evaporated

Cis-[1,3-diamino 2-(cyclopropene)propane]dichloride platinum (7)

A 1:1 molar equivalent of Pt(DMSO)₂Cl₂ or PtCl₄ and **5** are added to 4 equivalents of DBU to prevent the cyclopropene from being degraded. The reaction is stirred for 2 days in the dark followed by the reaction mixture being added dropwise to ice cold water. A yellow solid precipitates out of solution after stirring for 1 hour on ice. The precipitate is pelleted and washed with water (3x). The solid was washed with ether (1x) and allowed to dry.

Synthesis Scheme 2

The synthesis of compounds **3, 8 and 9** have been previously reported.

Cis-[1,2,3 triaminopropane]dichloride platinum (10)

1,3 platin (30mg, 0.08mmol) was dissolved in 5ml DMF with a catalytic amount of Pd/C. The reaction was reacted for 2 days under a hydrogen atmosphere at 1atm. The reaction was then filtered over celite and moved to the next reaction without purification.

Cis-[1,3-diamino 2-(cyclopropene)propane]dichloride platinum (7)

NHS ester cyclopropene was added to the crude mixture obtained from compound **10** along with triethyl amine (1ml). The reaction was shielded from light and allowed to react for 2 days. The crude mixture was rotovapped and dried.

Oxaliplatin mimic supplemental methods

Materials

Unless otherwise noted, all materials were Millipore sigma or TCI. The synthesis of compounds **11, 12, 13, and 14** are previously reported and modifications to the procedures shown below.

1,2-(ditert-butyl carbamate) 4-cyclohexene (11)

Boc₂O (1.56g, #mol) was added dropwise to a solution of 1,2-diamino 3-cyclopropene (209mg, #mol) at 0 °C. To the solution 1ml of triethylamine was added and reacted for 1 hour. The reaction was then rotovapped and dried to produce a white solid in quantitative yield.

1,2-(ditert-butyl carbamate) 4-acetamide cyclohexane (12)

Hg(NO₃)₂ (2g, 6.15mmol) was added to 10ml acetonitrile at 0 °C. Compound **11** (599mg, 1.9mmol) was added dropwise and reacted for 1 hour. The solution gradually became orange as the reaction proceeded. After, 10ml of 3M NaOH was added to the reaction followed by a 10% solution (W/V) of NaBH₄ in 3M NaOH was added. Upon addition of NaOH and NaBH₄ black metallic mercury is produced. It is allowed to react for another hour. The solution was filtered over celite and extracted using ethyl acetate (50mlx2). The ethyl acetate is dried using magnesium sulfate and rotovapped. The crude mixture is then separated using a silica column (20:1 DCM:methanol) to yield 225mg of a white solid (31% yield).

Cis-[1,2diamiono 4-acetamide cyclohexane]dichloride platinum (DACH-Am) (14)

Compound **12** (130mg, 0.34mmol) is reacted for 1 hour in 4M HCl in dioxane and then dried until the solid is no longer acidic. The salt is then dissolved in 1ml of water and DBU (69mg, 0.45mmol). Tetrachloroplatinate (180mg, 0.43mol) is then added and allowed to react overnight. The precipitated yellow or brown solid is centrifuged and allowed to air dry. If a yellow solid is produced, the product becomes brown after being allowed to air dry including when the product is shielded from light. DACH-am is produced in 71% yield (105mg).

Azide Oxaliplatin mimic (15)

DACH-am (105mg, 0.24mmol) was added to 5ml 3M HCl with 125 μ L TFA. The reaction mixture was refluxed for 1 day. The solution was neutralized using 3M NaOH and the NHS ester of 4-azido butanoic acid (127mg, 0.55mmol) was added. The solution was allowed to react for 1 day then another 125mg of 4-azido butanoic acid was added. The solution was rotovapped to dryness. TLC analysis shows the separation of 2 products using water as the mobile phase.

Supplemental NMRs

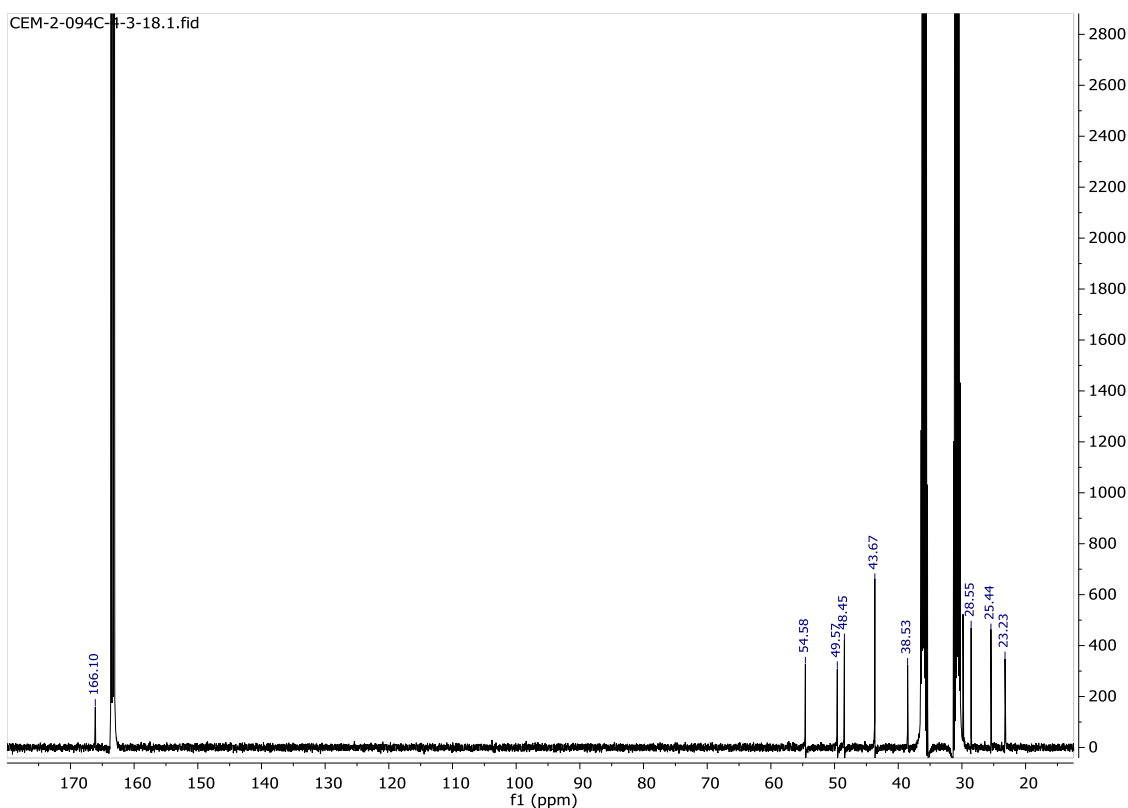


Figure D.1 Carbon NMR from cyclopropene scheme 1 compound **7** showing lack of electron rich double bond peaks around 95 and 115ppm.

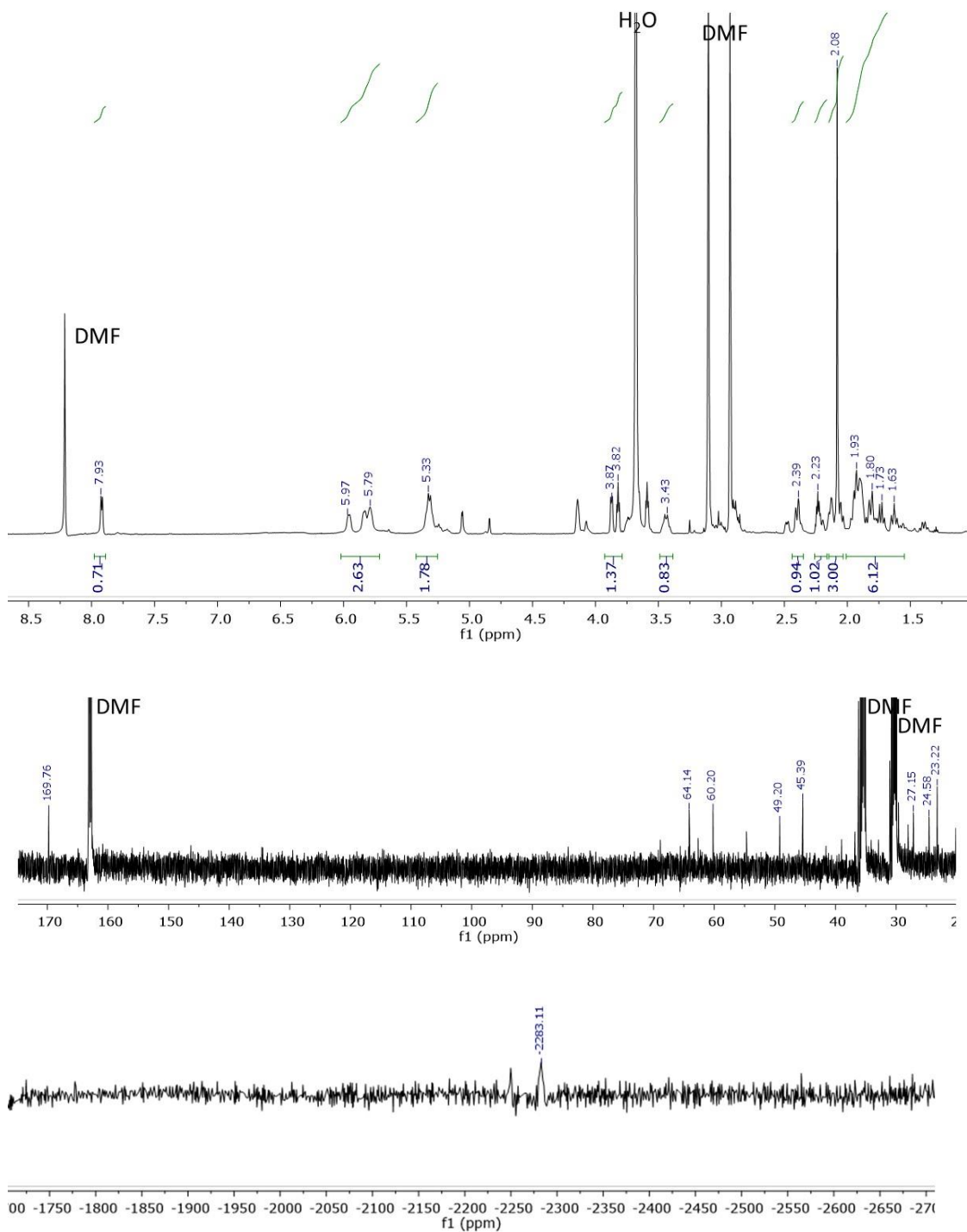


Figure D.3 NMRs of DACH-am

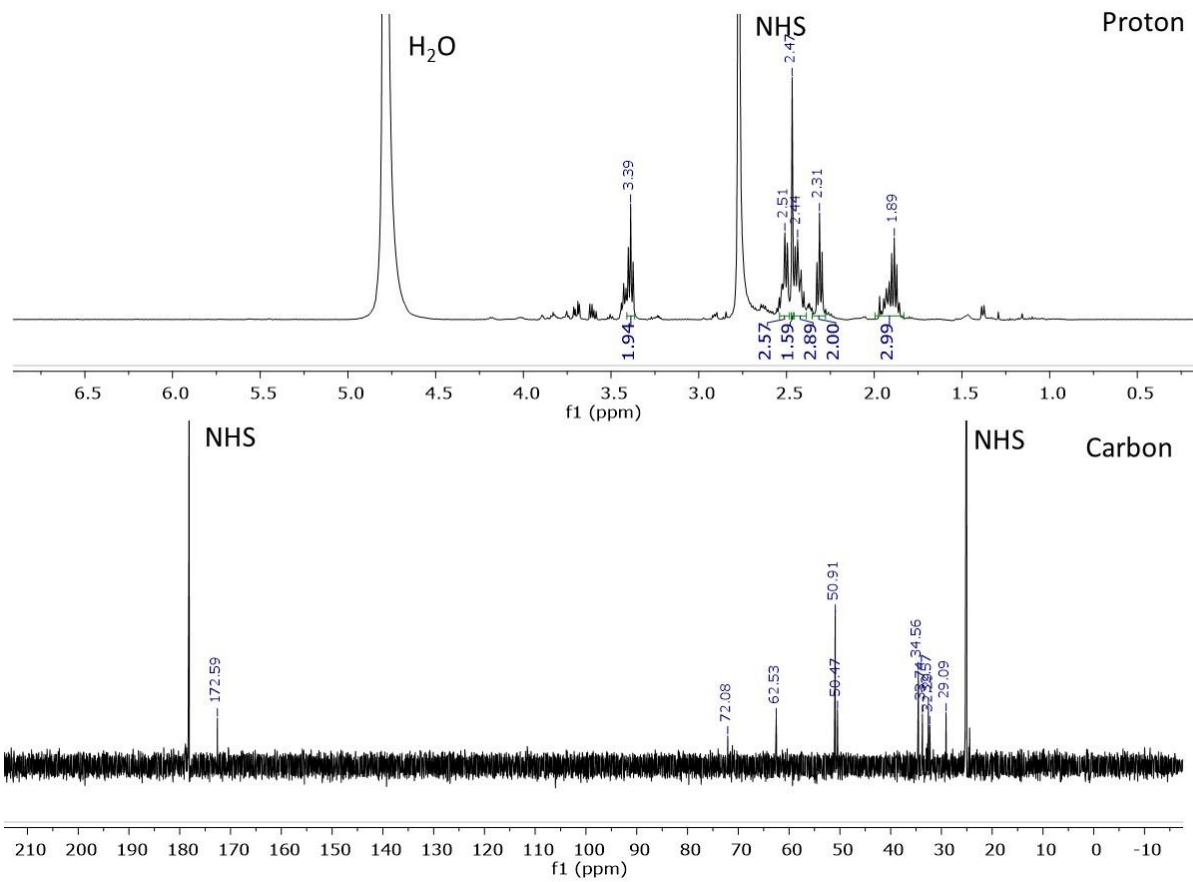


Figure D.4 Crude NMRs of azide containing oxaliplatin mimic (compound 15)

REFERENCES CITED

- (1) Discovery – Cisplatin and The Treatment of Testicular and Other Cancers - National Cancer Institute
<https://www.cancer.gov/research/progress/discovery/cisplatin> (accessed 2020 -09 -02).
- (2) Rosenberg, B.; Van Camp, L.; Krigas, T. Inhibition of Cell Division in Escherichia Coli by Electrolysis Products from a Platinum Electrode. *Nature* **1965**, *205* (4972), 698–699. <https://doi.org/10.1038/205698a0>.
- (3) Loretta VanCamp: Spartan, lab supervisor, lifesaver
<https://msutoday.msu.edu/news/2020/loretta-vancamp-spartan-lab-supervisor-lifesaver> (accessed 2021 -08 -03).
- (4) Rosenberg, B.; Camp, L. V.; Grimley, E. B.; Thomson, A. J. The Inhibition of Growth or Cell Division in Escherichia Coli by Different Ionic Species of Platinum(IV) Complexes. *Journal of Biological Chemistry* **1967**, *242* (6), 1347–1352. [https://doi.org/10.1016/S0021-9258\(18\)96186-7](https://doi.org/10.1016/S0021-9258(18)96186-7).
- (5) In Remembrance of Barnett Rosenberg. *Dalton Transactions* **2009**, *0* (48), 10648–10650. <https://doi.org/10.1039/B918993A>.
- (6) Kelland, L. The Resurgence of Platinum-Based Cancer Chemotherapy. *Nature Reviews Cancer* **2007**, *7* (8), nrc2167. <https://doi.org/10.1038/nrc2167>.
- (7) Wang, D.; Lippard, S. J. Cellular Processing of Platinum Anticancer Drugs. *Nature Reviews Drug Discovery* **2005**, *4* (4), 307–320. <https://doi.org/10.1038/nrd1691>.
- (8) Muhammad, N.; Guo, Z. Metal-Based Anticancer Chemotherapeutic Agents. *Current Opinion in Chemical Biology* **2014**, *19*, 144–153. <https://doi.org/10.1016/j.cbpa.2014.02.003>.
- (9) Johnstone, T. C.; Park, G. Y.; Lippard, S. J. Understanding and Improving Platinum Anticancer Drugs – Phenanthriplatin. *Anticancer Res* **2014**, *34* (1), 471–476.
- (10) Lazić, A.; Popović, J.; Paunesku, T.; Woloschak, G. E.; Stevanović, M. Insights into Platinum-Induced Peripheral Neuropathy–Current Perspective. *Neural Regen Res* **2020**, *15* (9), 1623–1630. <https://doi.org/10.4103/1673-5374.276321>.
- (11) Wang, D.; Lippard, S. J. Cellular Processing of Platinum Anticancer Drugs. *Nature Reviews Drug Delivery* **2005**, *4* (4), 307–320. <https://doi.org/10.1038/nrd1691>.

- (12) Groessl, M.; Zava, O.; Dyson, P. J. Cellular Uptake and Subcellular Distribution of Ruthenium-Based Metallodrugs under Clinical Investigation versus Cisplatin. *Metallomics* **2011**, *3* (6), 591–599. <https://doi.org/10.1039/C0MT00101E>.
- (13) DeConti, R. C.; Toftness, B. R.; Lange, R. C.; Creasey, W. A. Clinical and Pharmacological Studies with Cis-Diamminedichloroplatinum (II). *Cancer Res* **1973**, *33* (6), 1310–1315.
- (14) Akaboshi, M.; Kawai, K.; Maki, H.; Akuta, K.; Ujeno, Y.; Miyahara, T. The Number of Platinum Atoms Binding to DNA, RNA and Protein Molecules of HeLa Cells Treated with Cisplatin at Its Mean Lethal Concentration. *Jpn J Cancer Res* **1992**, *83* (5), 522–526. <https://doi.org/10.1111/j.1349-7006.1992.tb01959.x>.
- (15) Jamieson, E. R.; Lippard, S. J. Structure, Recognition, and Processing of Cisplatin–DNA Adducts. *Medicinal Chemistry* **1999**. <https://doi.org/10.1021/cr980421n>.
- (16) Chaney, S. G.; Campbell, S. L.; Bassett, E.; Wu, Y. Recognition and Processing of Cisplatin- and Oxaliplatin-DNA Adducts. *Critical Reviews in Oncology/Hematology* **2005**, *53* (1), 3–11. <https://doi.org/10.1016/j.critrevonc.2004.08.008>.
- (17) Wexselblatt, E.; Yavin, E.; Gibson, D. Cellular Interactions of Platinum Drugs. *Inorganica Chimica Acta* **2012**, *393*, 75–83. <https://doi.org/10.1016/j.ica.2012.07.013>.
- (18) Bruno, P. M.; Liu, Y.; Park, G. Y.; Murai, J.; Koch, C. E.; Eisen, T. J.; Pritchard, J. R.; Pommier, Y.; Lippard, S. J.; Hemann, M. T. A Subset of Platinum-Containing Chemotherapeutic Agents Kills Cells by Inducing Ribosome Biogenesis Stress. *Nature Medicine* **2017**, *23* (4), 461–471. <https://doi.org/10.1038/nm.4291>.
- (19) Bruno, P. M.; Liu, Y.; Park, G. Y.; Murai, J.; Koch, C. E.; Eisen, T. J.; Pritchard, J. R.; Pommier, Y.; Lippard, S. J.; Hemann, M. T. A Subset of Platinum-Containing Chemotherapeutic Agents Kills Cells by Inducing Ribosome Biogenesis Stress. *Nature Medicine* **2017**, *23* (4), 461–471. <https://doi.org/10.1038/nm.4291>.
- (20) Tsai, R. Y. L.; Pederson, T. Connecting the Nucleolus to the Cell Cycle and Human Disease. *FASEB journal : official publication of the Federation of American Societies for Experimental Biology* **2014**, *28* (8), 3290–3296. <https://doi.org/10.1096/fj.14-254680>.

- (21) Woods, S. J.; Hannan, K. M.; Pearson, R. B.; Hannan, R. D. The Nucleolus as a Fundamental Regulator of the P53 Response and a New Target for Cancer Therapy. *Biochimica et Biophysica Acta (BBA) - Gene Regulatory Mechanisms* **2015**, *1849* (7), 821–829. <https://doi.org/10.1016/j.bbagr.2014.10.007>.
- (22) Boulon, S.; Westman, B. J.; Hutten, S.; Boisvert, F.-M. M.; Lamond, A. I. The Nucleolus under Stress. *Molecular Cell* **2010**, *40* (2), 216–227. <https://doi.org/10.1016/j.molcel.2010.09.024>.
- (23) Farley-Barnes, K. I.; McCann, K. L.; Ogawa, L. M.; Merkel, J.; Surovtseva, Y. V.; Baserga, S. J. Diverse Regulators of Human Ribosome Biogenesis Discovered by Changes in Nucleolar Number. *Cell Reports* **2018**, *22* (7), 1923–1934. <https://doi.org/10.1016/j.celrep.2018.01.056>.
- (24) Pickard, A. J.; Bierbach, U. The Cell's Nucleolus: An Emerging Target for Chemotherapeutic Intervention. *ChemMedChem* **2013**, *8* (9), 1441–1449. <https://doi.org/10.1002/cmdc.201300262>.
- (25) Wirth, R.; White, J. D.; Moghaddam, A. D.; Ginzburg, A. L.; Zakharov, L. N.; Haley, M. M.; DeRose, V. J. Azide vs. Alkyne Functionalization in Pt(II) Complexes for Post-Treatment Click Modification: Solid State Structure, Fluorescent Labeling, and Cellular Fate. *Journal of the American Chemical Society* **2015**, No. Ii, jacs.5b09108. <https://doi.org/10.1021/jacs.5b09108>.
- (26) Plakos, K.; DeRose, V. J. Mapping Platinum Adducts on Yeast Ribosomal RNA Using High-Throughput Sequencing. *Chemical Communications* **2017**, *53* (95), 12746–12749. <https://doi.org/10.1039/C7CC06708A>.
- (27) Hostetter, A. A.; Osborn, M. F.; DeRose, V. J. Characterization of RNA-Pt Adducts Formed from Cisplatin Treatment of *Saccharomyces Cerevisiae*. *ACS Chem Biol.* **2012**, *7* (1), 218–225. <https://doi.org/10.1021/cb200279p.Characterization>.
- (28) Osborn, M. F.; White, J. D.; Haley, M. M.; DeRose, V. J. Platinum-RNA Modifications Following Drug Treatment in *S. Cerevisiae* Identified by Click Chemistry and Enzymatic Mapping. *ACS chemical biology* **2014**, No. Ii. <https://doi.org/10.1021/cb500395z>.
- (29) Melnikov, S. V.; Soll, D.; Steitz, T. A.; Polikanov, Y. S. Insights into RNA Binding by the Anticancer Drug Cisplatin from the Crystal Structure of Cisplatin-Modified Ribosome. *Nucleic acids research* **2016**, *44* (10), 4978–4987. <https://doi.org/10.1093/nar/gkw246>.
- (30) Rijal, K.; Chow, C. S. A New Role for Cisplatin: Probing Ribosomal RNA Structure. *Chem. Commun.* **2007**, *0* (1). <https://doi.org/10.1039/B816633A>.

- (31) Saunders, A. M.; DeRose, V. J. Beyond Mg²⁺: Functional Interactions between RNA and Transition Metals. *Current Opinion in Chemical Biology* **2016**, *31*, 153–159. <https://doi.org/10.1016/j.cbpa.2016.02.015>.
- (32) Sutton, E. C.; McDevitt, C. E.; Yglesias, M. V.; Cunningham, R. M.; DeRose, V. J. Tracking the Cellular Targets of Platinum Anticancer Drugs: Current Tools and Emergent Methods. *Inorganica Chimica Acta* **2019**, 118984. <https://doi.org/10.1016/j.ica.2019.118984>.
- (33) White, J. D.; Haley, M. M.; DeRose, V. J. Multifunctional Pt(II) Reagents: Covalent Modifications of Pt Complexes Enable Diverse Structural Variation and In-Cell Detection. *Acc. Chem. Res.* **2016**, *49* (1), 56–66. <https://doi.org/10.1021/acs.accounts.5b00322>.
- (34) Wexselblatt, E.; Yavin, E.; Gibson, D. Cellular Interactions of Platinum Drugs. *Inorganica Chimica Acta* **2012**, *393*, 75–83. <https://doi.org/10.1016/j.ica.2012.07.013>.
- (35) Galanski, M.; Yasemi, A.; Slaby, S.; Jakupec, M. A.; Arion, V. B.; Rausch, M.; Nazarov, A. A.; Keppler, B. K. Synthesis, Crystal Structure and Cytotoxicity of New Oxaliplatin Analogues Indicating That Improvement of Anticancer Activity Is Still Possible. *European Journal of Medicinal Chemistry* **2004**, *39* (8), 707–714. <https://doi.org/10.1016/j.ejmech.2004.04.003>.
- (36) Rijal, K.; Bao, X.; Chow, C. S. Amino Acid-Linked Platinum(II) Analogues Have Altered Specificity for RNA Compared to Cisplatin. *Chem. Commun.* **2014**, *50* (30), 3918–3920. <https://doi.org/10.1039/C3CC49035A>.
- (37) Kitteringham, E.; Wu, D.; Cheung, S.; Twamley, B.; O’Shea, D. F.; Griffith, D. M. Development of a Novel Carboplatin like Cytoplasmic Trackable near Infrared Fluorophore Conjugate via Strain-Promoted Azide Alkyne Cycloaddition. *Journal of Inorganic Biochemistry* **2018**, *182*, 150–157. <https://doi.org/10.1016/j.jinorgbio.2018.02.010>.
- (38) Kalayda, G. V.; Kullmann, M.; Galanski, M.; Gollos, S. A Fluorescent Oxaliplatin Derivative for Investigation of Oxaliplatin Resistance Using Imaging Techniques. *J Biol Inorg Chem* **2017**, *22* (8), 1295–1304. <https://doi.org/10.1007/s00775-017-1502-z>.
- (39) Ramu, V.; Gautam, S.; Garai, A.; Kondaiah, P.; Chakravarty, A. R. Glucose-Appended Platinum(II)-BODIPY Conjugates for Targeted Photodynamic Therapy in Red Light. *Inorganic Chemistry* **2018**, *57* (4), 1717–1726. <https://doi.org/10.1021/acs.inorgchem.7b02249>.

- (40) Xue, X.; Zhu, C.; Chen, H.; Bai, Y.; Shi, X.; Jiao, Y.; Chen, Z.; Miao, Y.; He, W.; Guo, Z. A New Approach to Sensitize Antitumor Monofunctional Platinum(II) Complexes via Short Time Photo-Irradiation. *Inorg. Chem.* **2017**, *56* (7), 3754–3762. <https://doi.org/10.1021/acs.inorgchem.6b02148>.
- (41) Yao, X.; Tracy, C. M.; Bierbach, U. Cysteine-Directed Bioconjugation of a Platinum(II)–Acridine Anticancer Agent. *Inorg. Chem.* **2019**, *58* (1), 43–46. <https://doi.org/10.1021/acs.inorgchem.8b02717>.
- (42) Yuan, Y.; Liu, B. Visualization of Drug Delivery Processes Using AIEgens. *Chemical Science* **2017**, *8* (4), 2537–2546. <https://doi.org/10.1039/C6SC05421H>.
- (43) Mayr, J.; Hager, S.; Koblmüller, B.; Klose, M. H. M.; Holste, K.; Fischer, B.; Pelivan, K.; Berger, W.; Heffeter, P.; Kowol, C. R.; Keppler, B. K. EGFR-Targeting Peptide-Coupled Platinum(IV) Complexes. *J Biol Inorg Chem* **2017**, *22* (4), 591–603. <https://doi.org/10.1007/s00775-017-1450-7>.
- (44) Kolb, H. C.; Finn, M. G.; Sharpless, K. B. Click Chemistry: Diverse Chemical Function from a Few Good Reactions. *Angew. Chem. Int. Ed. Engl.* **2001**, *40* (11), 2004–2021.
- (45) Cunningham, R. M.; Hickey, A. M.; Wilson, J. W.; Plakos, K. J. I.; DeRose, V. J. Pt-Induced Crosslinks Promote Target Enrichment and Protection from Serum Nucleases. *Journal of Inorganic Biochemistry* **2018**, *189*, 124–133. <https://doi.org/10.1016/j.jinorgbio.2018.09.007>.
- (46) Urankar, D.; Košmrlj, J. Preparation of Diazenecarboxamide–Carboplatin Conjugates by Click Chemistry. *Inorganica Chimica Acta* **2010**, *363* (14), 3817–3822. <https://doi.org/10.1016/j.ica.2010.07.031>.
- (47) Moghaddam, A. D.; White, J. D.; Cunningham, R. M.; Loes, A. N.; Haley, M. M.; DeRose, V. J. Convenient Detection of Metal–DNA, Metal–RNA, and Metal–Protein Adducts with a Click-Modified Pt(II) Complex. *Dalton Trans.* **2015**, *44* (8), 3536–3539. <https://doi.org/10.1039/C4DT02649G>.
- (48) Cunningham, R. M.; DeRose, V. J. Platinum Binds Proteins in the Endoplasmic Reticulum of *S. Cerevisiae* and Induces Endoplasmic Reticulum Stress. *ACS Chem. Biol.* **2017**. <https://doi.org/10.1021/acscchembio.7b00553>.
- (49) Osborn, M. F.; White, J. D.; Haley, M. M.; DeRose, V. J. Platinum-RNA Modifications Following Drug Treatment in *S. Cerevisiae* Identified by Click Chemistry and Enzymatic Mapping. *ACS Chem. Biol.* **2014**, *9* (10), 2404–2411. <https://doi.org/10.1021/cb500395z>.

- (50) Zacharioudakis, E.; Agarwal, P.; Bartoli, A.; Abell, N.; Kunalingam, L.; Bergoglio, V.; Xhemalce, B.; Miller, K. M.; Rodriguez, R. Chromatin Regulates Genome Targeting with Cisplatin. *Angew Chem Int Ed Engl* **2017**, *56* (23), 6483–6487. <https://doi.org/10.1002/anie.201701144>.
- (51) Qiao, X.; Ding, S.; Liu, F.; Kucera, G. L.; Bierbach, U. Investigating the Cellular Fate of a DNA-Targeted Platinum-Based Anticancer Agent by Orthogonal Double-Click Chemistry. *J Biol Inorg Chem* **2014**, *19* (3), 415–426. <https://doi.org/10.1007/s00775-013-1086-1>.
- (52) Ding, S.; Qiao, X.; Suryadi, J.; Marrs, G. S.; Kucera, G. L.; Bierbach, U. Using Fluorescent Post-Labeling To Probe the Subcellular Localization of DNA-Targeted Platinum Anticancer Agents. *Angewandte Chemie International Edition* **2013**, *52* (12), 3350–3354. <https://doi.org/10.1002/anie.201210079>.
- (53) Cañeque, T.; Müller, S.; Rodriguez, R. Visualizing Biologically Active Small Molecules in Cells Using Click Chemistry. *Nature Reviews Chemistry* **2018**, *2* (9), 202. <https://doi.org/10.1038/s41570-018-0030-x>.
- (54) Kelland, L. The Resurgence of Platinum-Based Cancer Chemotherapy. *Nature reviews. Cancer* **2007**, *7* (8), 573–584. <https://doi.org/10.1038/nrc2167>.
- (55) Wexselblatt, E.; Yavin, E.; Gibson, D. Cellular Interactions of Platinum Drugs. *Inorganica Chimica Acta* **2012**, *393*, 75–83. <https://doi.org/10.1016/j.ica.2012.07.013>.
- (56) Rubbi, C. P.; Milner, J. Disruption of the Nucleolus Mediates Stabilization of P53 in Response to DNA Damage and Other Stresses. *EMBO Journal* **2003**, *22* (22), 6068–6077. <https://doi.org/10.1093/emboj/cdg579>.
- (57) Yang, K.; Wang, M.; Zhao, Y.; Sun, X.; Yang, Y.; Li, X.; Zhou, A.; Chu, H.; Zhou, H.; Xu, J.; Wu, M.; Yang, J.; Yi, J. A Redox Mechanism Underlying Nucleolar Stress Sensing by Nucleophosmin. *Nature Communications* **2016**, *7*, 13599. <https://doi.org/10.1038/ncomms13599>.
- (58) Bursac, S.; Brdovcak, M. C.; Donati, G.; Volarevic, S. Activation of the Tumor Suppressor P53 upon Impairment of Ribosome Biogenesis. *Biochimica et biophysica acta* **2014**, *1842* (6), 817–830. <https://doi.org/10.1016/j.bbadis.2013.08.014>.
- (59) Nicolas, E.; Parisot, P.; Pinto-Monteiro, C.; de Walque, R.; De Vleeschouwer, C.; Lafontaine, D. L. J. Involvement of Human Ribosomal Proteins in Nucleolar Structure and P53-Dependent Nucleolar Stress. *Nature Communications* **2016**, *7* (June), 11390. <https://doi.org/10.1038/ncomms11390>.

- (60) McDevitt, C. E.; Yglesias, M. V.; Mroz, A. M.; Sutton, E. C.; Yang, M. C.; Hendon, C. H.; DeRose, V. J. Monofunctional Platinum(II) Compounds and Nucleolar Stress: Is Phenanthriplatin Unique? *J Biol Inorg Chem* **2019**. <https://doi.org/10.1007/s00775-019-01707-9>.
- (61) Faivre, S.; Chan, D.; Salinas, R.; Woynarowska, B.; Woynarowski, J. M. DNA Strand Breaks and Apoptosis Induced by Oxaliplatin in Cancer Cells. *Biochemical Pharmacology* **2003**, *66* (2), 225–237. [https://doi.org/10.1016/S0006-2952\(03\)00260-0](https://doi.org/10.1016/S0006-2952(03)00260-0).
- (62) Jerremalm, E.; Videhult, P.; Alvelius, G.; Griffiths, W. J.; Bergman, T.; Eksborg, S.; Ehrsson, H. Alkaline Hydrolysis of Oxaliplatin—Isolation and Identification of the Oxalato Monodentate Intermediate. *Journal of Pharmaceutical Sciences* **2002**, *91* (10), 2116–2121. <https://doi.org/10.1002/jps.10201>.
- (63) Zacharioudakis, E.; Agarwal, P.; Bartoli, A.; Abell, N.; Kunalingam, L.; Bergoglio, V.; Xhemalce, B.; Miller, K. M.; Rodriguez, R. Chromatin Regulates Genome Targeting with Cisplatin. *Angewandte Chemie* **2017**, *129* (23), 6583–6587. <https://doi.org/10.1002/ange.201701144>.
- (64) Brunner, H.; Schellerer, K.-M. New Porphyrin Platinum Conjugates for the Cytostatic and Photodynamic Tumor Therapy. *Inorganica Chimica Acta* **2003**, *350*, 39–48. [https://doi.org/10.1016/S0020-1693\(02\)01490-1](https://doi.org/10.1016/S0020-1693(02)01490-1).
- (65) Siew, Y.-Y.; Neo, S.-Y.; Yew, H.-C.; Lim, S.-W.; Ng, Y.-C.; Lew, S.-M.; Seetoh, W.-G.; Seow, S.-V.; Koh, H.-L. Oxaliplatin Regulates Expression of Stress Ligands in Ovarian Cancer Cells and Modulates Their Susceptibility to Natural Killer Cell-Mediated Cytotoxicity. *Int Immunol* **2015**, *27* (12), 621–632. <https://doi.org/10.1093/intimm/dxv041>.
- (66) Englinger, B.; Pirker, C.; Heffeter, P.; Terenzi, A.; Kowol, C. R.; Keppler, B. K.; Berger, W. Metal Drugs and the Anticancer Immune Response. *Chem. Rev.* **2019**, *119* (2), 1519–1624. <https://doi.org/10.1021/acs.chemrev.8b00396>.
- (67) Terenzi, A.; Pirker, C.; Keppler, B. K.; Berger, W. Anticancer Metal Drugs and Immunogenic Cell Death. *Journal of Inorganic Biochemistry* **2016**, *165*, 71–79. <https://doi.org/10.1016/j.jinorgbio.2016.06.021>.
- (68) McKeage, M. J.; Hsu, T.; Screnci, D.; Haddad, G.; Baguley, B. C. Nucleolar Damage Correlates with Neurotoxicity Induced by Different Platinum Drugs. *British Journal of Cancer* **2001**, *85* (8), 1219–1225. <https://doi.org/10.1054/bjoc.2001.2024>.

- (69) Toscano, F.; Parmentier, B.; Fajoui, Z. E.; Estornes, Y.; Chayvialle, J.-A.; Saurin, J.-C.; Abello, J. P53 Dependent and Independent Sensitivity to Oxaliplatin of Colon Cancer Cells. *Biochemical Pharmacology* **2007**, *74* (3), 392–406. <https://doi.org/10.1016/j.bcp.2007.05.001>.
- (70) Keck, M. V.; Lippard, S. J. Unwinding of Supercoiled DNA by Platinum-Ethidium and Related Complexes. *Journal of the American Chemical Society* **1992**, *114* (9), 3386–3390. <https://doi.org/10.1021/ja00035a033>.
- (71) Malina, J.; Novakova, O.; Vojtiskova, M.; Natile, G.; Brabec, V. Conformation of DNA GG Intrastrand Cross-Link of Antitumor Oxaliplatin and Its Enantiomeric Analog. *Biophysical Journal* **2007**, *93* (11), 3950–3962. <https://doi.org/10.1529/biophysj.107.116996>.
- (72) Park, G. Y.; Wilson, J. J.; Song, Y.; Lippard, S. J. Phenanthriplatin, a Monofunctional DNA-Binding Platinum Anticancer Drug Candidate with Unusual Potency and Cellular Activity Profile. *PNAS* **2012**, *109* (30), 11987–11992. <https://doi.org/10.1073/pnas.1207670109>.
- (73) Almaqwashi, A. A.; Zhou, W.; Naufer, M. N.; Riddell, I. A.; Yilmaz, Ö. H.; Lippard, S. J.; Williams, M. C. DNA Intercalation Facilitates Efficient DNA-Targeted Covalent Binding of Phenanthriplatin. *J. Am. Chem. Soc.* **2019**, *141* (4), 1537–1545. <https://doi.org/10.1021/jacs.8b10252>.
- (74) Riddell, I. A.; Agama, K.; Park, G. Y.; Pommier, Y.; Lippard, S. J. Phenanthriplatin Acts As a Covalent Poison of Topoisomerase II Cleavage Complexes. *ACS Chem. Biol.* **2016**, *11* (11), 2996–3001. <https://doi.org/10.1021/acscchembio.6b00565>.
- (75) Kellinger, M. W.; Park, G. Y.; Chong, J.; Lippard, S. J.; Wang, D. Effect of a Monofunctional Phenanthriplatin-DNA Adduct on RNA Polymerase II Transcriptional Fidelity and Translesion Synthesis. *J. Am. Chem. Soc.* **2013**, *135* (35), 13054–13061. <https://doi.org/10.1021/ja405475y>.
- (76) Gregory, M. T.; Park, G. Y.; Johnstone, T. C.; Lee, Y.-S.; Yang, W.; Lippard, S. J. Structural and Mechanistic Studies of Polymerase η Bypass of Phenanthriplatin DNA Damage. *Proc Natl Acad Sci U S A* **2014**, *111* (25), 9133–9138. <https://doi.org/10.1073/pnas.1405739111>.
- (77) Facchetti, G.; Rimoldi, I. Anticancer Platinum(II) Complexes Bearing N-Heterocycle Rings. *Bioorganic & Medicinal Chemistry Letters* **2019**, *29* (11), 1257–1263. <https://doi.org/10.1016/j.bmcl.2019.03.045>.

- (78) Yang, K.; Wang, M.; Zhao, Y.; Sun, X.; Yang, Y.; Li, X.; Zhou, A.; Chu, H.; Zhou, H.; Xu, J.; Wu, M.; Yang, J.; Yi, J. A Redox Mechanism Underlying Nucleolar Stress Sensing by Nucleophosmin. *Nature Communications* **2016**, *7* (1), 13599. <https://doi.org/10.1038/ncomms13599>.
- (79) Chen, Y.; Guo, Z.; Parsons, S.; Sadler, P. J. Stereospecific and Kinetic Control over the Hydrolysis of a Sterically Hindered Platinum Picoline Anticancer Complex. *Chemistry – A European Journal* **1998**, *4* (4), 672–676. [https://doi.org/10.1002/\(SICI\)1521-3765\(19980416\)4:4<672::AID-CHEM672>3.0.CO;2-8](https://doi.org/10.1002/(SICI)1521-3765(19980416)4:4<672::AID-CHEM672>3.0.CO;2-8).
- (80) Johnstone, T. C.; Lippard, S. J. The Chiral Potential of Phenanthriplatin and Its Influence on Guanine Binding. *J. Am. Chem. Soc.* **2014**, *136* (5), 2126–2134. <https://doi.org/10.1021/ja4125115>.
- (81) Sutton, E. C.; McDevitt, C. E.; Yglesias, M. V.; Cunningham, R. M.; DeRose, V. J. Tracking the Cellular Targets of Platinum Anticancer Drugs: Current Tools and Emergent Methods. *Inorganica Chimica Acta* **2019**, 118984. <https://doi.org/10.1016/j.ica.2019.118984>.
- (82) Sutton, E. C.; McDevitt, C. E.; Prochnau, J. Y.; Yglesias, M. V.; Mroz, A. M.; Yang, M. C.; Cunningham, R. M.; Hendon, C. H.; DeRose, V. J. Nucleolar Stress Induction by Oxaliplatin and Derivatives. *J. Am. Chem. Soc.* **2019**, *141* (46), 18411–18415. <https://doi.org/10.1021/jacs.9b10319>.
- (83) Sutton, E. C.; DeRose, V. J. Early Nucleolar Responses Differentiate Mechanisms of Cell Death Induced by Oxaliplatin and Cisplatin. *Journal of Biological Chemistry* **2021**, 296. <https://doi.org/10.1016/j.jbc.2021.100633>.
- (84) Johnstone, T. C.; Suntharalingam, K.; Lippard, S. J. The Next Generation of Platinum Drugs: Targeted Pt(II) Agents, Nanoparticle Delivery, and Pt(IV) Prodrugs. *Chem. Rev.* **2016**, *116* (5), 3436–3486. <https://doi.org/10.1021/acs.chemrev.5b00597>.
- (85) Pigg, H.; Sutton, E. C.; Yglesias, M. V.; McDevitt, C. E.; DeRose, V. J. Time-Dependent Studies of Oxaliplatin and Other Nucleolar StressInducing Derivatives. *Unpublished*.
- (86) Habala, L.; Galanski, M.; Yasemi, A.; Nazarov, A. A.; von Keyserlingk, N. G.; Keppler, B. K. Synthesis and Structure-Activity Relationships of Mono- and Dialkyl-Substituted Oxaliplatin Derivatives. *European Journal of Medicinal Chemistry* **2005**, *40* (11), 1149–1155. <https://doi.org/10.1016/j.ejmech.2005.06.003>.

- (87) Abramkin, S. A.; Jungwirth, U.; Valiahdhi, S. M.; Dworak, C.; Habala, L.; Meelich, K.; Berger, W.; Jakupec, M. A.; Hartinger, C. G.; Nazarov, A. A.; Galanski, M.; Keppler, B. K. {(1R,2R,4R)-4-Methyl-1,2-Cyclohexanediamine}oxalatoplatinum(II): A Novel Enantiomerically Pure Oxaliplatin Derivative Showing Improved Anticancer Activity in Vivo. *J. Med. Chem.* **2010**, *53* (20), 7356–7364. <https://doi.org/10.1021/jm100953c>.
- (88) Jungwirth, U.; Xanthos, D. N.; Gojo, J.; Bytzek, A. K.; Korner, W.; Heffeter, P.; Abramkin, S. A.; Jakupec, M. A.; Hartinger, C. G.; Windberger, U.; Galanski, M.; Keppler, B. K.; Berger, W. Anticancer Activity of Methyl-Substituted Oxaliplatin Analog. *Mol Pharmacol* **2012**. <https://doi.org/10.1124/mol.111.077321>.
- (89) Galanski, M.; Yasemi, A.; Slaby, S.; Jakupec, M. A.; Arion, V. B.; Rausch, M.; Nazarov, A. A.; Keppler, B. K. Synthesis, Crystal Structure and Cytotoxicity of New Oxaliplatin Analogues Indicating That Improvement of Anticancer Activity Is Still Possible. *European Journal of Medicinal Chemistry* **2004**, *39* (8), 707–714. <https://doi.org/10.1016/j.ejmech.2004.04.003>.
- (90) Habala, L.; Dworak, C.; Nazarov, A. A.; Hartinger, C. G.; Abramkin, S. A.; Arion, V. B.; Lindner, W.; Galanski, M.; Keppler, B. K. Methyl-Substituted Trans-1,2-Cyclohexanediamines as New Ligands for Oxaliplatin-Type Complexes. *Tetrahedron* **2008**, *64* (1), 137–146. <https://doi.org/10.1016/j.tet.2007.10.069>.
- (91) Wilson, J. J.; Lippard, S. J. Synthetic Methods for the Preparation of Platinum Anticancer Complexes. *Chem. Rev.* **2014**, *114* (8), 4470–4495. <https://doi.org/10.1021/cr4004314>.
- (92) Hall, M. D.; Telma, K. A.; Chang, K.-E.; Lee, T. D.; Madigan, J. P.; Lloyd, J. R.; Goldlust, I. S.; Hoeschele, J. D.; Gottesman, M. M. Say No to DMSO: Dimethylsulfoxide Inactivates Cisplatin, Carboplatin, and Other Platinum Complexes. *Cancer Res* **2014**, *74* (14), 3913–3922. <https://doi.org/10.1158/0008-5472.CAN-14-0247>.
- (93) Oliveira, B. L.; Guo, Z.; Bernardes, G. J. L. Inverse Electron Demand Diels–Alder Reactions in Chemical Biology. *Chem. Soc. Rev.* **2017**, *46* (16), 4895–4950. <https://doi.org/10.1039/C7CS00184C>.
- (94) Patterson, D. M.; Nazarova, L. A.; Prescher, J. A. Finding the Right (Bioorthogonal) Chemistry. *ACS Chem. Biol.* **2014**, *9* (3), 592–605. <https://doi.org/10.1021/cb400828a>.

- (95) Wirth, R.; White, J. D.; Moghaddam, A. D.; Ginzburg, A. L.; Zakharov, L. N.; Haley, M. M.; DeRose, V. J. Azide vs Alkyne Functionalization in Pt(II) Complexes for Post-Treatment Click Modification: Solid-State Structure, Fluorescent Labeling, and Cellular Fate. *J. Am. Chem. Soc.* **2015**, *137* (48), 15169–15175. <https://doi.org/10.1021/jacs.5b09108>.
- (96) Rodionov, V. O.; Fokin, V. V.; Finn, M. G. Mechanism of the Ligand-Free CuI-Catalyzed Azide–Alkyne Cycloaddition Reaction. *Angewandte Chemie* **2005**, *117* (15), 2250–2255. <https://doi.org/10.1002/ange.200461496>.
- (97) Lefebvre, J.; Guetta, C.; Poyer, F.; Mahuteau-Betzer, F.; Teulade-Fichou, M.-P. Copper-Alkyne Complexation Responsible for the Nucleolar Localization of Quadruplex Nucleic Acid Drugs Labeled by Click Reactions. *Angew. Chem. Int. Ed. Engl.* **2017**, *56* (38), 11365–11369. <https://doi.org/10.1002/anie.201703783>.
- (98) Tornøe, C. W.; Christensen, C.; Meldal, M. Peptidotriazoles on Solid Phase: [1,2,3]-Triazoles by Regiospecific Copper(I)-Catalyzed 1,3-Dipolar Cycloadditions of Terminal Alkynes to Azides. *J. Org. Chem.* **2002**, *67* (9), 3057–3064. <https://doi.org/10.1021/jo011148j>.
- (99) Saxon, E.; Armstrong, J. I.; Bertozzi, C. R. A “Traceless” Staudinger Ligation for the Chemoselective Synthesis of Amide Bonds. *Org. Lett.* **2000**, *2* (14), 2141–2143. <https://doi.org/10.1021/ol006054v>.
- (100) Agard, N. J.; Prescher, J. A.; Bertozzi, C. R. A Strain-Promoted [3 + 2] Azide–Alkyne Cycloaddition for Covalent Modification of Biomolecules in Living Systems. *J. Am. Chem. Soc.* **2004**, *126* (46), 15046–15047. <https://doi.org/10.1021/ja044996f>.
- (101) Blackman, M. L.; Royzen, M.; Fox, J. M. Tetrazine Ligation: Fast Bioconjugation Based on Inverse-Electron-Demand Diels–Alder Reactivity. *J. Am. Chem. Soc.* **2008**, *130* (41), 13518–13519. <https://doi.org/10.1021/ja8053805>.
- (102) Yang, J.; Šečutè, J.; Cole, C. M.; Devaraj, N. K. Live-Cell Imaging of Cyclopropene Tags with Fluorogenic Tetrazine Cycloadditions. *Angewandte Chemie International Edition* **2012**, *51* (30), 7476–7479. <https://doi.org/10.1002/anie.201202122>.
- (103) Row, R. D.; Shih, H.-W.; Alexander, A. T.; Mehl, R. A.; Prescher, J. A. Cyclopropenones for Metabolic Targeting and Sequential Bioorthogonal Labeling. *J. Am. Chem. Soc.* **2017**, *139* (21), 7370–7375. <https://doi.org/10.1021/jacs.7b03010>.

- (104) Barát, V.; Kasinathan, S.; Bates, R. W. Platinum-Catalysed Ring-Opening Isomerisation of Piperidine Cyclopropanes. *Asian Journal of Organic Chemistry* **2018**, 7 (4), 815–818. <https://doi.org/10.1002/ajoc.201700706>.
- (105) McDevitt, C. E.; Yglesias, M. V.; Mroz, A. M.; Sutton, E. C.; Yang, M. C.; Hendon, C. H.; DeRose, V. J. Monofunctional Platinum(II) Compounds and Nucleolar Stress: Is Phenanthriplatin Unique? *J Biol Inorg Chem* **2019**, 24 (6), 899–908. <https://doi.org/10.1007/s00775-019-01707-9>.
- (106) Cunningham, R. M.; DeRose, V. J. Platinum Binds Proteins in the Endoplasmic Reticulum of *S. Cerevisiae* and Induces Endoplasmic Reticulum Stress. *ACS Chem. Biol.* **2017**, 12 (11), 2737–2745. <https://doi.org/10.1021/acscchembio.7b00553>.
- (107) Plakos, K.; DeRose, V. J. Mapping Platinum Adducts on Yeast Ribosomal RNA Using High-Throughput Sequencing. *Chem. Commun.* **2017**. <https://doi.org/10.1039/C7CC06708A>.
- (108) Wirth, R.; White, J. D.; Moghaddam, A. D.; Ginzburg, A. L.; Zakharov, L. N.; Haley, M. M.; DeRose, V. J. Azide vs. Alkyne Functionalization in Pt(II) Complexes for Post-Treatment Click Modification: Solid State Structure, Fluorescent Labeling, and Cellular Fate. *Journal of the American Chemical Society* **2015**, No. 11, jacs.5b09108. <https://doi.org/10.1021/jacs.5b09108>.
- (109) Wu, Y.; Pradhan, P.; Havener, J.; Boysen, G.; Swenberg, J. A.; Campbell, S. L.; Chaney, S. G. NMR Solution Structure of an Oxaliplatin 1,2-d(GG) Intrastrand Cross-Link in a DNA Dodecamer Duplex. *Journal of Molecular Biology* **2004**, 341 (5), 1251–1269. <https://doi.org/10.1016/j.jmb.2004.06.066>.
- (110) Hanwell, M. D.; Curtis, D. E.; Lonie, D. C.; Vandermeersch, T.; Zurek, E.; Hutchison, G. R. Avogadro: An Advanced Semantic Chemical Editor, Visualization, and Analysis Platform. *Journal of Cheminformatics* **2012**, 4 (1), 17. <https://doi.org/10.1186/1758-2946-4-17>.
- (111) The PyMOL Molecular Graphics System, Version 2.0 Schrödinger, LLC.
- (112) Grummitt, C. G.; Townsley, F. M.; Johnson, C. M.; Warren, A. J.; Bycroft, M. Structural Consequences of Nucleophosmin Mutations in Acute Myeloid Leukemia *. *Journal of Biological Chemistry* **2008**, 283 (34), 23326–23332. <https://doi.org/10.1074/jbc.M801706200>.
- (113) Ritz, C.; Baty, F.; Streibig, J. C.; Gerhard, D. Dose-Response Analysis Using R. *PLOS ONE* **2015**, 10 (12), e0146021. <https://doi.org/10.1371/journal.pone.0146021>.

- (114) Rueden, C. T.; Schindelin, J.; Hiner, M. C.; DeZonia, B. E.; Walter, A. E.; Arena, E. T.; Eliceiri, K. W. ImageJ2: ImageJ for the next Generation of Scientific Image Data. *BMC Bioinformatics* **2017**, *18* (1), 529. <https://doi.org/10.1186/s12859-017-1934-z>.
- (115) Schindelin, J.; Arganda-Carreras, I.; Frise, E.; Kaynig, V.; Longair, M.; Pietzsch, T.; Preibisch, S.; Rueden, C.; Saalfeld, S.; Schmid, B.; Tinevez, J.-Y.; White, D. J.; Hartenstein, V.; Eliceiri, K.; Tomancak, P.; Cardona, A. Fiji: An Open-Source Platform for Biological-Image Analysis. *Nature Methods* **2012**, *9* (7), 676–682. <https://doi.org/10.1038/nmeth.2019>.
- (116) van der Walt, S.; Schönberger, J. L.; Nunez-Iglesias, J.; Boulogne, F.; Warner, J. D.; Yager, N.; Gouillart, E.; Yu, T. Scikit-Image: Image Processing in Python. *PeerJ* **2014**, *2*, e453. <https://doi.org/10.7717/peerj.453>.
- (117) Dhara, S.C. A Rapid Method for the Synthesis of Cis-[Pt (NH₃)₂Cl₂]. *Indian J Chem* **1970**, *8*, 193.
- (118) Wilson, J. J.; Lippard, S. J. Synthetic Methods for the Preparation of Platinum Anticancer Complexes. *Chem Rev* **2014**, *114* (8), 4470–4495. <https://doi.org/10.1021/cr4004314>.
- (119) Fanizzi, F. P.; Intini, F. P.; Maresca, L.; Natile, G.; Quaranta, R.; Coluccia, M.; Di Bari, L.; Giordano, D.; Mariggió, M. A. Biological Activity of Platinum Complexes Containing Chiral Centers on the Nitrogen or Carbon Atoms of a Chelate Diamine Ring. *Inorganica Chimica Acta* **1987**, *137* (1), 45–51. [https://doi.org/10.1016/S0020-1693\(00\)87114-5](https://doi.org/10.1016/S0020-1693(00)87114-5).
- (120) Garbutcheon-Singh, K. B.; Leverett, P.; Myers, S.; Aldrich-Wright, J. R. Cytotoxic Platinum(II) Intercalators That Incorporate 1R,2R-Diaminocyclopentane. *Dalton Trans.* **2012**, *42* (4), 918–926. <https://doi.org/10.1039/C2DT31323E>.
- (121) OECD. *Test No. 107: Partition Coefficient (n-Octanol/Water): Shake Flask Method, OECD Guidelines for the Testing of Chemicals, Section 1*; OECD Publishing: Paris, 1995.
- (122) Wilson, J. J.; Lippard, S. J. In Vitro Anticancer Activity of Cis-Diammineplatinum(II) Complexes with β -Diketonate Leaving Group Ligands. *J Med Chem* **2012**, *55* (11), 5326–5336. <https://doi.org/10.1021/jm3002857>.

- (123) Frisch, M.; Schlegel, H.; Scuseria, G.; Robb, M.; Cheeseman, J.; Scalmani, G.; Barone, V.; Petersson, G.; Nakatsuji, H.; Li, X.; Caricato, M.; Marenich, A.; Bloino, J.; Janesko, B.; Gomperts, R.; Mennucci, B.; Hratchian, H.; Ortiz, J.; Izmaylov, A.; Sonnenberg, J.; Williams-Young, D.; Ding, F.; Lipparini, F.; Egidi, F.; Goings, J.; Peng, B.; Petrone, A.; Henderson, T.; Ranasinghe, D.; Zakrzewski, V.; Gao, J.; Rega, N.; Zheng, G.; Liang, W.; Hada, M.; Ehara, M.; Toyota, K.; Fukuda, R.; Hasegawa, J.; Ishida, M.; Nakajima, T.; Honda, Y.; Kitao, O.; Nakai, H.; Vreven, T.; Throssell, K.; Montgomery, Jr, J.; Peralta, J.; Ogliaro, F.; Bearpark, M.; Heyd, J.; Brothers, E.; Kudin, K.; Staroverov, V.; Keith, T.; Kobayashi, R.; Normand, J.; Raghavachari, K.; Rendell, A.; Burant, J.; Iyengar, S.; Tomasi, J.; Cossi, M.; Millam, J.; Klene, M.; Adamo, C.; Cammi, R.; Ochterski, J.; Martin, R.; Morokuma, K.; Farkas, O.; Foresman, J.; Fox, D. *Gaussian09*; Gaussian Inc. Wallingford CT, 2016.
- (124) Perdew, J.; Burke, K.; Ernzerhof, M. Generalized Gradient Approximation Made Simple. *Phys. Rev. Lett.* **1996**, *77*, 3865–3868.
- (125) Perdew, J.; Burke, K.; Ernzerhof, M. Errata: Generalized Gradient Approximation Made Simple. *Phys. Rev. Lett.* **1997**, *78*, 1396.
- (126) Pansini, F.; Neto, A.; de Campos, M.; de Aquino R. Effects of All-Electron Basis Sets and the Scalar Relativistic Corrections in the Structure and Electronic Properties of Niobium Clusters. *J. Phys. Chem. A* **2017**, *121* (30), 5728–5734.
- (127) Butler, K.; Hendon, C.; Walsh, A. Electronic Chemical Potentials of Porous Metal-Organic Frameworks. *J. Am. Chem. Soc.* **2014**, *136*, 2703–2706.
- (128) Blöchl, P. E. Projector Augmented-Wave Method. *Phys Rev B Condens Matter* **1994**, *50* (24), 17953–17979. <https://doi.org/10.1103/physrevb.50.17953>.
- (129) Kresse, G.; Joubert, D. From Ultrasoft Pseudopotentials to the Projector Augmented-Wave Method. *Phys. Rev. B* **1999**, *59*, 1758.
- (130) Kresse, G.; Furthmüller, J. Efficient Iterative Schemes for Ab Initio Total-Energy Calculations Using a Plane-Wave Basis Set. *Phys. Rev. B* **1996**, *54*, 11169.
- (131) Kresse, G.; Hafner, J. Ab Initio Molecular Dynamics for Liquid Metals. *Phys. Rev. B* **1993**, *47*, 558.
- (132) Kresse, G.; Hafner, J. Ab Initio Molecular-Dynamics Simulation of the Liquid-Metal--Amorphous-Semiconductor Transition in Germanium. *Phys. Rev. B* **1994**, *49* (20), 14251–14269. <https://doi.org/10.1103/PhysRevB.49.14251>.

- (133) Okada, T.; El-Mehasseb, I. M.; Kodaka, M.; Tomohiro, T.; Okamoto, K.; Okuno, H. Mononuclear Platinum(II) Complex with 2-Phenylpyridine Ligands Showing High Cytotoxicity against Mouse Sarcoma 180 Cells Acquiring High Cisplatin Resistance. *J. Med. Chem.* **2001**, *44* (26), 4661–4667. <https://doi.org/10.1021/jm010203d>.
- (134) Walt, S. van der; Schönberger, J. L.; Nunez-Iglesias, J.; Boulogne, F.; Warner, J. D.; Yager, N.; Gouillart, E.; Yu, T. Scikit-Image: Image Processing in Python. *PeerJ* **2014**, *2*, e453. <https://doi.org/10.7717/peerj.453>.
- (135) Marenich, A.; Cramer, C.; Truhlar, D. Universal Solvation Model Based on Solute Electron Density and a Continuum Model of the Solvent Defined by the Bulk Dielectric Constant and Atomic Surface Tensions. *J. Phys. Chem. B* **2009**, *113*, 6378–6396.
- (136) Kresse, G.; Furthmüller, J. Efficiency of Ab-Initio Total Energy Calculations for Metals and Semiconductors Using a Plane-Wave Basis Set. *Computational Materials Science* **1996**, *6* (1), 15–50. [https://doi.org/10.1016/0927-0256\(96\)00008-0](https://doi.org/10.1016/0927-0256(96)00008-0).